

Wright State University

CORE Scholar

[Browse all Theses and Dissertations](#)

[Theses and Dissertations](#)

2014

Early Increase of CD11c in Human Monocyte-Derived Dendritic Cells in the Presence of A/California/07/2009 (H1N1pdm)

Amber M. Braddock
Wright State University

Follow this and additional works at: https://corescholar.libraries.wright.edu/etd_all



Part of the [Pharmacology, Toxicology and Environmental Health Commons](#)

Repository Citation

Braddock, Amber M., "Early Increase of CD11c in Human Monocyte-Derived Dendritic Cells in the Presence of A/California/07/2009 (H1N1pdm)" (2014). *Browse all Theses and Dissertations*. 1204. https://corescholar.libraries.wright.edu/etd_all/1204

This Thesis is brought to you for free and open access by the Theses and Dissertations at CORE Scholar. It has been accepted for inclusion in Browse all Theses and Dissertations by an authorized administrator of CORE Scholar. For more information, please contact library-corescholar@wright.edu.

**Early Increase of CD11c in Human Monocyte-derived Dendritic Cells in the
Presence of *A/California/07/2009 (H₁N₁pdm)***

A thesis submitted in partial fulfillment of the
requirements for the degree of
Master of Science

By

Amber Marie Braddock
B.S., Wright State University, 2011

2014
Wright State University

WRIGHT STATE UNIVERSITY

GRADUATE SCHOOL

May 27, 2014

I hereby recommend that the thesis prepared under my supervision by Amber Marie Braddock entitled Early Increase of CD11c in Human Monocyte-derived Dendritic Cells in the Presence of A/California/07/2009 (H₁N₁pdm) be accepted in partial fulfillment of the requirements for the degree of Master of Science.

Oswaldo Lopez, Ph.D.
Thesis Advisor

Cheryl Conley, Ph.D., M.T. (A.S.C.P.)
Co-Advisor

Norma Adragna, Ph.D.
Department Chair,
Pharmacology and Toxicology

Committee:

Mauricio Di Fulvio, Ph.D.

James B. Lucot, Ph.D.

Robert Fyffe, Ph.D.
Vice President for Research and
Dean of the Graduate School

ABSTRACT

Braddock, Amber Marie. M.S. Pharmacology and Toxicology, Wright State University, 2014. Early Increase of CD11c in Human Monocyte-derived Dendritic Cells in the Presence of *A/California/07/2009 (H₁N₁pdm)*.

Influenza A continues to cause significant morbidity and mortality. Vaccine production time, viral antigenic variability and low vaccine efficacy contribute to the annual pandemics and seasonal epidemics. A better understanding of human immune responses to influenza A could result in more effective vaccines. Dendritic cells (DCs) play an important role in the initiation of immune responses. Populations of B lymphocytes secrete protective antibodies but the role of different populations of B cells in the protective response is unknown. In this thesis we developed assays to determine subclasses of influenza specific antibodies. Mononuclear cells were assessed using flow cytometry to identify monocytes and marginal zone B lymphocytes. Monocyte-derived dendritic cells (MdDCs) were infected with influenza virus *A/California/07/2009 (H₁N₁pdm)* and activation markers were detected by using flow cytometry. Virus infected MdDCs exhibited enhanced expression of CD11c compared to MdDCs exposed to inactivated virus. We hypothesize that the early expression of CD11c activation marker is an important event in the early immune response against influenza virus. Expression of CD11c may help in the rapid activation of influenza-specific T cells leading to an early and robust immune response.

Table of Contents

Introduction.....	1
Purpose and Aim.....	9
Subjects	11
Chapter 1: Virus Work.....	12
Section 1: Propagation of Influenza Virus in Embryonated Chicken Eggs.....	12
1.1 Methods.....	12
1.2 Results.....	14
Section 2: Propagation of Influenza Virus in Madin Darby Canine Kidney-ATL cells (MDCK)	14
2.1 Methods.....	14
2.2 Results.....	16
Section 3: Titration of Virus using Hemagglutination.....	18
3.1 Methods.....	18
3.2 Results.....	19
Section 4: Titration of Virus using Tissue Culture Infectious Dose 50% Assay	21
4.1 Methods.....	21
4.2 Results.....	22

Chapter 2: Blood Processing and Analysis of Subclasses of Antibodies	27
Section 1: Red Blood Cell Lysis	27
1.1 Methods	27
1.1 Results	29
Section 2: Ficoll-Hypaque Separation	30
2.1 Methods	30
2.2 Results	33
Section 3: B cell Subpopulations	35
3.1 Results	35
Section 4: Enrichment of Monocytes from Mononuclear Cells	38
4.1 Methods	38
4.2 Results	40
Section 5: B cell Separation from Mononuclear Cells	43
5.1 Methods	43
5.2 Results	44
Section 6: Antibody Assay using Hemagglutination Inhibition	47
6.1 Methods	47
6.2 Results	49
Section 7: Detection of Subclasses of Antibodies	50

7.1 Methods.....	50
7.2 Results.....	55
Chapter 3: Dendritic Cell Production and Infection	71
Section 1: Differentiation of Monocytes to Dendritic Cells	71
1.1 Methods.....	71
1.2 Results.....	71
Section 2: Infection of Dendritic cells with <i>A/California/07/2009 (H₁N₁pdm)</i>	74
2.1 Methods.....	74
2.2 Results.....	75
Section 2: Detection of Markers	75
2.1 Methods.....	75
2.2 Results.....	76
Discussion	81
Appendices.....	85
Appendix A: Consent form for healthy volunteers	86
Appendix B: Reagent List.....	89
Appendix C: ELISA Antibodies	92
Works Cited	96

List of Figures

Figure 1: Experimental design for this thesis project	10
Figure 2: Propagation of Influenza A in embryonated chicken eggs.....	13
Figure 3: Injection of virus into chicken egg	13
Figure 4: MDCK-ATL cells in growth phase before reaching confluence	15
Figure 5: Propagation of H ₁ N ₁ in MDCK-ATL cells with different dilutions of stock virus	16
Figure 6: Propagation of H ₁ N ₁ in MDCK-ATL cells	17
Figure 7: H ₃ N ₂ did not propagate well in MDCK cells	17
Figure 8: HA assay.....	19
Figure 9: HA assay of H ₁ N ₁ propagated in MDCK cells.....	20
Figure 10: HA assay of H ₃ N ₂ propagation in MDCK cells	21
Figure 11: TCID ₅₀ % results from propagation of H ₁ N ₁ in MDCK cells.....	23
Figure 12: Side scatter and forward scatter of cells from a red blood cell lysis	30
Figure 13: Before (left) and after (right) Ficoll-Hypaque separation of MNCs	31
Figure 14: MNC separation with Accuspin tube	32
Figure 15: Monocyte (left) and lymphocyte (right), visualized using Wright Stain in whole blood.....	33
Figure 16: MNC populations after Ficoll-Hypaque separation	34
Figure 17: MZBC analysis, Donor A.....	36
Figure 18: B cell populations, Donor A.....	37

Figure 19: Overview of monocyte separation using Streptavidin Magnetic Microbeads	39
Figure 20: Flow data of the separation at each step.....	40
Figure 21: Purification analysis of monocytes from separation	42
Figure 22: B cell separation using Dynabeads.....	45
Figure 23: Flow cytometry analysis of MNCs depleted of CD3 and CD14.....	46
Figure 24: Antibody inhibition assay.....	48
Figure 25: Antibody inhibition assay results from donor S	49
Figure 26: ELISA method #1 overview.....	51
Figure 27: ELISA method #2 overview.....	53
Figure 28: ELISA method #3 overview.....	54
Figure 29: Curves to calculate unknown concentrations of IgG1.....	56
Figure 30: Multiple serum results	58
Figure 31: Multiple serum results	59
Figure 32: Preliminary data from donor L.....	60
Figure 33: ELISA method #2 multiple serums	61
Figure 34: ELISA method #2 multiple serums	62
Figure 35: Quantification of total IgG	65
Figure 36: Quantification of IgG1	66
Figure 37: Quantification of IgG2	67
Figure 38: Influenza specific antibodies donor A.....	68
Figure 39: Influenza specific antibodies donor S	69
Figure 40: Influenza specific antibodies donor S	70
Figure 41: DC production	72

Figure 42: Cells in DC culture	73
Figure 43: TCID50% Results of heat inactivated H ₁ N ₁	75
Figure 44: LPS stimulation of DCs.....	77
Figure 45: Infection of DC.....	78
Figure 46: Brightness of CD11c	80

List of Tables

Table 1: Subjects.....	11
Table 2: Example plate set up for a TCID ₅₀ % Assay	22
Table 3: Concentration of virus in stock vials from the IRR	25
Table 4: Concentration of virus from propagation of H ₁ N ₁ in MDCK cells	25
Table 5: MZBC analysis from different donors.....	36
Table 6: Quantification of IgGs in serum using Invitrogen Kit.....	57
Table 7: Known concentrations of myeloma standards	60
Table 8: Sensitivities of different methods	63
Table 9: Quantification of IgGs in donors	65
Table 10: CD11c mean brightness of DC infection.....	79
Table 11: ELISA Antibodies	95

Introduction

Despite modern medical advances and study, Influenza A viral infection is still a serious health problem. Influenza A has been responsible for several pandemics as well as seasonal epidemics during the autumn and winter in some climates, and has been known to be detectable all year in tropical climates. Seasonal influenza epidemics result in about three to five million cases of severe illness and 250,000-500,000 deaths worldwide according to the World Health Organization¹⁷. Deaths due to Influenza A viral infection can be caused by secondary infections such as pneumonia, or complications from other respiratory or cardiovascular problems¹⁹. Infection with influenza virus also has an economic impact due to loss of productivity and missed wages from sick days. It also puts a strain on the healthcare system during peak seasons when a large number of patients require care¹⁷. From 1918-1919 the Spanish Flu (H₁N₁) killed 50 million individuals, more than war-related casualties in World War I. The 1957 Asian Flu (H₂N₂) and 1968 Hong Kong Flu (H₃N₂) combined killed 2 million individuals. The H₅N₁ outbreak in 1997 had a 50% mortality rate¹⁶. More recently, the 2009 pandemic H₁N₁ pandemic virus has killed an estimated 283,000 individuals (respiratory and cardiovascular deaths) during the first 12 months, with 80% of the deaths in individuals less than 65 years of age¹⁸.

Influenza A is responsible for major pandemics and Influenza B only causes cold-like symptoms¹⁶. The nomenclature used to describe Influenza A is designated as follows: “type of virus/city of isolation/laboratory identification/year (Antigen (HA and

NA identifiers).” If the strain described produces a pandemic, the label “pdm” is used. For this research, the strains used were: *A/Brisbane/10/2007 (H₃N₂)* and the *A/California/07/2009 (H₁N₁pdm)* obtained from the Influenza Reagent Resource of the Center for Disease Control (CDC).

According to the CDC, the most effective mean to prevent influenza infection is through vaccination²⁶. There are several different types of influenza vaccines available. A standard intramuscular trivalent vaccine is produced in eggs and provides protection against three selected flu viruses for that season (usually Influenza B and two Influenza A strains). There is also an intradermal trivalent vaccine produced in cultured cells, essentially making the vaccine egg free for individuals with egg allergies. In addition, a high-dose trivalent vaccine is available for individuals older than 65. A quadrivalent flu vaccine protects against two selected Influenza A viruses and two selected Influenza B viruses. It is available as a standard vaccine and as a nasal spray. For the 2013 to 2014 flu season about 135-139 million vaccine doses were produced in the US²⁷. It is this trivalent vaccine that is the most commonly administered in the northern hemisphere. It contains *A/California/7/2009 (H₁N₁)*, A H₃N₂ virus like *A/Victoria/361/2011*, and *B/Massachusetts/2/2012* like virus²⁹.

In spite of available vaccines, predicting which influenza strains will prevail during future seasons is a challenge and therefore, effective vaccine production for future infections remains non-practical. Throughout the year, samples from individuals suspected of having influenza are sent to the National Influenza Centers from around the world. Here specific strains are identified and details sent to the Collaborating Centers for Influenza Reference and Research. Twice a year this data is evaluated by the WHO

Collaborating Center. Then the strains of influenza likely to cause disease in the next season are reviewed and suggestions made for next season's flu vaccine. Northern hemisphere vaccines are reviewed in February and the southern hemisphere in September. Subsequent to this evaluation, manufacturing companies have about 6 months to produce their vaccine supply. The majority of the vaccine supply is produced in chicken eggs²⁸. There are two types of vaccines, attenuated and inactivated. Attenuated vaccines contain a weakened form of the live virus that does not cause disease in normal individuals. Inactivated vaccines contain the virus killed by heat or radiation. These vaccines do not require special storage conditions⁴⁴.

Serum anti-influenza antibodies after vaccination with inactivated vaccines increase in humans two weeks after vaccination. This protects individuals during the influenza season when the highest risk for exposure is present³¹. Clinical studies on "Afluria" (trivalent inactivated vaccine currently available) showed a vaccine efficacy was 60% (lower limit of the 95% confidence interval: 42%) for the 2013-2014 formula³².

According to the CDC, for the 2013-14 flu season, only 40% of the eligible population in the United States had been vaccinated with the seasonal flu vaccine by the early part of the season (November 2013)³⁶. Data is not available for late season vaccine coverage but the CDC has estimated it to be around 45% for that time period³⁷. As of the end of February 2014, 95% and 3.8% of the reported influenza associated hospitalizations have occurred from Influenza A and Influenza B strains, respectively. The majority of the hospitalizations (61.2%) have occurred in adults age 18-64 years. Adults over 65 years of age have only accounted for 24.8% of influenza associated hospitalizations this season. It is important to note that of the Influenza A related hospitalizations, 98.6%

were caused by the pandemic H₁N₁ strain³⁶. This strain has been present in the vaccine for several seasons in a row. Therefore H₁N₁ is still the major cause of influenza cases occurring in non-elderly populations.

The influenza virion is enveloped with a segmented single-stranded negative RNA genome. It also contains a matrix between the envelope and the nucleocapsid. The influenza virus has 8 genes. Genes 1-3 are related to RNA polymerization and duplication of the viral genome. Gene 4 regulates expression of the HA antigen, or hemagglutinin, the viral attachment protein target of neutralizing antibodies. Gene 5 regulates expression of NP or nucleoprotein. The NP is associated with the viral RNA and a target for cellular immunity. Gene 6 regulates expression of NA, or neuraminidase, which cleaves sialic acid and promotes viral release from the host cell. Neuraminidase is a target for neuraminidase inhibitor drugs and neutralizing antibodies of the host. Gene 7 codes for the matrix protein 1 (M1), or the viral structure protein, and M2, a membrane protein. Gene 8 codes for Nonstructural Protein 1 and 2 (NS1 or NS2)¹³.

The HA and NA combine to form different variants of the influenza virus. Human influenza virus strains bind sialic acid attached to galactose in an alpha 2, 6 configuration present in the glycocalyx of cells, in particular the upper respiratory tract. Avian influenza viruses bind the alpha 2, 3 configuration. Pigs have either configuration which causes them to be easily infected with human and avian virus strains, increasing the potential for creating novel influenza viruses that could cause human pandemics¹⁶. If a pig becomes infected simultaneously with both avian and human Influenza A, a recombinant form of the virus may emerge. This may have an environmental advantage and infect new hosts easily because of a lack of herd immunity against the new strain.

Influenza is transmitted through droplets and aerosols suspended in the air and moved by currents. The human infectious dose is between one and five viral particles. In the infective mode, the virus enters the cell by receptor-mediated endocytosis. The low pH in the endosome allows the membrane of the virus to fuse with the endosome while the RNA is delivered to the nucleus. There, the negative stranded viral RNA transcribes to positive RNA to create mRNA. In the ER transcribed viral mRNAs are translated. HA and NA antigens are transported with the help of M2 proteins from the Golgi network to the plasma membrane on the apical side of the respiratory epithelium. The negative RNA and other structural proteins move to the cell membrane where the virus is assembled. The virus then buds through the plasma membrane whilst still attached to the sialic acid receptors via HA interaction. NA then cleaves the attaching sialic acid releasing the virions into the lumen of the respiratory tract^{16, 21}.

The incubation period for influenza is about two days. Thereafter, the onset of the disease is fast. Symptoms include high fever, headaches, chills, cough, congestion, sore throat, muscle pain, and loss of appetite. It takes about a week for the respiratory symptoms to subside, but cough and general weakness lasts for up to two weeks. Influenza infection leads to cell death and desquamation of the epithelium. This increases the possibility of secondary infections to occur as well as other complications if the human immune system cannot stop viral replication. Secondary bacterial infections can occur after influenza infection, causing increased complications and health risks including hospitalization and death¹⁶.

An effective vaccine induces host protection by prompting a virus-specific neutralizing antibody response. There are a number of antibody isotypes present in

human serum. Immunoglobulin G (IgG) makes up about 75% of serum immunoglobulin and is involved in the secondary immune response, i.e., the one elicited after an initial and subsequent exposure to the same antigens. IgGs come in several subclasses; IgG1, 2, 3, and 4. IgG1 binds Fc- receptors on phagocytic cells and to platelets with high affinity. IgG1 has a freely flexing hinge, 15 amino acids in length, and a kappa to lambda light chain ratio of 2.4. It makes up 60.3-71.5% of IgG in healthy adult serum (5-12 g/L). In contrast, IgG2 is the only IgG that cannot cross the placental barrier, and is lacking in children less than 2 years of age. It has a very short hinge that cannot pivot, and is 12 amino acids long. The light chain is joined about one fourth the distance from the gamma, and has a kappa to lambda ratio of 1.1. IgG2 constitutes 19.4-31% of IgG in healthy human serum (2-6 g/L). The circulating concentration of IgG2 is highly correlated to polysaccharide vaccine responses. IgG3 makes up 5-8.4% of IgG in healthy adult serum (0.5-1 g/L) and has a very long hinge region that is 62 amino acids long. Complement component C1q binds IgG3 more readily than others. IgG4 makes up 0.7-4.2% of IgG in healthy adults serum (0.2-1 g/L), and has a kappa to lambda binding ratio of 8. IgG4 has the shortest hinge (12 amino acids), and is thought to not be able to bind complement through the classical pathway¹⁴.

Contrary to IgGs, Immunoglobulin M (IgM) is less abundant in (1.5 mg/ml of serum) and has a pentameric structure. IgM is the first antibody response detected during an infection²³. Its structure allows it to bind antigen with high avidity and agglutinate. IgM removes antigen and apoptotic cells from the site of inflammation. Over the course of an infection, the antibody response changes from IgM to IgG⁴⁰.

Dendritic cells (DCs) are also found on mucosal surfaces in the respiratory tract.

Because of the pivotal role of DCs in initiating and enhancing specific immune responses, DCs are used to study the immune system *in vitro* in many different infection models. The immune response to pathogens not only includes the humoral response i.e., antibodies, it also starts with antigen presentation, a task mainly executed by DCs. These cells capture, process, and present antigens. A process that may be further stimulated by foreign particles or by inflammation. Processed antigens are then bound to the Major Histocompatibility Complex (MHC) class I, which then are presented by DCs to CD8 cytotoxic T cells to activate them to kill the infected targets. Influenza proteins acquired by the exogenous pathway are associated with MHC II proteins and presented by DCs to CD4 follicular T helper cells. Once T helper cells are activated they modulate the response of other immune cells such as B cells to induce antibody production i.e., the humoral response. DC-activated T helper cells are involved in class switching of activated B cells i.e., the change in the humoral response from isotype IgM to isotype IgG⁴¹.

All populations of B cells express CD19, a pan-B cell marker. A cell population of importance in the early antibody response is a B cell subpopulation called the Marginal Zone B cells (MZBCs). The existence of the counterpart of the MZBCs in humans was initially controversial but it is now becoming widely accepted³. MZBCs originate from the marginal zone of the spleen, where they come into contact with pathogens in the blood⁴. The main markers that allow for characterization of the MZBC population in humans are CD27 and surface immunoglobulin (Ig) IgD and IgM. MZBCs differ from naïve B cells in their expression of CD27, and differ from memory B cells in their expression of IgD and IgM. MZBCs are classified as an innate-like population of B cells

and seem to be responsible for the early antibody response in acute infection. Our lab has previously demonstrated that this population produces the first wave of neutralizing antibodies in mice infected with foot-and-mouth disease virus (FMDV), a virus that produces acute infections, is characterized by the secretion of IgM and IgG3^{1,2}.

As previously mentioned, T helper cells are necessary to activate B cells in humans and to induce the class switch of immunoglobulins from IgM to IgG as part of the normal immune response. However, experiments done by researchers working with several viruses producing acute infection including influenza virus^{5,6} as well as the work in our lab with FMDV demonstrated that the early immune response against these viruses is T cell independent though there is switch to the IgG isotype^{1,2}. These experiments showed that the immune response induced by infection is different than the one elicited by vaccination with inactivated virus, which are typically T cell dependent. Nevertheless, vaccination with inactivated virus induces a weak and short-lasting antibody response compared to the strong and long-lasting antibody response induced by the infection. A better understanding of these different pathways involved in early and late immune responses to infection as well as the humoral responses to infection or inactivated vaccines may help design and produce more efficient next-generation vaccines to prevent future influenza infections.

Purpose and Aim

The purpose of this study was to analyze the role of DCs in the early immune response against infectious and inactivated influenza virus *A/California/07/2009 (H₁N₁pdm)* and to determine the isotype and IgG subclass responses to influenza vaccine in normal healthy donors.

The first specific aim of this study was to determine the expression of activation markers in DCs infected with H₁N₁, inactivated H₁N₁, and mock infected. This was completed by optimizing the following methods: propagation of influenza virus, titration of virus using hemagglutination assay, Tissue Culture Infectious Dose 50% assay (TCID₅₀), enrichment of monocytes from PBMCs, differentiation of monocytes to DCs, infection of DCs, and detection of different activation markers using flow cytometry.

We tested the hypothesis that DCs respond differentially to infectious or inactivated virus impacting the antibody response against virus presented by DCs.

The second specific aim of this research was to study the formation of different immunoglobulin isotypes both before and after vaccination of normal healthy subjects. For this purpose, a series of sandwich Enzyme Linked Immunosorbent Assays (ELISAs) were developed to determine the immune of total Immunoglobulin M, total IgG, and subclasses IgG1, IgG2, IgG3, and IgG4 and to develop H1 and H3 Influenza A specific ELISAs to study IgG Subclass generation post-vaccination.

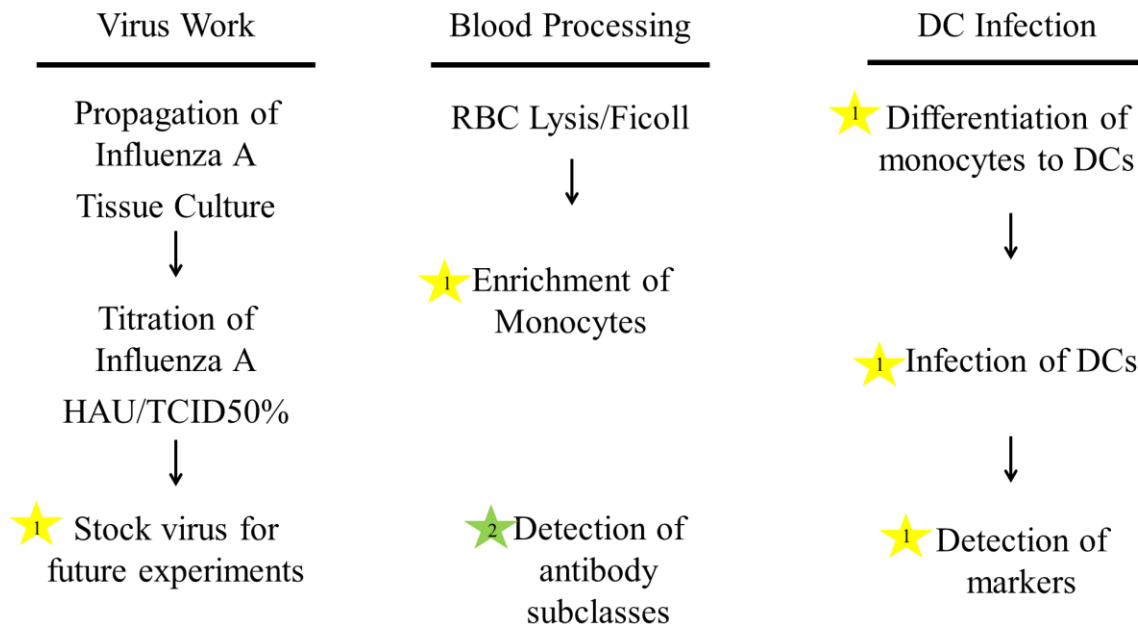


Figure 1: Experimental design for this thesis project. Numbers indicate which specific aim the protocol is related to.

Subjects

This study used healthy volunteers with no known clinical influenza infections in the past 2 years, under an approved IRB# 4884 (see appendix A for consent form).

Table 1: Subjects

Donor	Age at collection	Gender
A	23 years	Female
B	28 years	Male
C	22 years	Male
D	24 years	Male
E	23 years	Male
F	24 years	Female
H	22 years	Male
I	60 years	Female
L	49 years	Female
S	24 years	Female

Chapter 1: Virus Work

Section 1: Propagation of Influenza Virus in Embryonated Chicken Eggs

1.1 Methods

Stock virus obtained from Influenza Reagent Resource (IRR) was propagated to produce enough virus stock for future experiments. Fertilized chicken eggs were obtained for this use (see Figure 2 for an overview). Each egg was candled to confirm the presence of a yolk, insure shell integrity, and location of the air sac. A piece of tape was placed on one side, and the eggs were laid tape up in an incubator at 37 degrees Celsius with a beaker of water at the bottom. Each morning at the same time eggs were candled to check for embryo growth, and turned 180 degrees. On day 10 or 11, eggs were candled again, and those with embryos were marked for the air sac location and placed into groups. Dilutions of stock virus were made in sterile 1% Pen-Strep HBSS. In a sterile hood, each embryonated egg was swabbed with 70% ethanol, allowed to dry, and a tiny hole was punched at the top where the air sac was. This hole was then swabbed with 70% ethanol again and allowed to dry. Once dried, 0.2 mls of viral dilution was injected at a 45 degree angle into the allantoic sac (0.1 to 0.01 HAU, see Figure 3). The hole was then swabbed with 70% ethanol, allowed to dry, and the hole taped and labeled. The eggs were placed back into the incubator for 48 hours and turned daily at the same time. After 48 hours eggs were placed at 4°C overnight to clot the blood. Allantoic fluid was collected in a sterile environment using a syringe. If a large volume was obtained,

the tubes were spun at 500xG at 4 degrees Celsius for 15 minutes to pellet the protein.

The supernatant was collected, aliquoted and stored at -80 degrees Celsius.

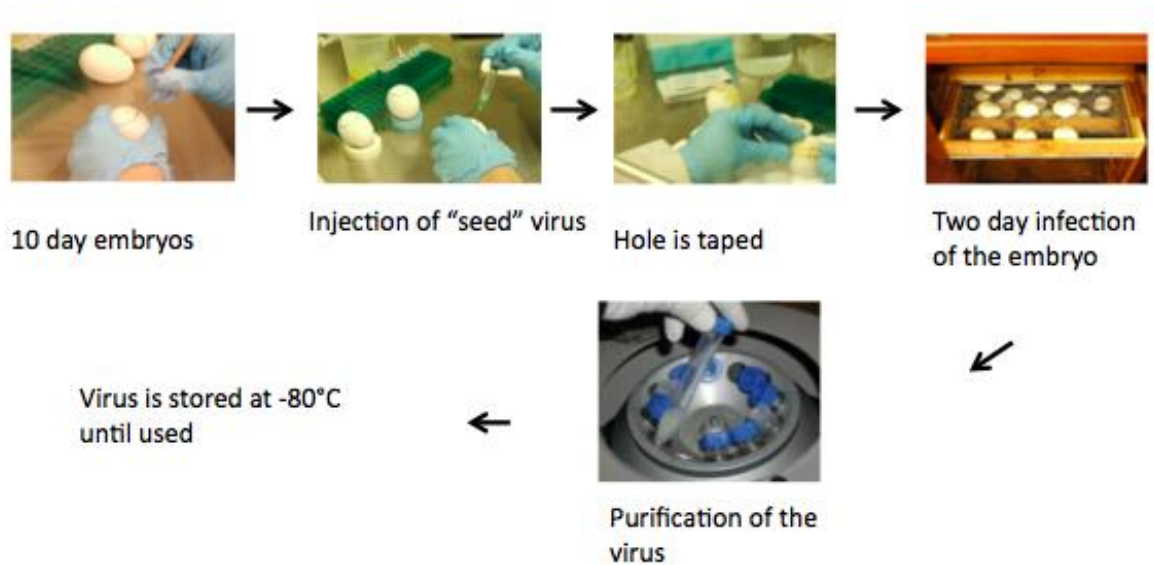


Figure 2: Propagation of Influenza A in embryonated chicken eggs.
Overview of methods.

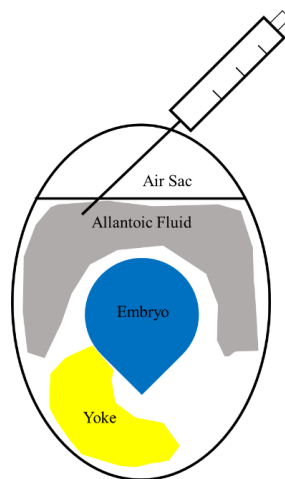


Figure 3: Injection of virus into chicken egg.
Needle was inserted at an angle to ensure that virus was injected into the allantoic fluid and not the embryo.

1.2 Results

Allantoic fluid was collected according to the protocol described, and frozen at -80 degrees Celsius. Virus presence was determined by using a Hemagglutination Assay (HA), as described in section 3. Because virus propagation in embryonated chicken eggs did not produce consistent results, propagation of virus was assayed in MDCK cells.

Section 2: Propagation of Influenza Virus in Madin Darby Canine Kidney-ATL cells (MDCK)

2.1 Methods

MDCK cells were grown in Dulbecco's Modified Essential Medium (DMEM) with 5-10% fetal calf serum (FCS). FCS was heat inactivated by incubation at 56 degrees Celsius for 40 minutes. The original cell line was obtained from the Influenza Reagent Resource. This was thawed and diluted into a final volume of 10 mls of DMEM-10%FCS and washed twice at 250xG for 5 minutes at room temperature. The cell pellet was resuspended in 5 mls of DMEM-10%FCS and placed in a 25cm² tissue culture flask and allowed to grow to confluence. Once confluent, cells were detached by using 0.25% Trypsin solution (Thermo Scientific CAT# SH30042.02). A stock of cells from the second passage was frozen back for future use. Briefly, cells were pelleted by spinning at 250xG for 5 minutes at room temperature. The supernatant was removed and the cell pellet was resuspended in 10% Dimethyl Sulfoxide (DMSO) DMEM-20% solution at a concentration of 1 million cells per ml and dispensed into 1 ml aliquots in cryo-vials. These tubes were stored at -80 degrees Celsius for 2 days, then transferred to liquid nitrogen for long term storage. Once cells reached a passage of 30, a new vial of fresh cells was thawed and used.

For infection, MDCK-ATL cells were grown to confluence in a 75cm² tissue culture flask, see Figure 4 for an image on the growth of the cell line. Once at confluence the growth media was removed and the monolayer washed two times with 5 mls sterile Hank's Balanced Salt Solution (HBSS) with 1% Pen Strep at room temperature. The virus samples were diluted in Influenza Virus Growth Media (0.1 HAU-0.0001 HAU). Each flask was inoculated with 1 ml of virus dilution and rotated so solution covered the monolayer. Flasks were incubated at 37 degrees Celsius with 5% CO₂ for one hour and rotated every 15 minutes to ensure the monolayer did not dry out. After inoculation, 14 mls of DMEM-5%FCS was added to each flask, and returned to the incubator. Cytopathic effect (CPE) was observed daily, and when 75% of the cell monolayer had rounded up and detached the supernatant was removed. Supernatant was spun at 250xG for 20 minutes to pellet cellular debris and the clarified supernatant was aliquoted and frozen at -80 degrees Celsius.

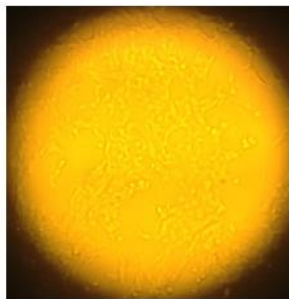


Figure 4: MDCK-ATL cells in growth phase before reaching confluence

2.2 Results

Cytopathic effect (CPE) was observed in the flasks inoculated with H₁N₁ virus usually on day 3 of infection compared to the controls. CPE in this project is seen when the cell monolayer begins to round up and detach. When 75% or more of the cells exhibited CPE, the supernatant was collected and purified according to the protocol. Virus was quantified using a Tissue Culture Infectious Dose 50% Assay (TCID₅₀), and a Hemagglutination Assay (HA), as described in section 3. H₁N₁ was easily propagated in tissue culture. As described, dilutions of the stock virus were infected to the MDCK cell monolayer, and 0.01 HAU of H₁N₁ was determined to be optimal for viral propagation after the initial experiment (see Figure 5) and used in all remaining propagations. Figure 6 shows an example of an optimized propagation of H₁N₁ done in tissue culture. On Day 3 CPE was seen, and the virus was collected.

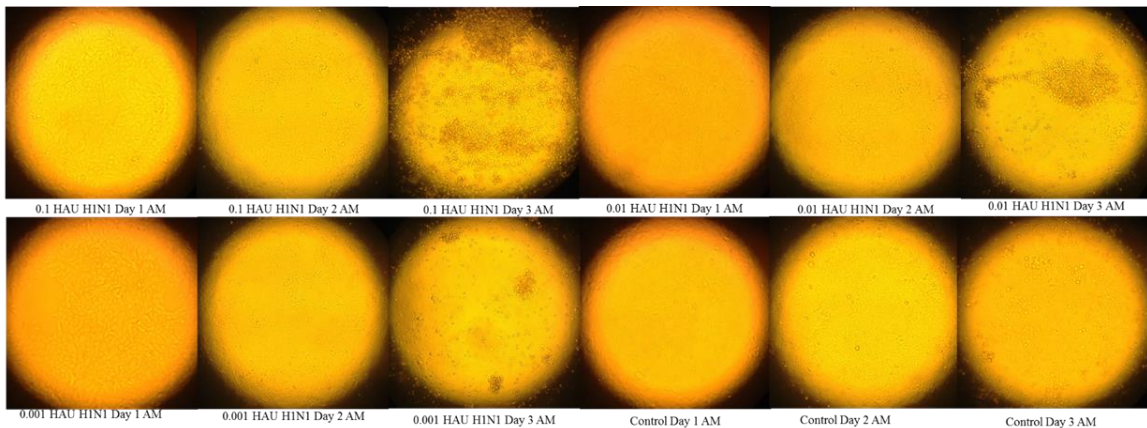


Figure 5: Propagation of H₁N₁ in MDCK-ATL cells with different dilutions of stock virus, 0.01 HAU of H₁N₁ was found to be optimal, and used for all subsequent infections.

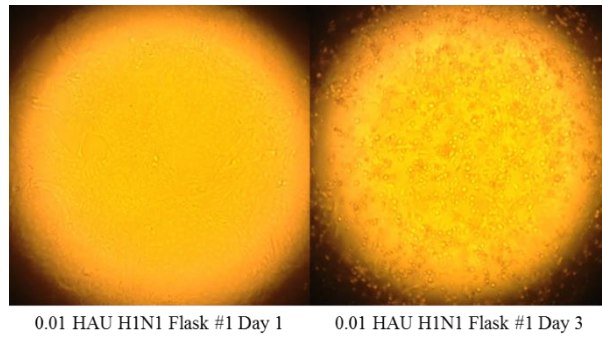


Figure 6: Propagation of H₁N₁ in MDCK-ATL cells. Typical CPE observed on day 3. Multiple flasks/propagations completed until enough stock virus was produced for future experiments.

Propagation of H₃N₂ was not as efficient in tissue culture when compared to H₁N₁. This can be seen by the low amount of CPE in H₃N₂ infected samples in Figure 7. Because H₃N₂ did not propagate well in tissue culture, it was not used for this thesis work.

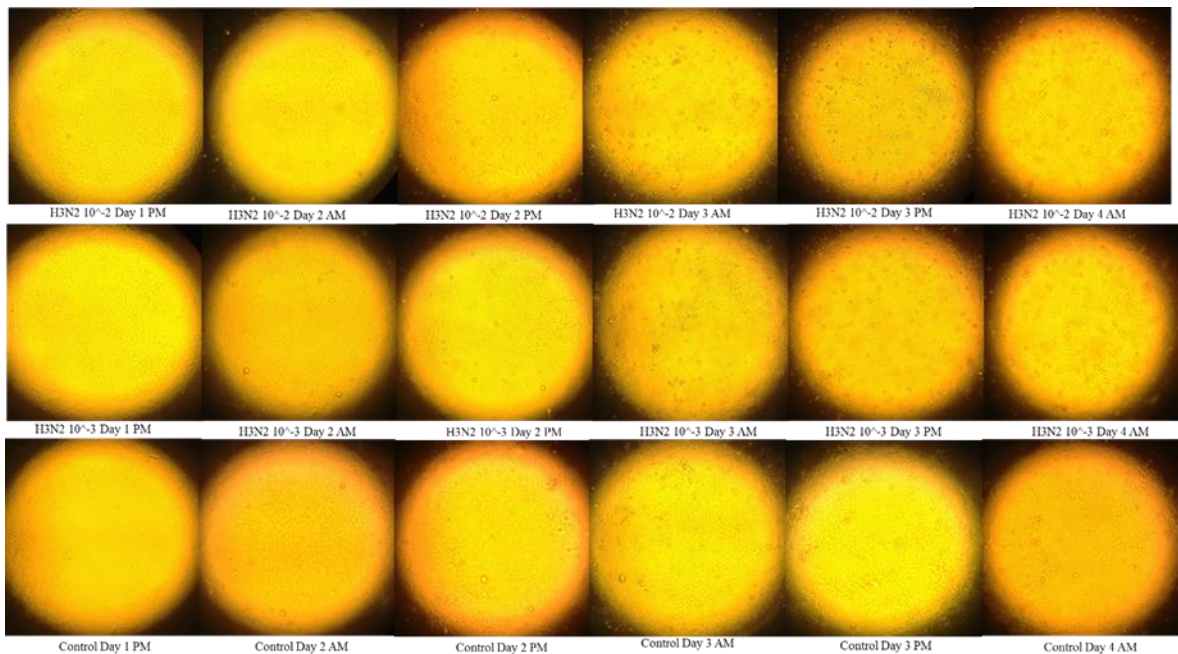


Figure 7: H₃N₂ did not propagate well in MDCK cells, as seen by the low amount of CPE compared to the control through day 4

In conclusion, H₁N₁ was propagated in MDCK cells, as seen in Figure 5 and 6. H₃N₂ did not show any CPE when propagated in MDCK cells, as seen in Figure 7.

In order for a productive infection to be produced, the virus must be released from the host cell. HA must be cleaved and the NA must be released, as described in the introduction. MDCK cells lack the protease needed to cleave HA into the two subunits. By adding tosyl-phenylalanyl-chloromethyl ketone (TPCK)-Treated Trypsin, the HA can now be cleaved, and a productive infection can occur²².

Section 3: Titration of Virus using Hemagglutination

3.1 Methods

A 1% Turkey red blood cell (TRBCs) or chicken red blood cell solutions were prepared from a stock 5% solution in cold Alsever's solution. A white 96 well round bottom plate was used to make viral dilutions. Fifty microliters of 1x Phosphate Buffered Saline (PBS) were dispensed in each well. One row served as controls, receiving no virus but vehicle. In the first column 50 µl of virus sample being tested was added to make the first 1:2 dilution. A multichannel pipette was used to mix the well 5 times. Two fold dilutions were performed, mixing between each step. Fifty microliters of 1% TRBCs were then added to each well. The plate was covered, and placed at 4 degrees Celsius 45 minutes or until agglutination of the blood was observed.

Hemagglutination assay determines the number of particles present per unit volume of the virus, but it does not determine if the particles are infectious. The viral hemagglutinin protein attaches to the RBCs and binds or agglutinates them, preventing them from settling out of suspension and forming red cell agglutination or cell button. This button can be seen in the negative control in Figure 8, where the RBCs have pooled

to the bottom of the well making a red circle. RBCs not bound by virus sink to the bottom. This is shown in Figure 8. The dilution demonstrating agglutination is one hemagglutination unit or HAU.

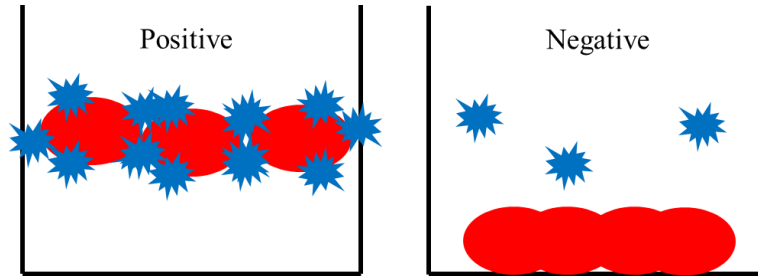


Figure 8: HA assay. Hemagglutination occurs when virions and red blood cells bind together, and produce a net. As a consequence of the net, the virions and red blood cells remain in suspension. A negative result is detected when there is not enough virus present to agglutinate the RBCs, which sink to the bottom of the well creating a distinct red button.

3.2 Results

Stock virus from the IRR was shipped with no reported concentration of total virus particles. HA assay was used for the stock virus strains to determine the starting amount of virus that was used to propagate in MDCK cells, as described previously in this chapter. For influenza virus, 1 HAU= 10^6 virus particles⁴². The HAU titer was determined for both H₁N₁ and H₃N₂ stock vial strains from the IRR. For H₁N₁ the 1:32 dilution of virus was 1 HAU. For H₃N₂ the 1:128 dilution of virus was 1 HAU.

One example of typical results can be seen in Figure 9. The last dilution that the TRBCs are still being held into suspension (no button) is seen at a 1:64 dilution of the virus for this example. A 1:64 dilution of the propagated virus was 1 HAU, or 10^6 total viral particles.

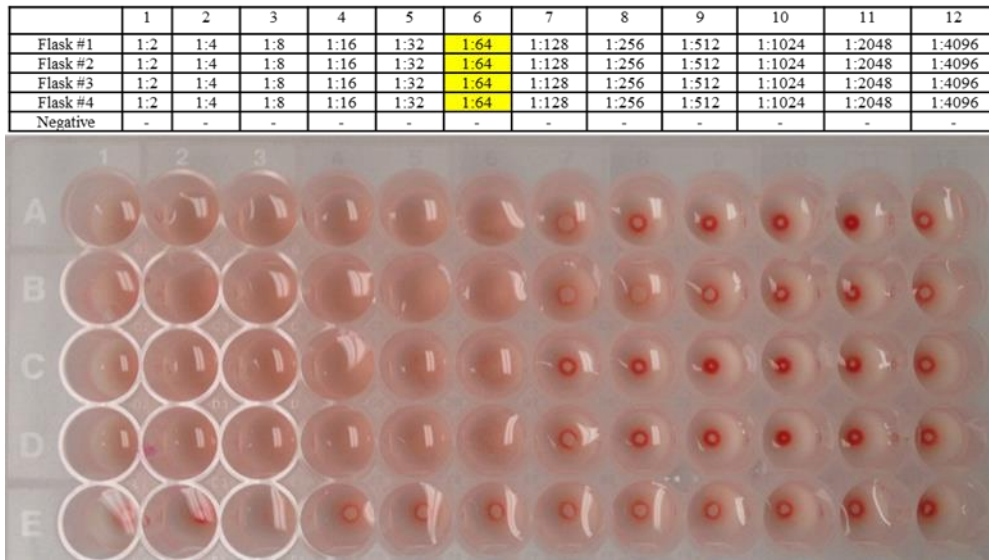


Figure 9: HA assay of H₁N₁ propagated in MDCK cells. The endpoint was 1:64 dilution, thus the titer of the virus is 64 HAU. The last row was a negative control that received no virus.

The H₃N₂ virus did not show CPE during the propagation in MDCK cells, as previously stated. When a HA assay was completed on the supernatant from this propagation, all results were negative, as seen in Figure 10. This confirmed the results seen in Figure 7, and H₃N₂ was not able to be grown in this way.

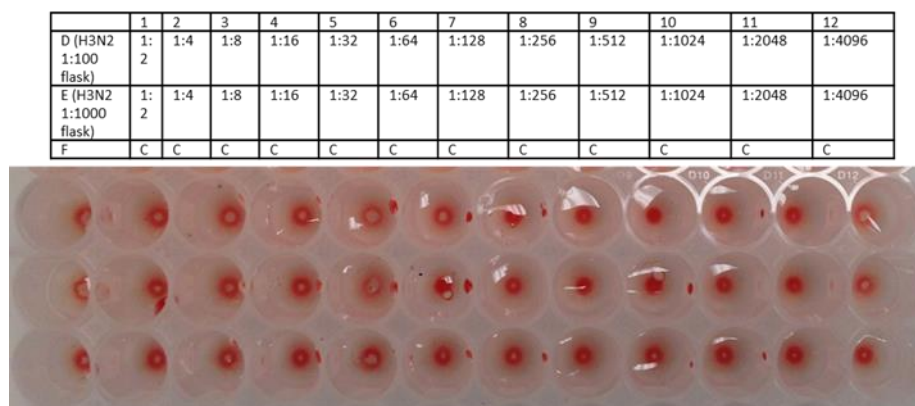


Figure 10: HA assay of H₃N₂ propagation in MDCK cells. The first two rows contained dilutions of the media from the propagation. The last row (F) was a negative control that just received buffer. All results were negative, indicating that there was no virus present and H₃N₂ was not propagated using this method.

In conclusion, the HA assay detects total virus particles of H₁N₁ propagated in MDCK cells, which confirmed the presence of virus after propagation and CPE that was seen as seen in Figure 9. The assay did not detect virus particles in the propagation of H₃N₂ in tissue culture. CPE was also not seen for this virus, confirming these negative results, as seen in Figure 10.

Section 4: Titration of Virus using Tissue Culture Infectious Dose 50% Assay

4.1 Methods

A TCID₅₀ assay was used with a MDCK-ATL cell line following established protocols²². This assay determines the number of infectious viral particles per milliliter. Briefly, cells were seeded into a 96 well plate and allowed to attach for 24 hours. Viral dilutions were performed in viral dilution media of 1% Pen Strep 1ug/ml tosyl-phenylalanyl-chloromethyl ketone (TPCK)-Treated Trypsin 1xDMEM. Media was

removed from each well and washed once with 100 μ l of 1% Pen Strep HBSS. One hundred microliters of viral dilutions were added down each column to inoculate the monolayer, seen in Table 2. Plates were placed in the incubator at 37 degrees Celsius 5% CO₂ for 45 minutes. Once infection had occurred, 100 μ l of DMEM-5%FCS was added to each well, and CPE was observed daily for four to seven days, or until 75% of the cells showed CPE. Once completed, the Reed Muench Method for approximation of TCID₅₀% was used to calculate the titer of the virus.

Table 2: Example plate set up for a TCID₅₀% Assay. Each sample was diluted and added in a set of six across an entire plate. Each column was a 1:10 dilution. An additional plate for each experiment was done with no virus as a negative control.

	1	2	3	4	5	6	7	8	9	10	11	12
A	10 ⁻²	10 ⁻³	10 ⁻⁴	10 ⁻⁵	10 ⁻⁶	10 ⁻⁷	10 ⁻⁸	10 ⁻⁹	10 ⁻¹⁰	10 ⁻¹¹	10 ⁻¹²	10 ⁻¹³
B	10 ⁻²	10 ⁻³	10 ⁻⁴	10 ⁻⁵	10 ⁻⁶	10 ⁻⁷	10 ⁻⁸	10 ⁻⁹	10 ⁻¹⁰	10 ⁻¹¹	10 ⁻¹²	10 ⁻¹³
C	10 ⁻²	10 ⁻³	10 ⁻⁴	10 ⁻⁵	10 ⁻⁶	10 ⁻⁷	10 ⁻⁸	10 ⁻⁹	10 ⁻¹⁰	10 ⁻¹¹	10 ⁻¹²	10 ⁻¹³
D	10 ⁻²	10 ⁻³	10 ⁻⁴	10 ⁻⁵	10 ⁻⁶	10 ⁻⁷	10 ⁻⁸	10 ⁻⁹	10 ⁻¹⁰	10 ⁻¹¹	10 ⁻¹²	10 ⁻¹³
E	10 ⁻²	10 ⁻³	10 ⁻⁴	10 ⁻⁵	10 ⁻⁶	10 ⁻⁷	10 ⁻⁸	10 ⁻⁹	10 ⁻¹⁰	10 ⁻¹¹	10 ⁻¹²	10 ⁻¹³
F	10 ⁻²	10 ⁻³	10 ⁻⁴	10 ⁻⁵	10 ⁻⁶	10 ⁻⁷	10 ⁻⁸	10 ⁻⁹	10 ⁻¹⁰	10 ⁻¹¹	10 ⁻¹²	10 ⁻¹³

4.2 Results

A TCID₅₀% assay must be completed to determine if the viral particles are infectious. Wells were checked daily and marked when CPE was visible. For H₁N₁, CPE was typically seen by day 3. The most concentrated virus dilutions showed CPE early, while the wells containing the most diluted virus (10⁻¹³) did not show CPE compared to the control, indicating that the virus was too dilute for productive infection in MDCK cells. Figure 11 shows typical results of a TCID₅₀% assay completed on the H₁N₁ virus propagated in MDCK cells. CPE is clearly visible on day 3, indicating that infectious virus are present.

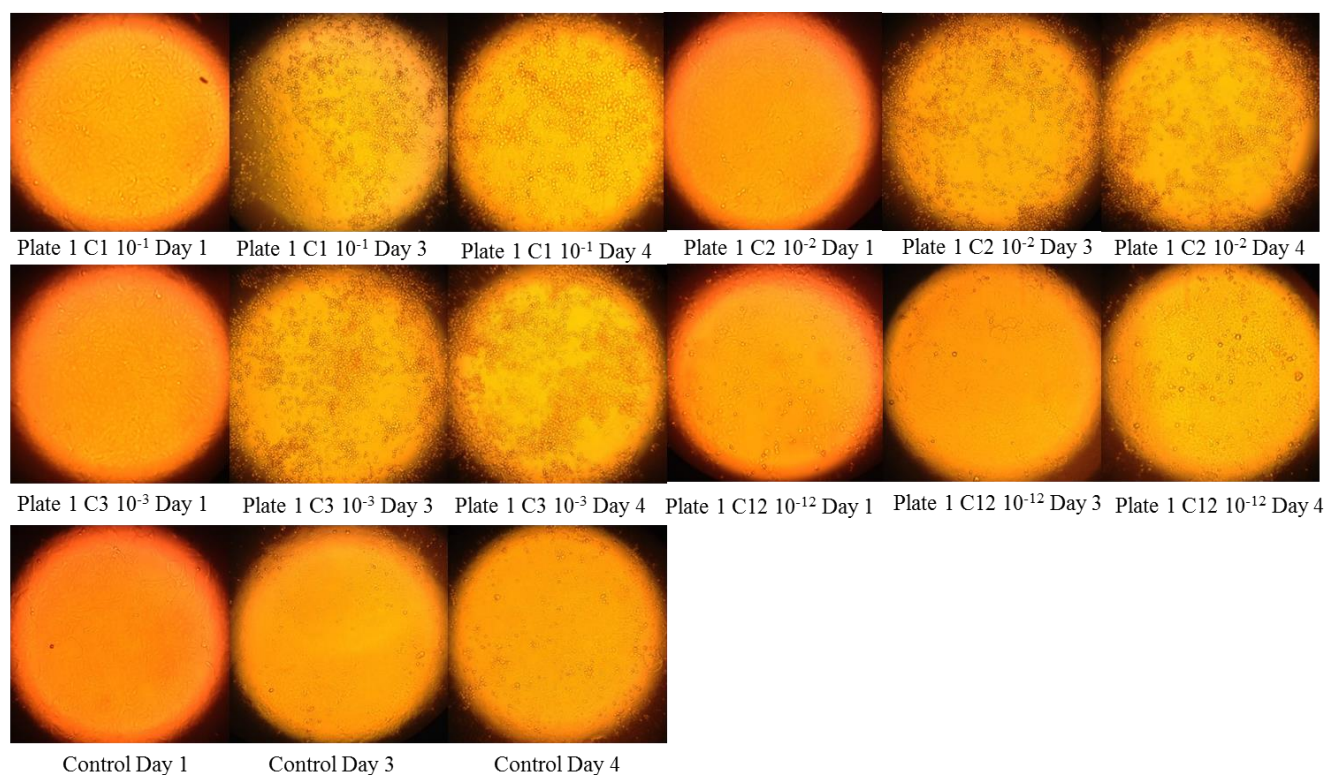


Figure 11: TCID50% results from propagation of H₁N₁ in MDCK cells. CPE is clearly visible on day 3 in wells incubated with the most concentrated virus, but absent in wells with more dilute virus (10^{-12}) or the negative control. CPE indicates the presence of infectious virus.

Once the results from the TCID50% assay have been obtained, the concentration of infectious particles can be determined. The Reed Muench Method for approximation of TCID50% was used to calculate the titer of the virus²². Briefly, the number of wells showing CPE for each dilution of virus was recorded daily. After the assay was completed the percent infected at each dilution was calculated. The proportional distance formula was used to calculate the log of the infectious dose for the virus. This calculation was used in conjunction with the inoculate volume to determine the Infectious Dose 50% per unit volume for each virus. Below is an example of how this is calculated.

Log of Virus dilution	Infected samples	Cumulative positive (A)	Cumulative negative (B)	Ratio of A/(A+B)	Percent infected
-2	6	6	0	6/6	100%
-3	6	6	0	6/6	100%
-4	4	4	2	4/6	66.7%
-5	2	2	4	2/6	33.3%
-6	0	0	6	0/6	0%
-7	0	0	6	0/6	0%
-8	0	0	6	0/6	0%
-9	0	0	6	0/6	0%
-10	0	0	6	0/6	0%
-11	0	0	6	0/6	0%
-12	0	0	6	0/6	0%
-13	0	0	6	0/6	0%

Proportional Distance Formula= [(% positive value >50%)-50%]/ [(% positive value >50%)-(% positive value <50%)]

Log infectious dose₅₀= (log dilution >50%) + (proportional distance x log dilution factor)

Proportional Distance Formula= (66.7%-50%) / (66.7%-33.3%) = 0.5

Log infectious dose₅₀= -4+ (0.5x1) = -4.5

Infectious dose 50 % titer: $10^{4.5}$ ID₅₀/0.1ml or $10^{5.5}$ ID₅₀/ml

Stock virus from the IRR was shipped with no reported concentration of total virus particles. HA assay was used for the stock virus strains to determine the starting amount of virus that was used to propagate in MDCK cells, as described previously in this chapter. A TCID₅₀ assay was then completed to determine how many of these particles were infectious. The ID₅₀/ml was calculated for each virus stock. Once determined, the plaque forming units per milliliter can be calculated by using the Poisson Distribution³³. Table 3 shows the titer determined by using these methods in the influenza stock vials from the IRR. H₃N₂ had almost four times more total viral particles,

as seen by a HAU titer of a 128 versus a 32 in H₁N₁. However, H₃N₂ has less infectious particles with a titer of 3.9x10⁴ PFU/ml versus H₁N₁ titer of 3.9x10⁵ PFU/ml. This shows that the virus stocks of H₃N₂ had far more noninfectious particles than H₁N₁.

Table 3: Concentration of virus in stock vials from the IRR, determined by HA assay and TCID₅₀% assay

Virus Stock	1 HAU	ID ₅₀ /ml	PFU/ml
H ₁ N ₁ Stock Vial #1	1:32	10 ^{5.5} ID ₅₀ /ml	2.2 x10 ⁵ PFU/ml
H ₁ N ₁ Stock Vial #2	1:32	10 ^{5.75} ID ₅₀ /ml	3.9x10 ⁵ PFU/ml
H ₃ N ₂ Stock Vial #1	1:128	10 ^{4.75} ID ₅₀ /ml	3.9x10 ⁴ PFU/ml
H ₃ N ₂ Stock Vial #2	1:128	10 ^{4.6} ID ₅₀ /ml	2.8x10 ⁴ PFU/ml

For use in future experiments, H₁N₁ virus was propagated several times to obtain a virus stock that could be frozen back. Six flasks could be completed at once. Flasks that had the same HA titer could be pooled together to minimize storage space. Table 4 shows the titer obtained by propagating H₁N₁ in several sequential propagations.

Table 4: Concentration of virus from propagation of H₁N₁ in MDCK cells, determined by HA assay and TCID₅₀% assay

Virus Propagation	1 HAU	ID ₅₀ /ml	PFU/ml
Propagation #1 0.1 HAU H ₁ N ₁	1:256	10 ^{6.4} ID ₅₀ /ml	1.76x10 ⁶ PFU/ml
Propagation #1 0.01 HAU H ₁ N ₁	1:128	10 ^{6.5} ID ₅₀ /ml	2.2x10 ⁶ PFU/ml
Propagation #1 0.001 HAU H ₁ N ₁	1:256	10 ^{5.25} ID ₅₀ /ml	1.2x10 ⁵ PFU/ml
Propagation #2 H ₁ N ₁ All Flasks	1:64	10 ^{6.66} ID ₅₀ /ml	3.2x10 ⁶ PFU/ml
Propagation #3 H ₁ N ₁ Flasks 1, 2, 5, and 6	1:64	10 ^{6.65} ID ₅₀ /ml	2.2x10 ⁶ PFU/ml
Propagation #3 H ₁ N ₁ Flasks 3 and 4	1:32	10 ^{6.34} ID ₅₀ /ml	1.53x10 ⁶ PFU/ml
Propagation #4 H ₁ N ₁ Flasks 1, 3 and 6	1:64	10 ^{6.66} ID ₅₀ /ml	3.2x10 ⁶ PFU/ml
Propagation #4 H ₁ N ₁ Flasks 2 and 4	1:128	10 ^{7.66} ID ₅₀ /ml	3.2x10 ⁷ PFU/ml
Propagation #5 H ₁ N ₁ Flasks 1 and 2	1:64	10 ^{6.25} ID ₅₀ /ml	1.2x10 ⁶ PFU/ml
Propagation #5 H ₁ N ₁ Flasks 4, 5, and 6	1:128	10 ^{6.25} ID ₅₀ /ml	1.2x10 ⁶ PFU/ml

In conclusion, the TCID₅₀% assay was used to find the concentration of infectious particles in the stock vials of virus from the IRR, as well as in each of the propagations completed for H₁N₁ in tissue culture. The titer obtained on the stock vials showed that H₁N₁ had a higher titer of infectious particles (3.9×10^5 PFU/ml), than H₃N₂ (3.9×10^4 PFU/ml). The HA Assay showed that H₃N₂ had four times more total particles as seen in Table 3. This shows that H₃N₂ stock had more defective particles than H₁N₁. The titer obtained for H₁N₁ propagated in MDCK cells after optimization ranged from 1.2×10^6 PFU/ml to 3.2×10^7 PFU/ml, as referenced in Table 4.

Chapter 2: Blood Processing and Analysis of Subclasses of Antibodies

In human peripheral blood 48-70% are neutrophils ($2.3-8.1 \times 10^3/\mu\text{l}$), 18-42% are lymphocytes ($0.8-4.8 \times 10^3/\mu\text{l}$), 1-10% are monocytes ($0.45-1.3 \times 10^3/\mu\text{l}$), 1-4% are eosinophils ($0-0.4 \times 10^3/\mu\text{l}$), and 0-2% are basophils ($0-0.1 \times 10^3/\mu\text{l}$)²⁰. We used Ficoll-Hypaque to isolate the mononuclear cells (monocytes and lymphocytes) from whole blood. This procedure separates the mononuclear cells from the red blood cells, neutrophils, and the plasma. The majority of these cells are lymphocytes (~60%) and the minority are monocytes (~30%). Lymphocytes consist of T cells and B cells. Red Blood Cell Lysis can also be used which removes the red blood cells only leaving the neutrophils and the mononuclear cells.

Section 1: Red Blood Cell Lysis

1.1 Methods

Whole blood was collected via venipuncture under approved IRB#4884 after obtaining informed consent. Blood was collected into sterile EDTA Vacutainer tubes. Blood was stored using approved methods at 4 degrees Celsius before use. Consent forms were securely maintained and donor samples labeled to insure anonymity. Only demographics such as gender and age were used for labeling. Proper personal protective equipment (PPE) was used at all times. Fifteen milliliter falcon tubes were prepared. 500 μl of whole blood was added to 10 mls of 1xRBC Lysis Buffer. Tubes were inverted to mix and incubated at room temperature in the dark for 15 minutes. Every 5 minutes the tubes were inverted and checked for turbidity. After the incubation was complete, the

tubes were spun at 250xG for 5 minutes at room temperature. The supernatant was decanted into a 20% bleach solution. The cell pellet was dislodged and resuspended in 10 mls of cell buffer (1% BSA 1mM EDTA 1xPBS). The cells were spun at 250xG for 5 minutes at room temperature. After the wash, cells were resuspended in 3 mls of cell buffer. Then cells were counted using a hemocytometer according to published protocols²⁰. Once cells were counted, aliquots were taken for flow analysis. Each sample was incubated with the appropriate labeled antibodies and was prepared in a final volume of 100 µl in the cell buffer per manufacturer's directions. At least 300,000 cells were aliquoted for labeling, mixed with the labeled monoclonal antibodies and incubated on ice in the dark for 30 minutes. Then samples were washed twice with 400 µl of cell buffer and centrifuged at 400xG for 5 minutes at 4 degrees Celsius. If a secondary antibody was needed (streptavidin) pellets were resuspended in 95 µl of cell buffer and 5 µl of the fluorphore conjugated to streptavidin. These tubes were incubated and washed as previously described. All samples prepared for flow cytometry analysis were pelleted after the last wash and resuspended in 200 µl of 1% paraformaldehyde (PFA) 1mM EDTA 1xPBS. Samples were analyzed using an Accuri C6 Flow Cytometer and CFlow Plus or FCS Express V3 software according to the manufacturer's guidelines.

The flow cytometer used in this thesis is a BD Accuri C6 Flow Cytometer System. It contains two lasers, a blue (488nm), and a red (640nm). It also has two light scatter detectors for side and forward scatter, and four fluorescence detectors. The forward scatter detector indicates relative size of the cells, and the side scatter detector indicates complexity of the cells. Relative forward and side scatter can differentiate between different cell types such as small lymphocytes versus larger and more granular monocytes

in a mononuclear cell sample. Different monoclonal antibodies can be purchased, that are conjugated to different flurophores. The flurophore absorbs light from the lasers, then emits light that is detected by one of the four different detectors. These detectors separate out the emitted light based on its wavelength. Based on this data, a researcher can determine cell types and concentrations in each sample based on the antibody used which is conjugated to a particular flurophore³⁸. In this flow cytometer system, FL1 is the 533/30 detector for Fluorescein Isothiocyanate (FITC), Phycoerythrin (PE) is detected by FL2 with a filter of 585/40, Phycoerythrin-Cy7 Tandem (PE-Cy7) is detected by FL3, with a filter of 670LP, and Allophycocyanin (APC) is detected by FL4 with a filter of 675/2539. For example, if Anti-Human CD19 APC is used for labeling in a mononuclear cell sample, a positive peak on filter FL4 will be detected. The software assists in determining the percent of cells or events that are in the positive peak for FL4 in the entire sample, and by using a labeled monoclonal antibody, a specific cell populations can be identified. For example cells positive for CD19 identifies B cell populations.

1.1 Results

Cells remaining after red blood cell lysis include the mononuclear cells and neutrophils from whole blood. Figure 12 shows three cell populations (neutrophils, monocytes, and lymphocytes) based on side and forward scatter. Neutrophils are the larger and more complex cells which make up the majority of the cell populations. For this thesis project, purification of the monocytes was necessary. Monocytes and neutrophils are both CD14+. In order to use CD14 in a way to facilitate this separation, the red blood cell lysis method could not be used, because of the neutrophil contamination.

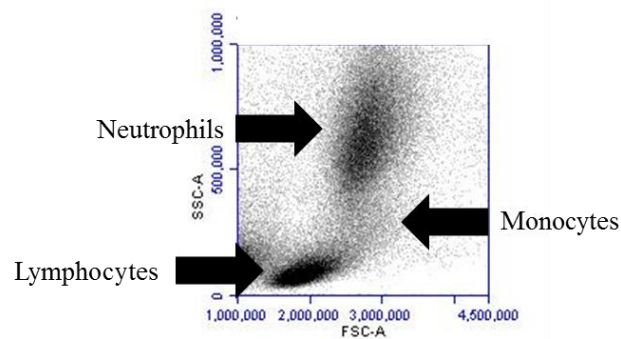


Figure 12: Side scatter and forward scatter of cells from a red blood cell lysis. Three populations are shown, the lymphocytes, monocytes, and neutrophils. The neutrophils are in the majority, and the largest and most complex.

Section 2: Ficoll-Hypaque Separation

2.1 Methods

Ficoll-Hypaque (Hystopaque 1077 Sigma-Aldrich) isolation of mononuclear cells from whole blood, non Accuspin assisted.

Blood was stored using approved methods at 4 degrees Celsius before use. Ficoll-Hypaque separation was performed according to manufacturer specifications⁴³. After separation, cells were counted using the hemocytometer and labeled for flow analysis as described earlier. Ficoll-Hypaque is a polymer that will separate out the mononuclear cells using a density gradient when centrifuged. The red blood cells and neutrophils are found on the bottom of the tube, Ficoll-Hypaque composes the next clear layer, and a white buffy layer is above the Ficoll-Hypaque that contains the cells of interest, with the plasma at the top as seen in Figure 13.

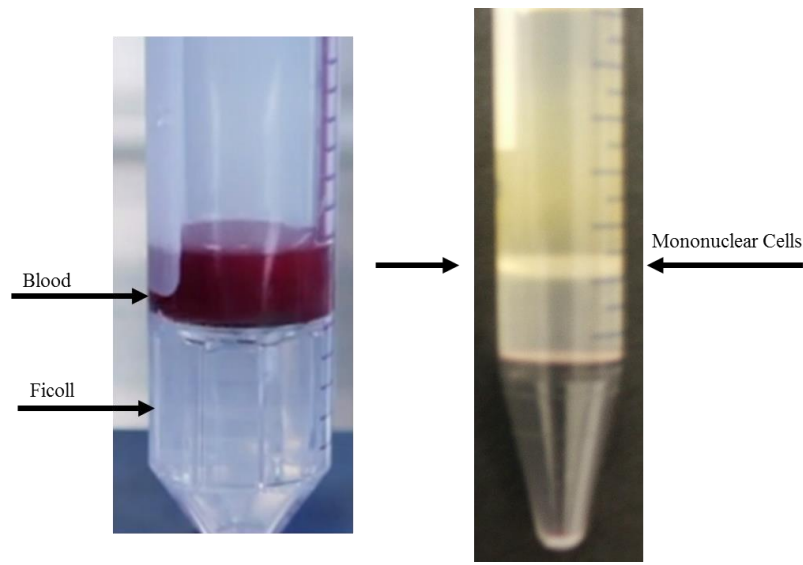


Figure 13: Before (left) and after (right) Ficoll-Hypaque separation of MNCs. After spinning MNCs are found above the Ficoll-Hypaque. Plasma is the top layer and red blood cells and neutrophils are at the bottom.

Ficoll-Hypaque (Hystopaque 1077 Sigma-Aldrich) isolation of mononuclear cells from whole blood, Accuspin assisted.

Whole blood was collected as described. A 50 ml tube holds 15 mls of Ficoll-Hypaque and 15 to 30 mls of undiluted blood. The 15 ml tube holds 3 mls of Ficoll-Hypaque and 3 to 6 mls of undiluted blood. Ficoll-Hypaque was pipetted into the Accuspin tube, and spun for 30 seconds at 800xG to move the Ficoll-Hypaque to the lower chamber below the frit. The Ficoll-Hypaque was then brought to room temperature on the bench while protected from light. Whole blood was poured into the Accuspin tube along the side, and spun for 15 minutes at 800xG. Once complete, the buffy layer was

retrieved, washed, and counted as previously referenced. The mononuclear cells are separated as previously described, and shown in Figure 14.

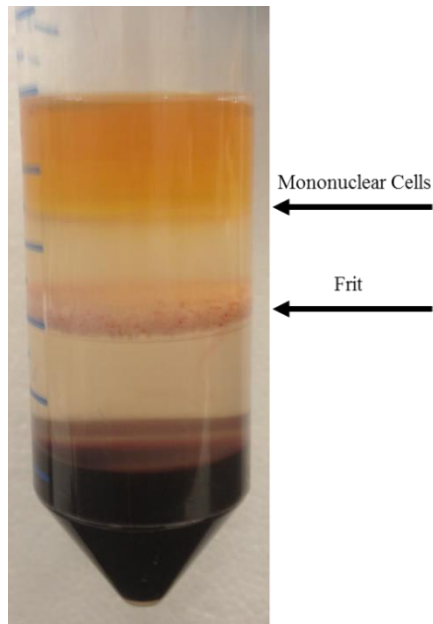
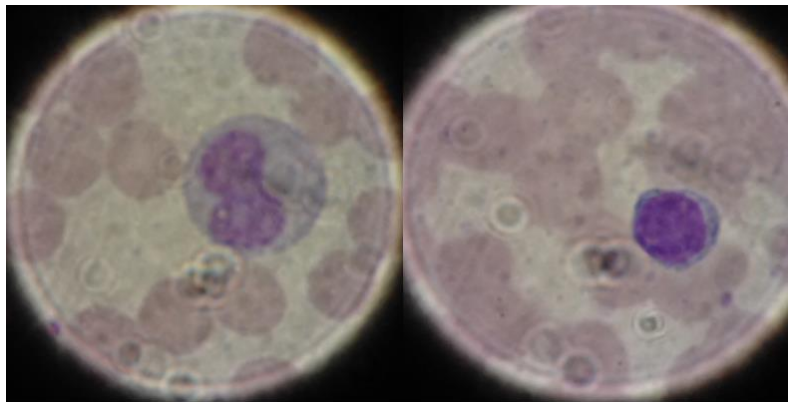


Figure 14: MNC separation with Accuspin tube. Mononuclear cells are above the Ficoll-Hypaque. Plasma takes up the top layer, and red blood cells and neutrophils make up the bottom.

Wright-Giemsa Stain

Wright Stain technique was used to visualize white blood cell populations during experiments. An aliquot of the cells was washed with 22% BSA, and then resuspended again in the 22% BSA. Five μl of whole blood or cells in BSA was added to each slide, and a smear was made. Once dried slides are dipped in the Wright Stain from the Thermo Scientific Modified Wright-Giemsa Stain Pack for 45 seconds, then dipped in the accompanying buffer solution containing phosphate salts for 30 seconds, then finally the

wash containing methanol for 5 seconds. A second type of Wright stain was obtained for use, Thermo Scientific Buffered Wright Stain. These slides were first fixed in methanol for 30 seconds, and then dipped in the stain for 30-60 seconds. Finally, the slides were rinsed in distilled water for 10 seconds and allowed to dry. A monocyte and lymphocyte visualized using this can be seen below in Figure 15.



Monocyte, Wright Stain

Lymphocyte, Wright Stain

Figure 15: Monocyte (left) and lymphocyte (right), visualized using Wright Stain in whole blood

2.2 Results

Ficoll-Hypaque facilitates isolation of the mononuclear cells, eliminating the contaminating neutrophils and enriches for a population of lymphocytes and monocytes only, as described in the methods section. Below in Figure 16 normal mononuclear cell populations can be seen after Ficoll-Hypaque separation. First, the side scatter and forward scatter is analyzed (graph 1 and 6), and the monocyte (P4) and lymphocyte (P3) populations are gated (graph 1) based on their size and complexity. These populations are graphed as average forward scatter (FSCA) vs forward scatter heights (FSCH) to

remove any doublets (graph 2 and 7). The remaining events are analyzed for populations of interest. Below, CD14+ cells represent monocytes (graph 3), CD3+ T cells (graph 4), CD4+ helper T cells, CD8+ cytotoxic T cells (graph 8), CD56+ natural killer cells (graph 5), and CD19+ B cells (graphs 3 and 4). These results are typical of a healthy donor.

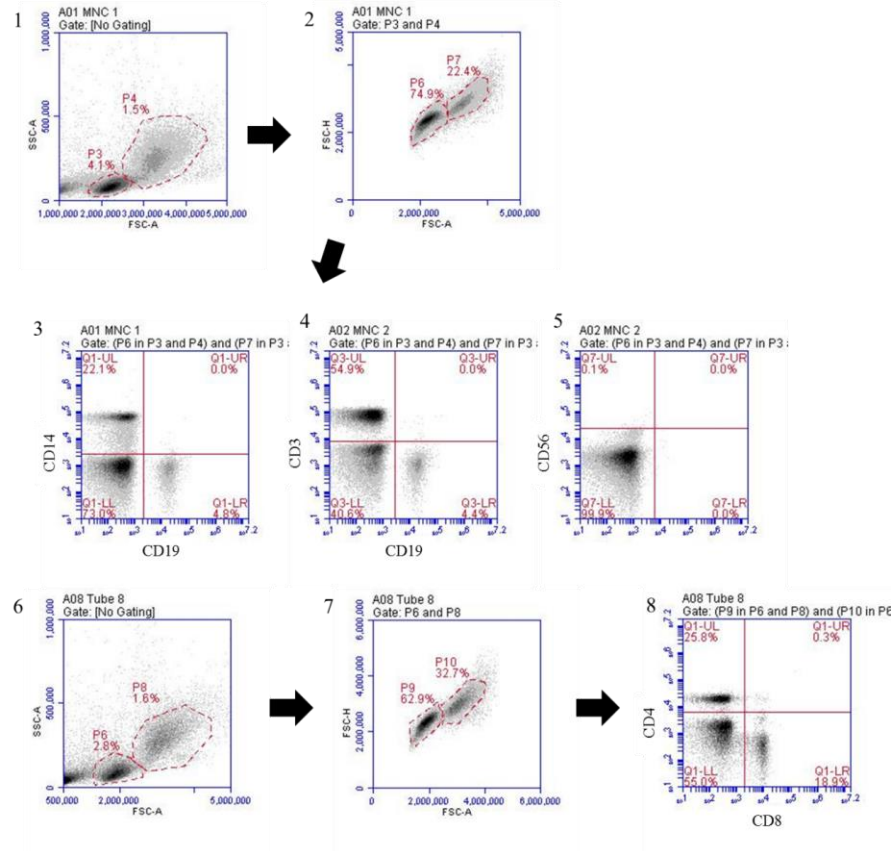


Figure 16: MNC populations after Ficoll-Hypaque separation. Graphs 1-5 Donor A, Graphs 6-8 Donor Q. CD14 is a monocyte marker, CD3 is a T cell marker, CD19 is a B cell marker, CD4 is a T helper cell marker, and CD8 is a cytotoxic T cell marker. Results represent typical cell populations in normal healthy donors.

In summary, Ficoll-Hypaque separation was used to separate mononuclear cells from whole blood. Flow cytometry was then used to study and quantify different cell populations like monocytes, T cells, and B cells. As seen in Figure 16 and described in the first paragraph of section 2, T cells make up the majority of the mononuclear cells

after Ficoll-Hypaque separation, 50-60% of cells are CD3+. In healthy individuals, CD4+ T cells make up the majority. The monocytes constitute the next prevalent cell type, with approximately 30% of the cell population expressing CD14+. B cells range from approximately 4-10% of all mononuclear cells and express CD19+. Natural killer cells may also be present, and will be CD56+, but are usually less than 2% of the mononuclear cells and not usually seen.

Section 3: B cell Subpopulations

3.1 Results

As described previously, our lab is interested in a B cell population known as the Marginal Zone B cells (MZBCs). MZBCs are IgD^{low} IgM^{high} CD27+ CD19+. These B cells are in the minority, making them difficult to analyze. Labeling for the MZBCs was completed and analyzed using flow cytometry. Data was analyzed as previously described. Cells were gated for CD19+ cells (B cell marker, graph 3), then graphed with IgD vs IgM (graph 4). The IgD^{low} IgM^{high} cells were then analyzed for the CD27+ marker. The MZBC population can be observed in Figure 17 below, graph 5. Cells of several different healthy donors were analyzed for MZBCs, seen in Table 5. Between 5-10% of the mononuclear cells were B cells, which is in the known range described at the beginning of this chapter. MZBCs made up between 5-11% of those B cells.

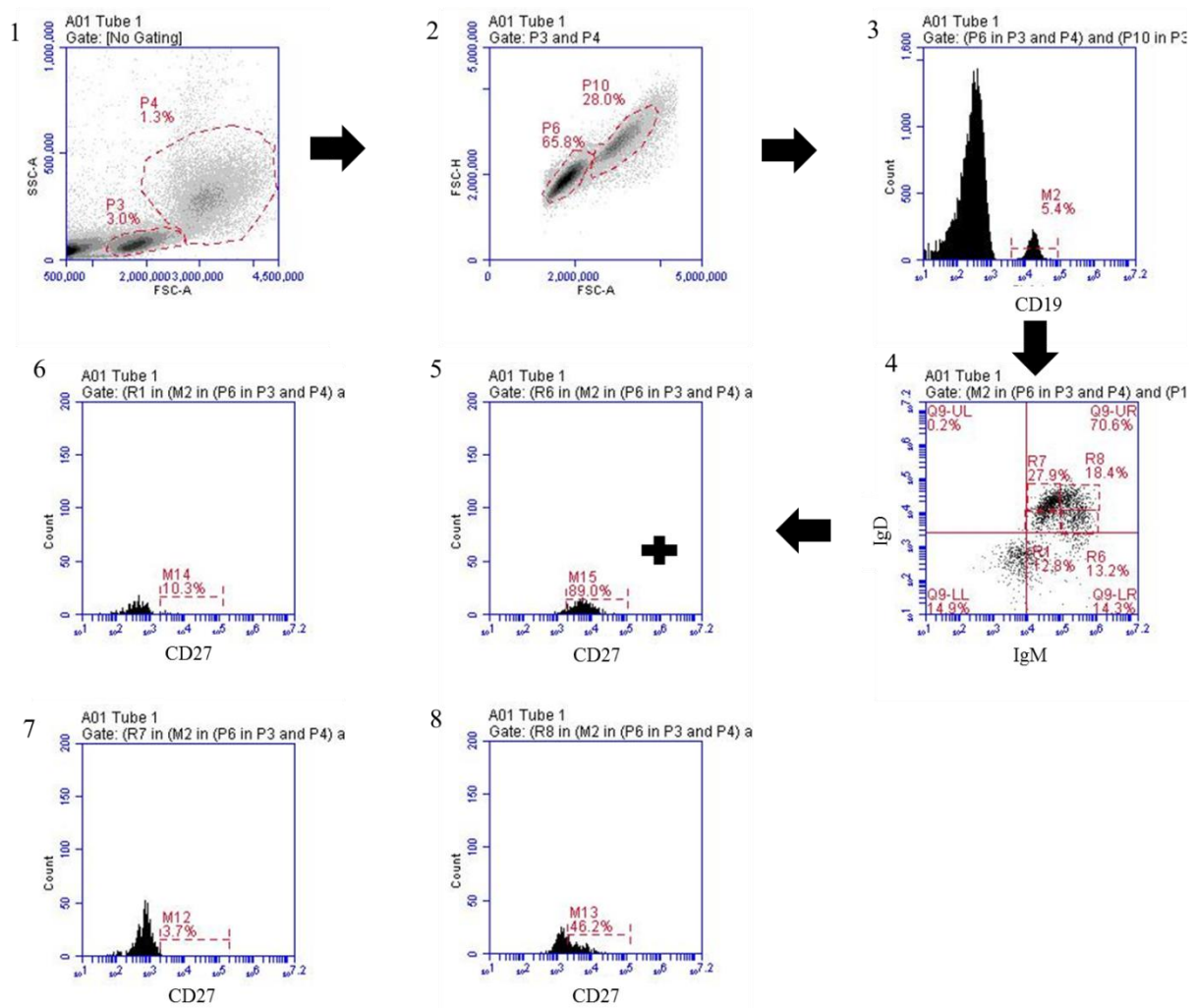


Figure 17: MZBC analysis, Donor A

Table 5: MZBC analysis from different donors

Donor	Percent CD19+ of monocyte and lymphocyte gate	Percent MZBCs of CD19+ cells
Donor Q, 10-31-12	8.3%	8.6%
Donor C, 11-6-12	7.9%	4.3%
Donor A, 11-19-12	6.7%	5.1%
Donor A, 3-12-14	5.4%	11.7%

Once the flow cytometry analysis was performed for a normal healthy donor population, a sample was obtained from a patient with recurrent infections (IBC protocol

#211). Preliminary data indicate that 2% of the mononuclear cells were B cells, less than half of what is seen in the healthy donors. However the MZBCs from this patient, though low compared to healthy donors, was found to be normal relative to the total number of B cells present when compared to the healthy donors (3.5%).

Along with MZBCs, other B cell populations can be analyzed using this method. As described in Figure 18, Naïve B cells shown in green are IgD^{high} IgM^{low} CD27- (graph 7). Memory B cells shown in blue are CD27+ (graph 5).

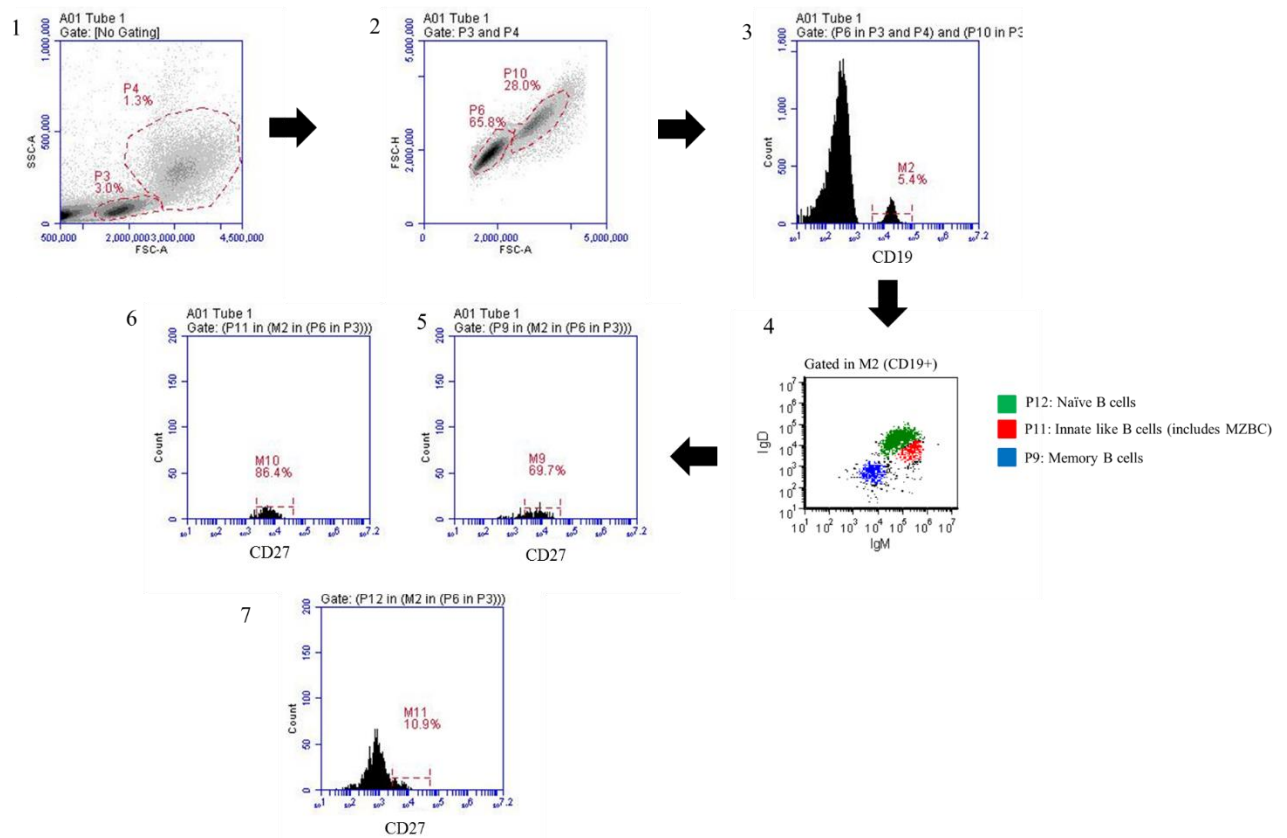


Figure 18: B cell populations, Donor A

In summary, using the optimized method different populations of B cells, including MZBCs, Naïve B cells, and Memory B cells, can be identified and analyzed. B

cells on average made up 4-10% of the mononuclear cells, with MZBCs making up 5-11% of the B cell population. This will be used for future experiments studying the interaction of B cells and infected DCs.

Section 4: Enrichment of Monocytes from Mononuclear Cells

4.1 Methods

Monocytes can be differentiated into DCs in culture using interleukin 4 (IL-4) and granulocyte macrophage colony-stimulating factor (GM-CSF). DCs are used in this thesis as a model for influenza virus infection *in vitro*.

Mononuclear cells were separated from whole blood as described previously. Ten microliters of Anti-Human CD14 Biotin (eBioscience) was diluted into 90 μ l of cell buffer and kept on ice. Mononuclear cells were pelleted and resuspended in the presence of the antibody and incubated on ice in the dark for 30 minutes. After incubation cells were washed twice with 1 ml of labeling buffer at 400xG for 10 minutes at 4 degrees Celsius. The pellet was then resuspended in 90 μ l of labeling buffer and 10 μ l of Miltenyi Biotec Streptavidin MicroBeads (10 μ l of beads for 10^7 target cells). The beads were thoroughly mixed with cells, and incubated on ice in the dark for 15 minutes. After the incubation period cells were washed with 1 ml of labeling buffer at 400xG for 10 minutes at 4 degrees Celsius. The final pellet was resuspended in 500 μ l of cold separation buffer. A prepared magnetic column apparatus and sterile MS column was removed from the -20 degree Celsius freezer. The MS column for positive selection could hold a max of 2×10^8 total cells, see Figure 19 for an overview of this process. The MS column was purged with 500ul of cold separation buffer. Once purged, 500ul of cells with the microbeads was added to the column before it went dry, and allowed to

flow through into a 1.5 ml tube. The cell prep was passed through the column twice. Subsequently, 500 µl of additional cold separation buffer was added to rinse the column, and repeated two more times. The flow through volume collected from the column was the unlabeled cell fraction. The column was then removed from the magnetic field, and one milliliter of cold separation buffer was added to the column and quickly plunged. This process removed all of the labeled cells (CD14+) from the column. This cell population was then collected in another 1.5 ml tube. Cells were counted and labeled as described above. Antibodies used included: CD14, CD3, CD56, CD19, CD80, CD11c, and HLA-DR (MHC Class II).

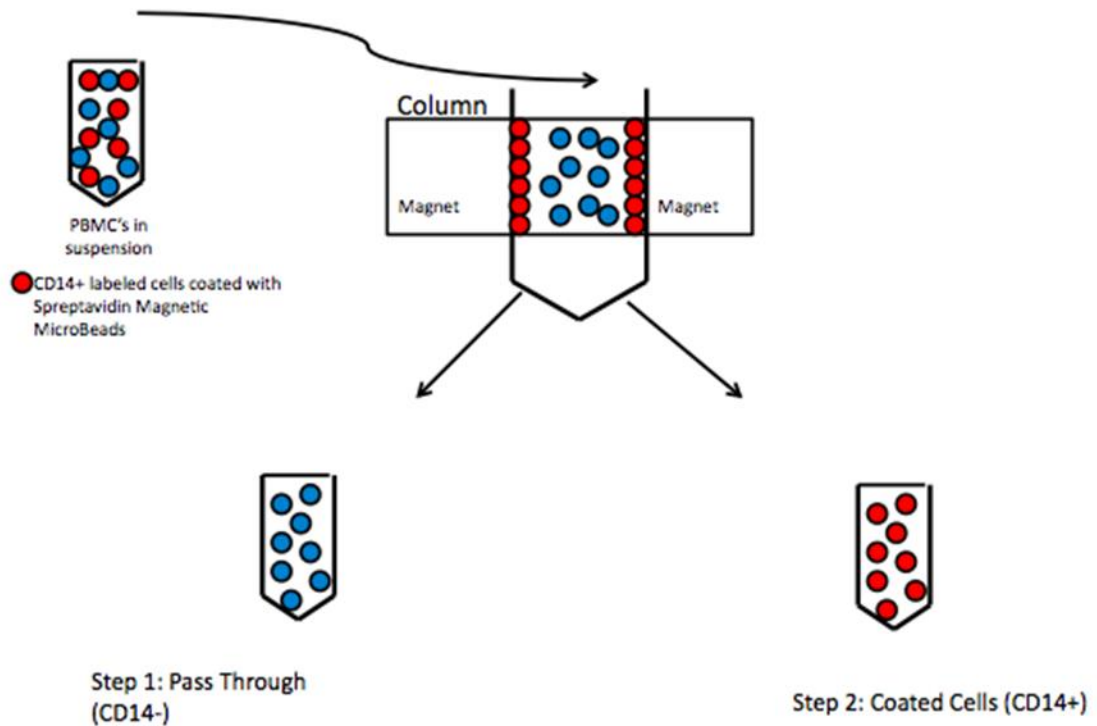


Figure 19: Overview of monocyte separation using Streptavidin Magnetic Microbeads

4.2 Results

Figure 20 shows the flow data of the separation at each step. Total mononuclear cells were placed in the column with CD14 labeled cells attached to magnetic beads. The passed cells come out in step one. In step two, the bound cells were plunged out. A greater number of cells are seen in gate P7, the monocyte gate, in the flow data of this step. The flow data indicates that the magnetic bead separation enriches for the CD14 cell population.

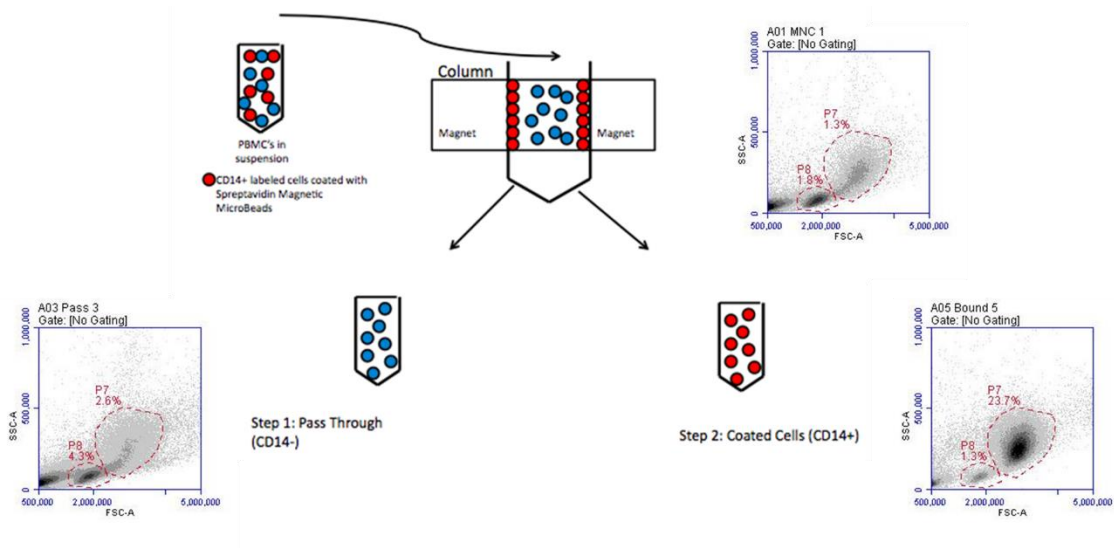


Figure 20: Flow data of the separation at each step, side scatter and forward scatter shown.

Additional cell labeling was performed to determine the purity of the separation and to identify any contamination that may be present. A typical example of this is seen in Figure 21. Analysis was completed as previously described, gating to remove any doublets. Labeling for flow cytometry was done for CD14 (monocytes), CD3 (T cells), CD19 (B cells), and CD56 (natural killer cells) to verify purification. A purity as high as

95% was achieved of CD14+ cells, seen in graph 3 which represents CD14+ cells in the column bound population. These monocytes would be used for future experiments, and differentiated into DCs, described later. There is less than 1% contamination of B cells (CD19+ in graph 3), and about 1.6 % contamination of T cells (CD3+, graph 6).

Labeling for CD11c (human pan DC marker) was used as a negative control before the monocytes were put into DC culture (graph 7). The presence of CD11c after culture was used to verify that DC were produced⁴⁵.

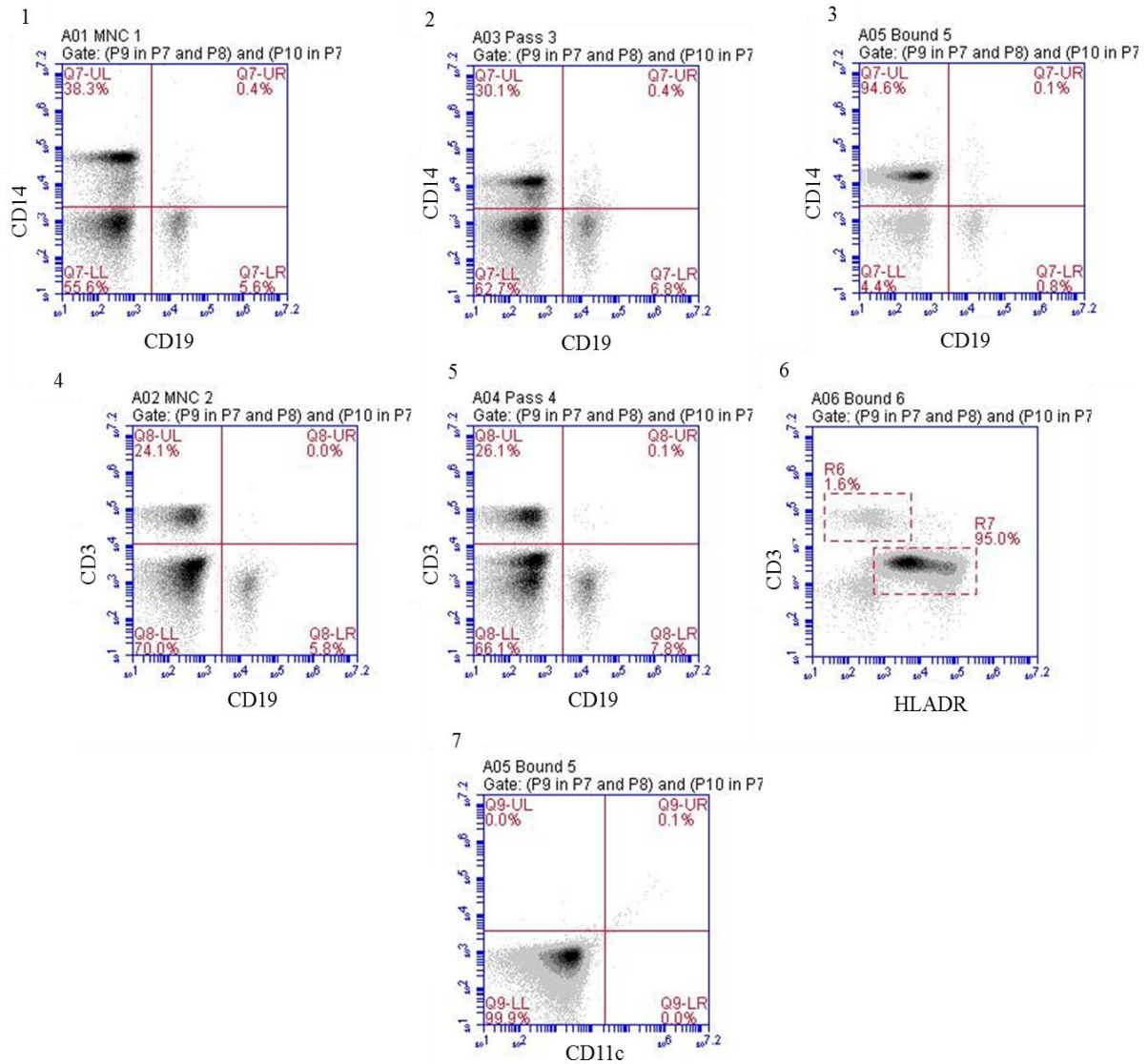


Figure 21: Purification analysis of monocytes from separation. 95% purity achieved, seen in graph 3. Cells are negative for CD11c seen in graph 7, as expected, before going into DC culture.

In conclusion, the flow cytometry data in Figure 21 shows that using this method monocytes could be successfully separated from the mononuclear cells with high yield

and purity of up to 95%. These cells were added to conditioned medium to induce differentiation to DC. These DCs are used as an *in vitro* model for influenza infection.

Section 5: B cell Separation from Mononuclear Cells

5.1 Methods

To study the interaction of B cells and infected DCs *in vitro*, a protocol was optimized to separate B cells (about 10% of mononuclear cells) with high purity and yield.

Mononuclear cells were isolated from whole blood using Accuspin tubes as described previously. After counting, cells were resuspended to a concentration not exceeding 10^8 cells per milliliter in Dynabead buffer. Five microliters of Anti-Human CD3 Biotin (eBioscience) were added to the cells in buffer. These cells were placed on ice, protected from light and incubated in a shaker set at 100RPM for 30 minutes. After incubation, the cells were washed with 1 ml of Dynabead buffer for 8 minutes at 4 degrees Celsius at 400xG. After the wash, cells were resuspended in 1 ml of Dynabead buffer. Life Technologies Dynabead Biotin Binders (CAT# 11047) were prepared according to the manufacturers specifications. There were 4×10^8 beads per milliliter and was adjusted after each depletion to a concentration of 5 beads per target cell for the depletion. Once the volume of beads was calculated, the volume was removed from the stock bottle and placed in a small tube inside the Dynabead magnet for 1 minute. The supernatant was discarded, and the beads were resuspended in the original volume with Dynabead buffer. Once the beads were prepared, they were added to the washed cells. One milliliter of Dynabead buffer was added to limit the trapping of unbound cells. These cells were placed on ice, protected from light and incubated in a shaker set at

100RPM for 30 minutes. After incubation, the tube was placed in the magnet for 3 minutes, and the supernatant was removed and transferred to a new tube on ice. The beads were resuspended in 1 ml of Dynabead buffer. The magnetic depletion step above was then repeated. After completed, the beads were resuspended in 1 ml of Dynabead buffer and kept on ice. Aliquots of each step were taken for photographs, Wright Stain, and flow analysis. Cells in each step, including those bound to beads, were counted using a hemocytometer. A second depletion was completed with 5ul of Anti-Human CD3 Biotin (eBioscience) and 5 µl of Anti-Human CD14 Biotin (eBioscience) used together. A third depletion was completed using 5 µl of Anti-Human CD14 Biotin (eBioscience).

5.2 Results

After three depletions CD19+ cells were separated from MNCs. As seen in Figure 22, beads appear as metallic balls around cells. They can be easily seen bound to beads in clumps in the bound population. In the population that passed through the magnet, no beads can be seen. Wright Stain was also used to determine visually the cell populations that were present. Wright staining facilitates differentiation between lymphocytes and monocytes, and this provides information about the cell populations that are present. This stain, however, cannot differentiate between different lymphocyte populations. In order to determine the purity of the lymphocyte populations, flow cytometry was used.

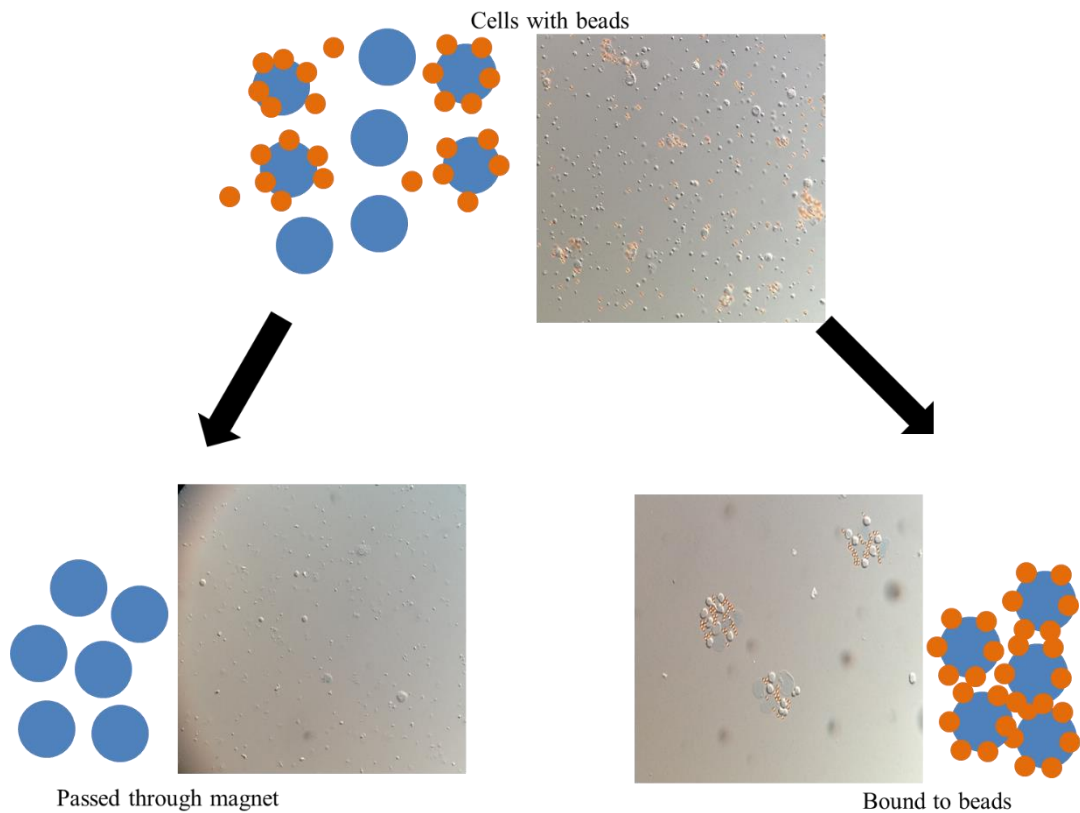


Figure 22: B cell separation using Dynabeads. The beads appear colored around cells. The cells that passed through the magnet do not contain any beads, but in the bound population the cells are surrounded by them.

In Figure 23, typical flow cytometry results are shown of B cell depletion. As described previously, the cells are gated to remove doublets (graph 3). Graph 1 and 2 show the side and forward scatter from the flow analysis. After three depletions, the lymphocyte gate (P5) contains a higher percentage of cells compared to before depletion, indicating that a lymphocyte population is being purified. In graphs 7, 8, and 9 after the depletion is completed CD3 disappears and only a small amount of CD14 remains (2.3%). The percentage of CD19+ cells increases from 6 to 17%.

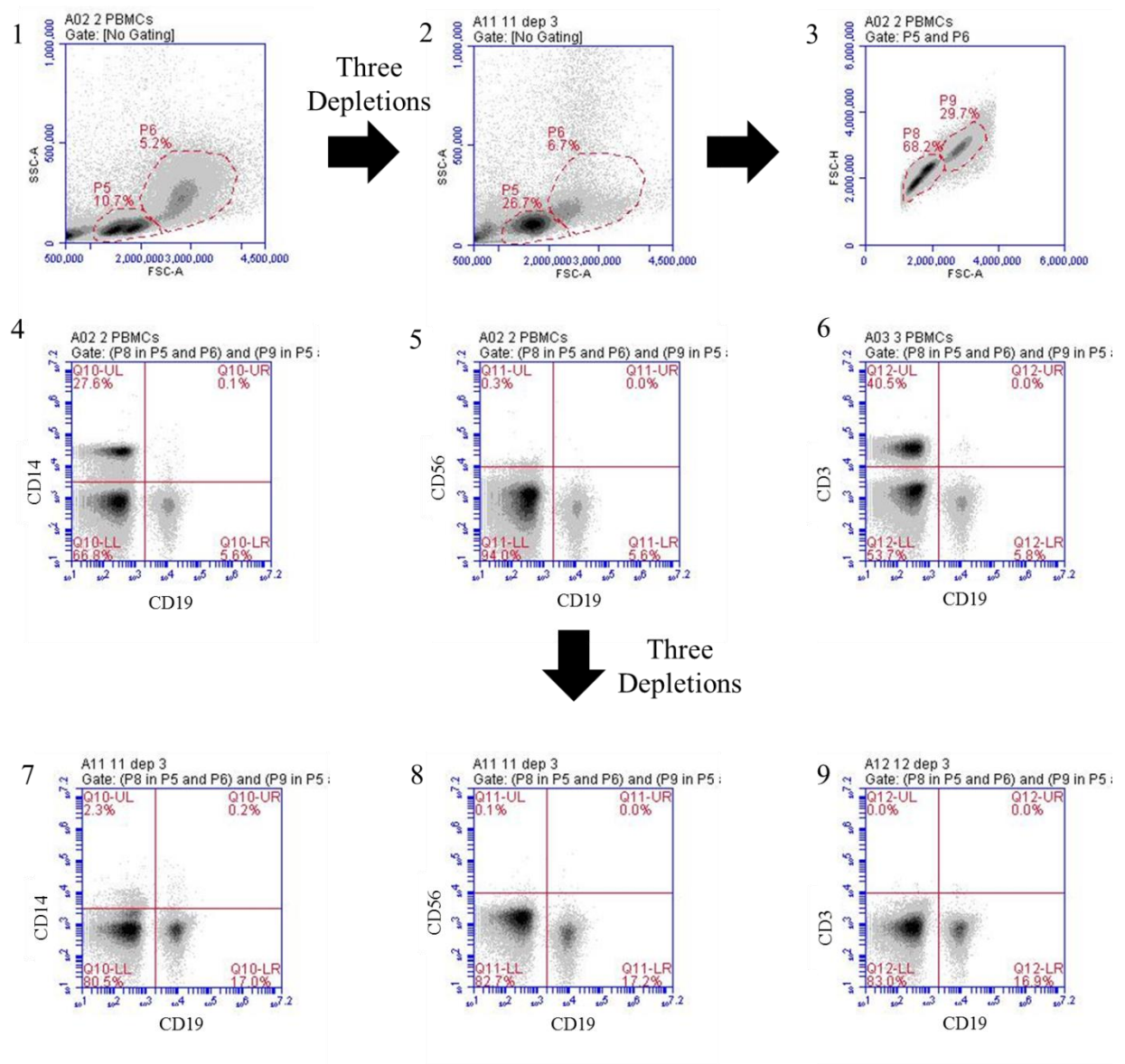


Figure 23: Flow cytometry analysis of MNCs depleted of CD3 and CD14

The flow cytometry data indicates that the B cells were purified, but there were many unlabeled cells in the population. This was found to be typical of these experiments, as it appears that 80% of the mononuclear cells were unlabeled. Markers to detect all mononuclear cells are used for labeling, so no cell types are missing. Wright

stain analysis of the above experiment showed 96% lymphocytes and 4% monocytes. This microscopic examination confirms the flow data, indicating that there is little monocyte contamination, and that the majority of the cells are lymphocytes. After many replicates of the depletion with the same results, these unlabeled cells can be attributed to debris, because positive and negative controls show that the antibodies used to label are fully functional, and the Wright stain microscopic examinations confirm the results. Taking this into account, the true purity of the CD19+ cells is 88% for this experiment, which is what is typically seen using this protocol. The largest concern for this future in vitro experiment is presence of contaminating T cells which could affect data interpretation. However, T cells were almost completely depleted whereas little monocyte contamination was noticed (11.7%).

In conclusion, the data presented in Figure 23 shows that this method can be used to obtain a population of CD19+ cells for future experiments with high yield (88% purity). Isolation of this B cell population was done by negative selection. Hence magnetic beads were not used to positively select for these cells since manipulation could cause this cell population to become activated, adversely affecting results.

Section 6: Antibody Assay using Hemagglutination Inhibition

6.1 Methods

Volunteer serum was collected before influenza vaccination and 30 days post influenza vaccination. It was necessary to confirm the presence of influenza specific antibodies in this serum before and after vaccination because this serum would be used in future experiments to optimize the influenza specific ELISA. A white 96 well round bottom plate was used to make viral dilutions. Fifty microliters of H₁N₁ or H₃N₂ virus

dilution were added to each well. Two HAU of influenza were added to each well to confirm a positive result would occur. Negative control wells received 1x PBS with no virus. Fifty microliters of pre and post flu vaccine serum from the volunteers were added to the first well (1:2 dilution). A multichannel pipette was used to mix the well 5 times. Two fold serum dilutions were performed, mixing between each step. The positive control wells with virus did not receive serum. The plate was covered and incubated at 4 degrees Celsius for 20 minutes. After the incubation, 50 μ l of a 1% TRBC solution in Alsever's were added to each well, and the plate incubated for an additional 45 minutes.

Hemagglutination is inhibited when specific HA antibodies are present in the sample, precluding the viral HA to agglutinate red blood cells. Figure 24 demonstrates the principle of this assay. The highest dilution of the serum that prevents hemagglutination is the HA titer of the serum. If the serum contained no antibodies against the virus strain, then hemagglutination is expected in all wells.

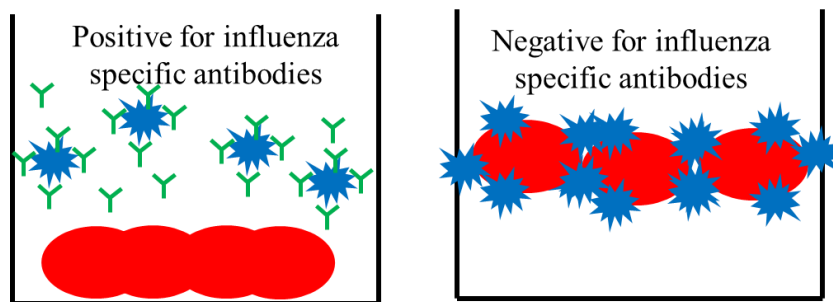


Figure 24: Antibody inhibition assay. If enough influenza specific antibodies are present, they bind influenza particles, and RBCs will form a button on the bottom of the well

6.2 Results

The results of the antibody inhibition assay can be seen in Figure 25 below. The serum contained influenza specific antibodies for both H₁N₁ and H₃N₂, showing that it could be used to optimize later assays. The influenza specific antibody titer was lower in the pre vaccination then the post vaccination for both viral strains. This is expected, because vaccination with the seasonal influenza vaccine should increase the influenza specific antibody titer. It is expected to see some antibodies against influenza to be present before vaccination. This is because influenza virus is very common, and individuals are exposed to it on a regular basis, which would cause them to produce some antibodies against it even though they did not develop an active infection.

	1	2	3	4	5	6	7	8	9	10	11	12
H1N1 Pre Vac	1:2	1:4	1:8	1:16	1:32	1:64	1:128	1:256	1:512	1:1024	1:2048	1:4096
H1N1 Post Vac	1:2	1:4	1:8	1:16	1:32	1:64	1:128	1:256	1:512	1:1024	1:2048	1:4096
H3N2 Pre Vac	1:2	1:4	1:8	1:16	1:32	1:64	1:128	1:256	1:512	1:1024	1:2048	1:4096
H3N2 Post Vac	1:2	1:4	1:8	1:16	1:32	1:64	1:128	1:256	1:512	1:1024	1:2048	1:4096
Positive Control	H1N1	H1N1	H1N1	H1N1	H1N1	H1N1	H3N2	H3N2	H3N2	H3N2	H3N2	H3N2
Negative Control	-	-	-	-	-	-	-	-	-	-	-	-

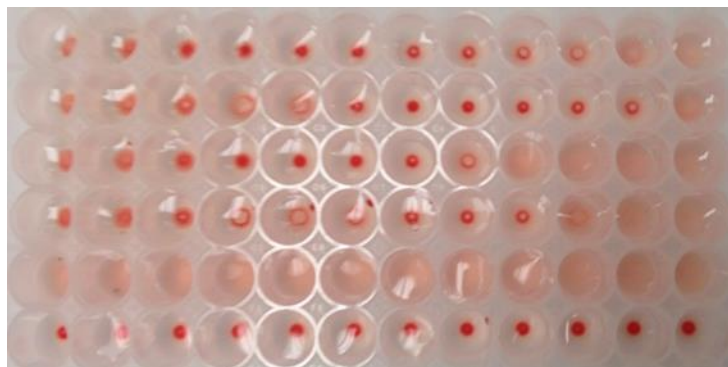


Figure 25: Antibody inhibition assay results from donor S

In summary, the assay showed that influenza-specific antibodies to both H₁N₁ and H₃N₂ were present in the specimen. The amount of these antibodies increased after

vaccination with the inactivated influenza vaccine, as expected. This serum was used to optimize assays for the determination of subclasses of influenza specific antibodies.

Section 7: Detection of Subclasses of Antibodies

7.1 Methods

Future studies will involve the interaction of B cells and infected DCs *in vitro*, so a protocol was optimized to separate un-manipulated B cells (about 10% of mononuclear cells) with high purity and yield. This was accomplished as described in Chapter 2, 5.2. Included in this study, the subclass of antibodies secreted needs to be analyzed. These antibodies may be secreted *in vitro* in much lower concentration than normal, so highly sensitive Enzyme Linked Immunosorbent Assays (ELISAs) were developed. See Appendix C for a list of the different Antibodies used for each ELISA method.

Enzyme Linked Immunosorbent Assay (ELISA) Method #1: Pierce Goat Anti-Human IgG Kappa and Pierce Goat Anti-Human IgG Lambda Sensitized, BD Pharmingen Biotin Mouse Anti-Human IgGs secondary.

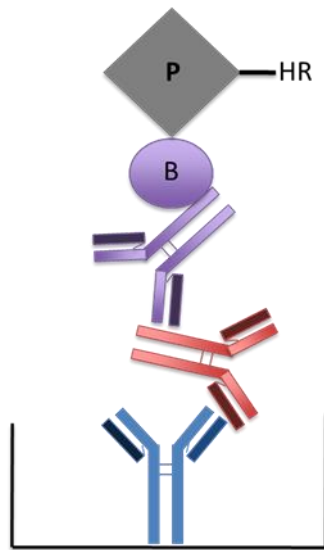


Figure 26: ELISA method #1 overview

For the detection of IgGs and associated light chains in human serum, primary antibody was diluted into bicarbonate buffer. Pierce Goat Anti-Human IgG Lambda or Pierce Goat Anti-Human IgG Kappa was diluted 1:40 in bicarbonate buffer, and 50 μ l was added to each assigned well in a Thermo Immulon 2HB 96 well flat bottom ELISA plate. The plate was incubated at room temperature for 1 hour covered. After incubation, the plate was then washed three times with 100 μ l of 1xPBS. To block for non-specific binding, 200 μ l of blocking buffer (5% nonfat dry milk 0.1% Tween 1xPBS) was added to each well, and incubated covered overnight at 4 degrees Celsius. The next morning the wells were washed three times with 100 μ l of 1xPBS 0.1% Tween. Fifty microliters of the sera (standard or unknown serum dilutions) diluted in blocking buffer was added to the assigned wells. Standard serum samples used are as follows; Sigma IgG1 Kappa from human myeloma plasma (CAT# I5154 Lot# 081M6276 1.13mg/ml), Sigma IgG1

Lambda from human myeloma plasma (CAT# I5029 Lot# 091M6298 1.18 mg/ml), Sigma IgG2 Kappa from human myeloma plasma (CAT# I5404 Lot#067K6026 1.1mg/ml), Sigma IgG2 Lambda from human myeloma plasma (CAT# I5279 Lot#061M6247 1.00mg/ml). Sera dilutions were incubated for 1 hour covered at room temperature. After incubation, the wells were washed three times with 100 μ l of 1xPBS 0.1% Tween. The secondary antibody was added to assigned wells diluted in blocking buffer. Secondary antibodies are as follows; BD Pharmigen Biotin Mouse Anti-Human IgG, BD Pharmigen Biotin Mouse Anti-Human IgG1, BD Pharmigen Biotin Mouse Anti-Human IgG2, Abcam Mouse Anti-Human IgG3 HRPeroxidase, BD Pharmigen Mouse Anti-Human IgG4, and Pierce Goat Anti-Human IgG Peroxidase. Secondary antibody was incubated at room temperature for 1 hour covered. After the incubation time was completed, the wells were washed three times with 1xPBS 0.1% Tween. Fifty microliters of a 1:1000 dilution in 1xPBS of the detector Thermo Scientific ImmunoPure Streptavidin Horseradish Peroxidase (CAT# 21126 Lot: MD157646) was added if required by the secondary antibody, and incubated at room temperature for 1 hour covered. After this final incubation, the wells were washed three times with 1xPBS 0.1% Tween, and 50 μ l of 3, 3', 5, 5' Tetramethyl Benzdine (1xTMB) substrate was added. The reaction was allowed to continue until a blue color was seen, monitoring the control wells for background which reacted in approximately 10-15 minutes. During this time, the plate was placed in the 37 degree Celsius incubator for one minute, and checked each minute after. After completion, the reaction was stopped by adding 1M H₂SO₄, and read at 450nm with a Bio-Tek Instruments Automated Microplate Reader ELx800. See Figure 26 for an overview of the described protocol.

ELISA Method #2: BD Pharmigen Purified Mouse Anti-Human IgGs Sensitized,
BD Pharmigen Biotin Mouse Anti-Human Ig Kappa Light Chain and Lambda light chain
secondary.

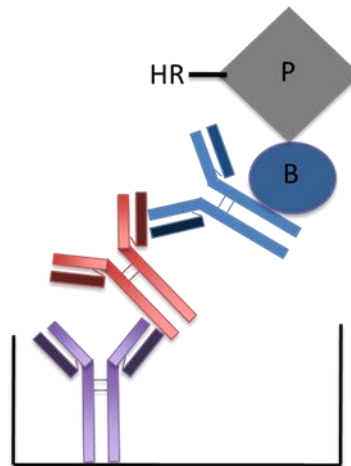


Figure 27: ELISA method
#2 overview

For the detection of IgGs and associated light chains in human serum, primary antibody was diluted in carbonate buffer. BD Pharmigen Purified Mouse Anti-Human IgG, BD Pharmigen Purified Mouse Anti-Human IgG1, or BD Pharmigen Purified Mouse Anti-Human IgG2 were diluted in carbonate buffer and 50 μ l of the dilution was added to the assigned wells on a Thermo Immulon 2HB 96 well flat bottom plate. Assay was completed as previously described. Secondary antibodies are as follows; BD Pharmigen Biotin Mouse Anti-Human Ig Kappa Light C, or BD Pharmigen Biotin Mouse Anti-Human Ig Lambda Light Chain. Figure 27 shows an overview of the described protocol.

In order to standardize the concentrations of IgGs in serum from a single volunteer, a Human IgG Subclass Profile kit was purchased from Invitrogen (CAT#

991000). This kit was used to determine the amount of IgG1, IgG2, IgG3, and IgG4 in a single volunteer, so that serum could be used as a standard for unknowns in the future. The kit was used according to the specifications by the manufacturer, and following the protocol it was determined that the volunteer had 6.76 mg/ml of IgG1, 3.27 mg/ml of IgG2, 0.82 mg/ml of IgG3, and 0.98 mg/ml of IgG4, all within the normal ranges for the volunteers age.

ELISA Method #3: IRR Influenza A H1 and H3 Control antigen sensitized, BD Pharmigen Biotin Mouse Anti-Human IgGs and IgM secondary.

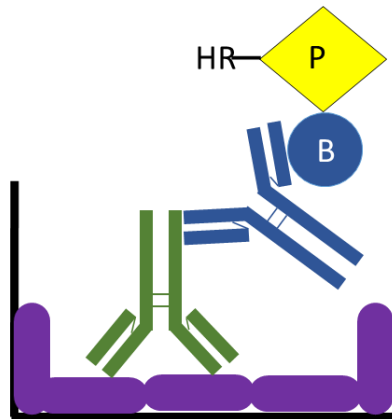


Figure 28: ELISA method #3 overview

For the detection of IgGs and IgM specific to H1 and H3 influenza antigens, antigen was diluted into bicarbonate buffer. Influenza Reagent Resource (IRR) Influenza A (H1) pdm09 Control Antigen or IRR Influenza A (H3) were diluted 1:50 in bicarbonate buffer, and 50 μ l was added to each assigned well in a Thermo Immulon 2HB 96 well flat bottom plate. This assay was completed as previously described, with unknown samples diluted in DMEM-5%FCS. Secondary antibodies included: BD Pharmigen Biotin Mouse

Anti-Human IgG, BD Pharmingen Biotin Mouse Anti-Human IgG1, BD Pharmingen Biotin Mouse Anti-Human IgG2, Abcam Mouse Anti-Human IgG3 HRPeroxidase, BD Pharmingen Biotin Mouse Anti-Human IgG4 and BD Pharmingen Biotin Mouse Anti-Human IgM. See Figure 28 for a summary of the described protocol.

As a positive and negative control for the influenza ELISA, a combination of the H1 and H3 antigens described were used in conjunction with IRR Mouse Monoclonal Antibody Influenza Type A H3, IRR Mouse Monoclonal Antibody Influenza Type A H1 pdm09, and IRR Mouse Monoclonal Antibody Influenza A pool at a 1:50 dilution with a detector of Thermo Scientific Stabilized Peroxidase Conjugated Goat Anti-Mouse H+L IgG at a 1:500 dilution.

All results were expressed as the average of a set of triplicates. Results were considered significant above background if the average of the Optical Density (OD) was three times the standard deviation of the negative control group, as described by John Crowther in *The Elisa Guidebook*³⁴.

All experiments were completed with positive and negative controls of each step to verify that each antibody or detector was working, and there was no cross reactivity between different steps in the sandwich ELISA. Background for all ELISAs was an average OD of 0.05-0.06. Unless otherwise indicated, graphs of ODs are represented as the geometric mean of the triplicate with standard deviation bars.

The sera collected from volunteers are described in the subject section.

7.2 Results

All ELISAs were optimized by completing serial dilutions of the different antibodies or detectors. These dilutions were tested with the system, and the dilution that

gave the brightest color change was chosen. The optimized working dilution of each ingredient was described in the methods section earlier in this section.

Enzyme Linked Immunosorbent Assay (ELISA) Method #1: Pierce Goat Anti-Human IgG Kappa and Pierce Goat Anti-Human IgG Lambda Sensitized, BD Pharmingen Biotin Mouse Anti-Human IgGs secondary.

To determine concentrations of IgGs in an unknown serum (Serum A), the Human IgG Subclass Profile Kit (CAT# 991000 Lot# 844404) was purchased from *Invitrogen*, and was followed according to the manufacturer's directions. Other standards were used also, as described earlier in this chapter. To determine the unknown quantities, the standard was plotted with the average OD and known concentration of the antibody. The unknown sera were tested in parallel and plotted. The unknown OD was used in the linear equation for the slope of the best fit line of the standard. This was used to quantify the unknown concentration of IgG subclasses. This unknown concentration was then multiplied by the dilution factor taking into account the volume that was added to the well. For example, in Figure 29, the standard and unknown graphs for IgG1 are shown. In Table 6, the concentrations determined by this method are shown.

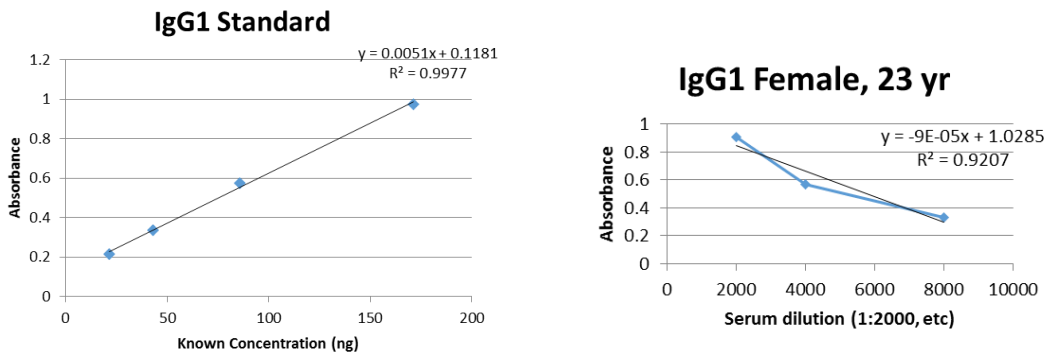


Figure 29: Curves to calculate unknown concentrations of IgG1

Table 6: Quantification of IgGs in serum using Invitrogen Kit

	IgG1	IgG2	IgG3	IgG4
Unknown Concentration (mg/ml)	6.6 mg/ml	3.3 mg/ml	0.8 mg/ml	0.98 mg/ml
Normal Range (mg/ml)	5-12 mg/ml	2-6 mg/ml	0.5-1 mg/ml	0.2-1 mg/ml

Ten different sera from volunteers as well as a mixed serum standard from Biorbyt were used in this ELISA to determine reproducibility with IgG1 and IgG2. Assays for IgG3 and IgG4 were not performed for these sera because the subclasses of interest in this project were IgG1 and IgG2. The data shown in Figures 30 and 31 demonstrate that the system is optimized and functional using sera from normal healthy subjects.

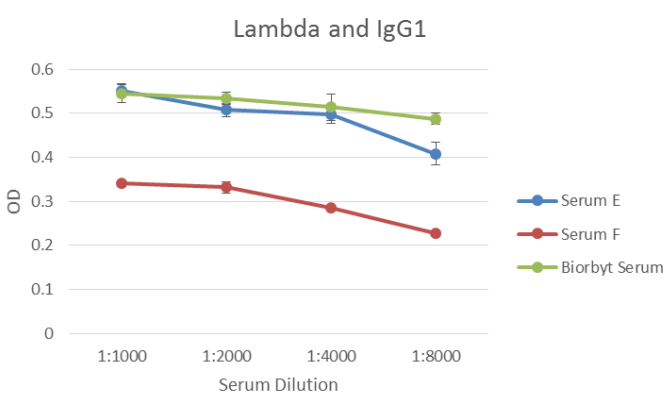
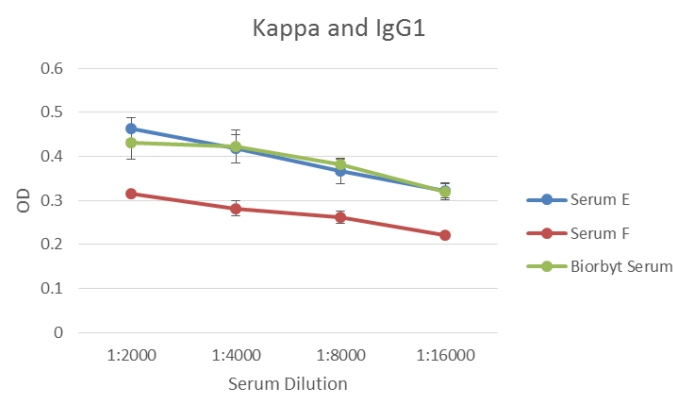
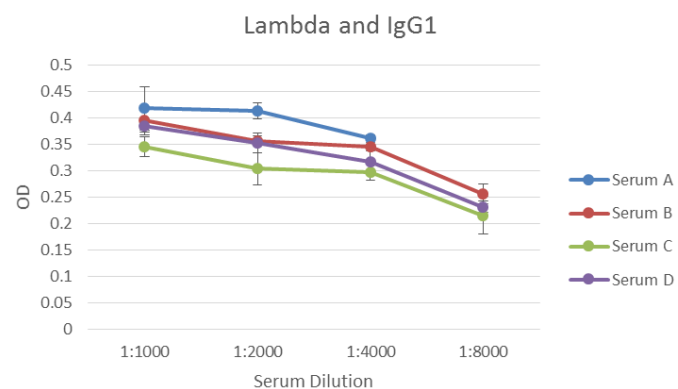
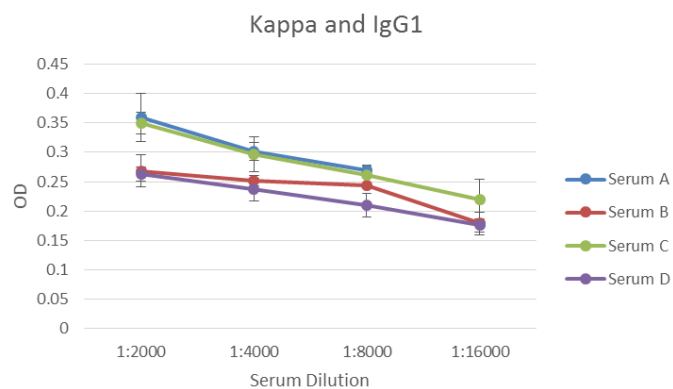


Figure 30: Multiple serum results

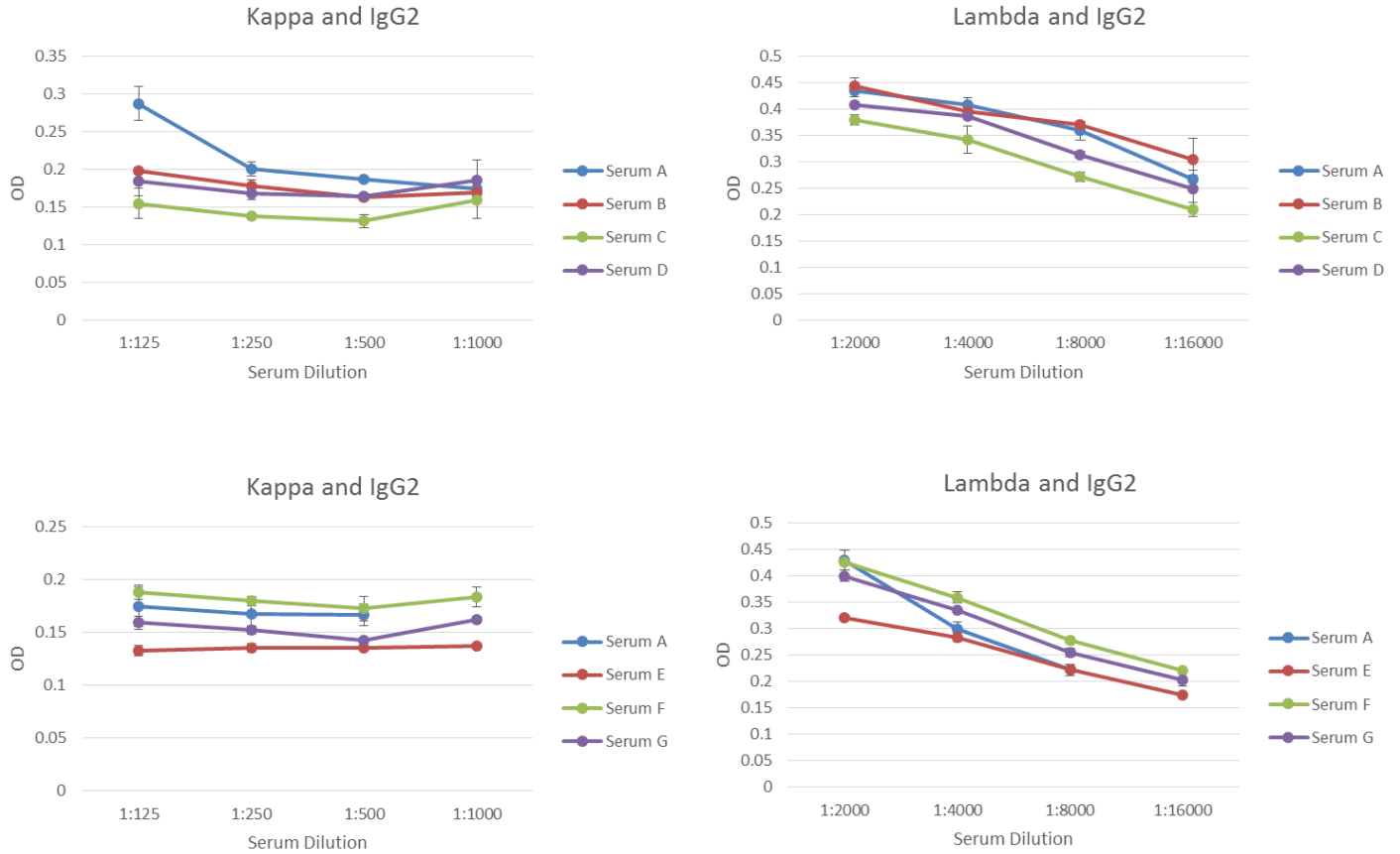


Figure 31: Multiple serum results

A sample was obtained from a patient with recurrent infections (IBC protocol #211), as described previously as donor L. This patient serum sample was assayed using the optimized system. Preliminary data is shown in Figure 32. The IgG2 from this patient does not appear to be detectable with the kappa light chain.

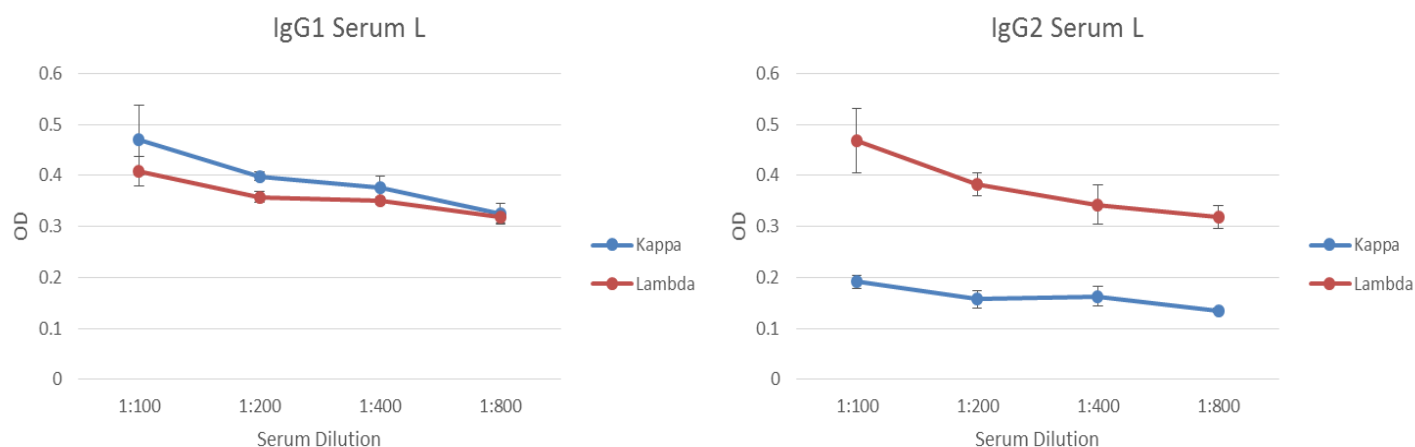


Figure 32: Preliminary data from donor L

The Purified Myeloma Standards listed earlier in this chapter had a known concentration value with at least 95% purity. These were diluted and used to determine the sensitivity of the optimized ELISA using the methods described earlier. Table 7 shows the known concentrations of the Myeloma Standards that were used for both ELISA method #1 and #2 described below. The sensitivity of this ELISA and the second ELISA type is shown in Table 8.

Table 7: Known concentrations of myeloma standards

Human IgG1 Kappa	Human IgG1 Lambda	Human IgG2 Kappa	Human IgG2 Lambda
1.13 mg/ml	1.18 mg/ml	1.1 mg/ml	1.00 mg/ml

In summary, this ELISA was optimized to detect total IgG, along with subclasses IgG1, IgG2, IgG3, and IgG4 and the associated light chains of kappa and lambda in human serum from several different donors. Capture antibodies of Pierce Goat Anti-

Human IgG Lambda or Pierce Goat Anti-Human IgG Kappa were used along with secondary antibodies of BD Pharmingen Biotin Mouse Anti-Human IgG, IgG1, IgG2, and IgG4 along with Abcam Mouse Anti-Human IgG3 HRPeroxidase.

ELISA Method #2: BD Pharmingen Purified Mouse Anti-Human IgGs Sensitized, BD Pharmingen Biotin Mouse Anti-Human Ig Kappa Light Chain and Lambda Light Chain secondary.

As in ELISA method #1, multiple donors were used to test the optimization of this second ELISA method, and be sure that the system was working across multiple samples. The results of these experiments can be seen below in Figures 33 and 34.

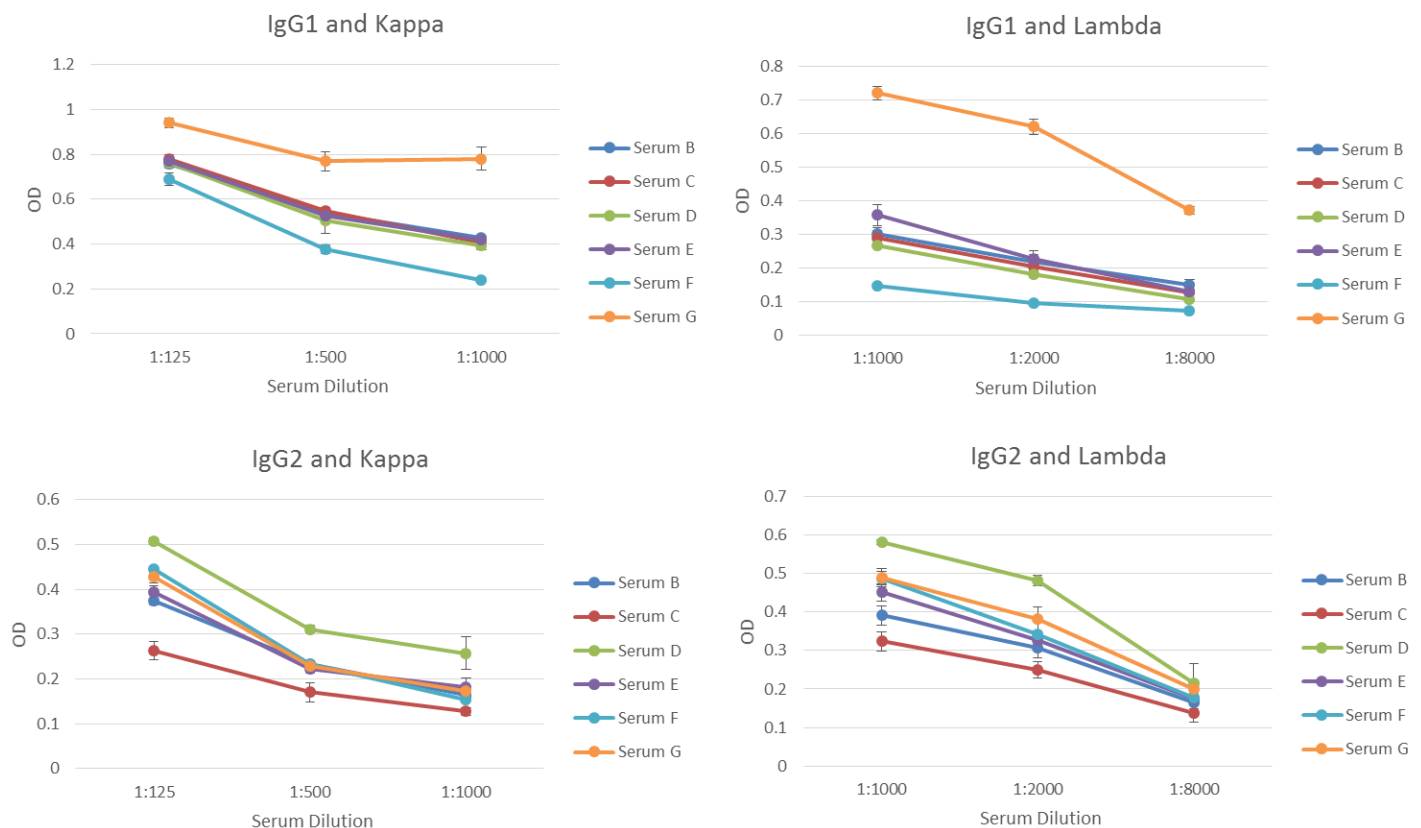


Figure 33: ELISA method #2 multiple serums

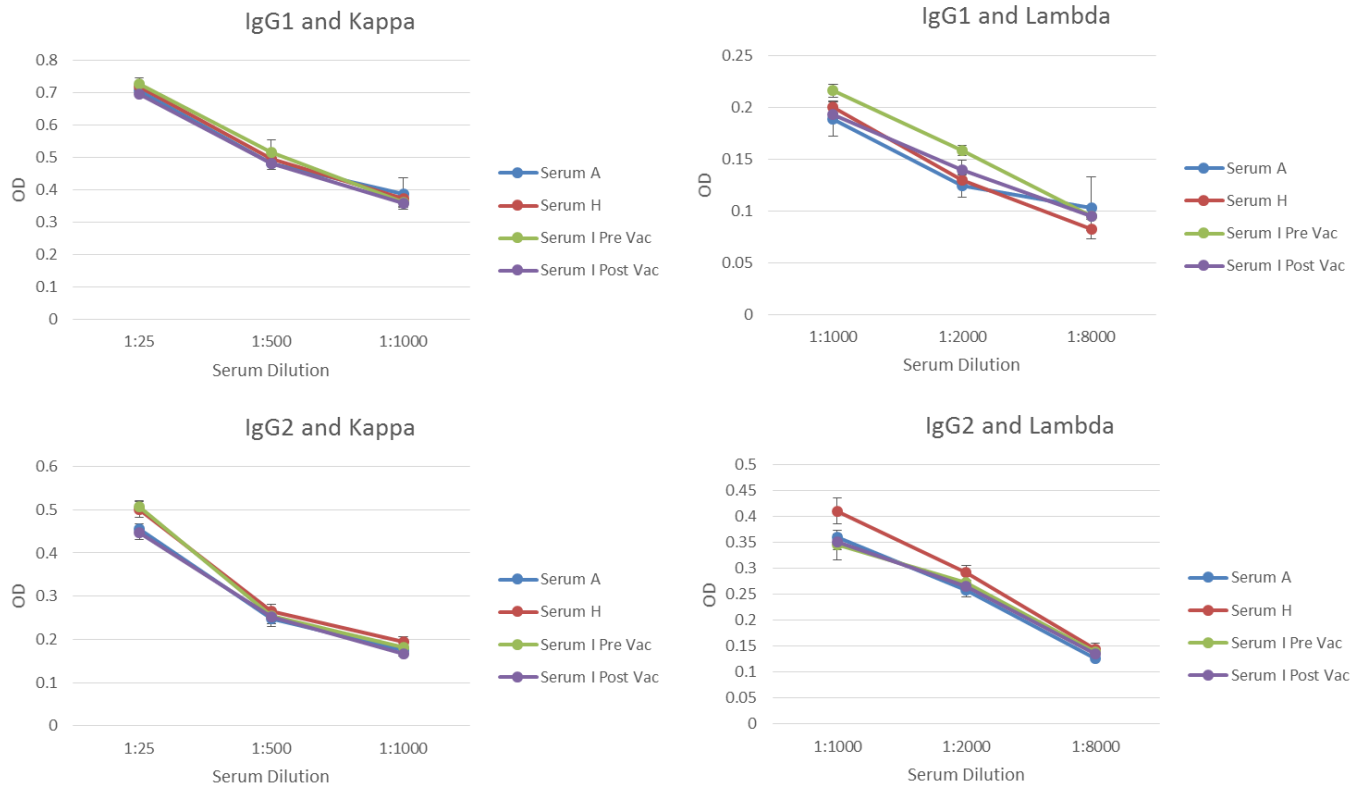


Figure 34: ELISA method #2 multiple serums

In summary, this ELISA was optimized to detect total IgG, along with subclasses IgG1, IgG2, IgG3, and IgG4 and the associated light chains of kappa and lambda in human serum from several different donors. Capture antibodies of BD Pharmingen Purified Mouse Anti-Human IgG, IgG1, and IgG2 were used along with secondary antibodies of BD Pharmingen Biotin Mouse Anti-Human Ig Kappa Light chain and Lambda Light chain, as described previously.

As described previously in this chapter and shown in Table 7, the standards were diluted to determine the sensitivity of the different ELISA methods. The sensitivities

with different combinations of capture antibody or antigen and detectors are shown in Table 8. The ELISA methods developed are very sensitive, and can detect nanogram amounts of antibodies. This sensitivity may prove helpful when detecting antibodies in the future co-culture studies referenced in the purpose section.

Table 8: Sensitivities of different methods

Capture	Detector	Detects at least x ng per well * Indicates lowest dilution tested	Target
Anti-Lambda (Polyclonal)	Anti-IgG1 (Monoclonal)	9.22 ng*	Myeloma IgG1 Lambda
Anti-IgG (Monoclonal)	Anti-Lambda (Monoclonal)	9.22 ng*	Myeloma IgG1 Lambda
Anti-IgG (Monoclonal)	Anti-IgG1 (Monoclonal)	18.44 ng	Myeloma IgG1 Lambda
Anti-IgG (Monoclonal)	Anti-Kappa (Monoclonal)	34.38 ng	Myeloma IgG2 Kappa
Anti-Lambda (Polyclonal)	Anti-IgG2 (Monoclonal)	7.81 ng*	Myeloma IgG2 Lambda
Anti-IgG (Monoclonal)	Anti-Lambda (Monoclonal)	7.81 ng*	Myeloma IgG2 Lambda
Anti-IgM (Polyclonal)	Anti-Kappa (Monoclonal)	0.9766 ng*	IgM Standard
Anti-IgM (Polyclonal)	Anti-Lambda (Monoclonal)	1.953 ng*	IgM Standard
Anti-IgG1 (Monoclonal)	Anti-Kappa (Monoclonal)	278.50 ng*	Biorbyt Standard
Anti-IgG1 (Monoclonal)	Anti-Lambda (Monoclonal)	34.81 ng*	Biorbyt Standard

Anti-IgG2 (Monoclonal)	Anti-Lambda (Monoclonal)	77.00 ng	Biorbyt Standard
Anti-Kappa (Polyclonal)	Anti-IgG1 (Monoclonal)	17.41 ng*	Biorbyt Standard

As stated in the Purpose and Specific Aims section, the future goal of this research is to understand the interaction between different populations of B cells in the presence of DCs loaded with inactivated virus as well as infected DCs in the antibody response to influenza infection *in vitro*. The intent of this study will be to co-culture MZBCs with Influenza A-infected DCs, or B cells with inactivated Influenza A DCs and compare with mock-infected controls. Antibody isotypes and IgG subclasses will be analyzed. These antibodies may be secreted in a concentration much lower than normal *in vitro*, so highly sensitive ELISAs were developed to determine if there was a detection system that would produce results before this future work could begin. Results in Table 8 demonstrate adequate sensitivity for future assays.

In summary, the optimized ELISAS are highly sensitive, which is important for future work with subclasses of antibodies that may be in lower concentrations than what is normally found in circulation.

ELISA Method #3: IRR Influenza A H1 and H3 Control antigen sensitized, BD Pharmingen Biotin Mouse Anti-Human IgGs and IgM detector

This ELISA was optimized to detect influenza specific antibodies. We hypothesize that these antibodies will be secreted in the co-culture of influenza infected DCs and separated B cells.

Pre flu vaccine serum and 30 days post flu vaccine serum was used from three

different volunteers (A, I, and S) to make sure the optimized ELISA for influenza specific antibodies was working. First, total IgG1 and IgG2 for the volunteers was quantified with the standard using methods described previously. The standard was used as a control, to determine that the volunteers had total IgG1 and IgG2 present, before looking for influenza specific antibodies of those subclasses. The known values determined using this method are shown in Table 9. All values are in the normal reported range, as expected. Data can be seen in Figures 35-37.

Table 9: Quantification of IgGs in donors

Quantification using ELISA				
Sample	IgG1 mg/ml	IgG2 mg/ml	Reference Range	Concentration in Standard
Serum A	4.16	7.04	IgG1: 5-12 IgG2 2-6	IgG1: 5.57 IgG2: 3.08
Serum I	9.05	2.9		
Serum S	6.23	5.09		

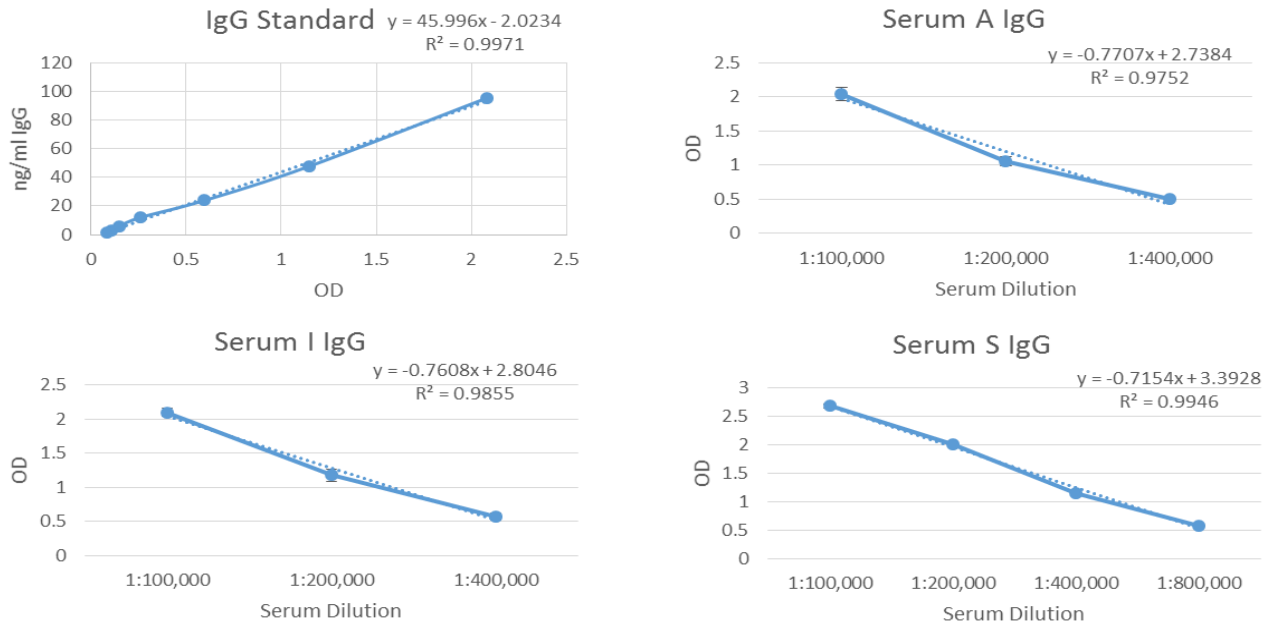


Figure 35: Quantification of total IgG

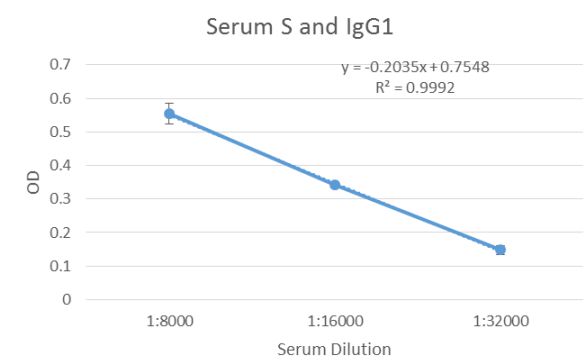
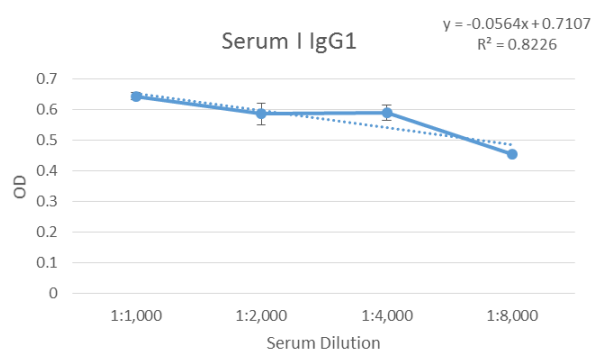
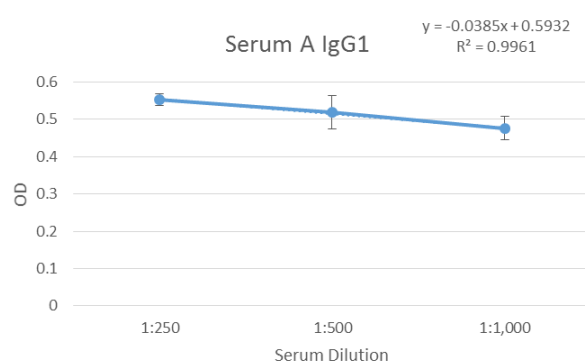
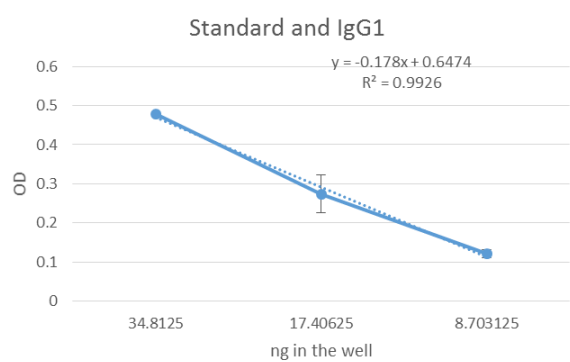


Figure 36: Quantification of IgG1

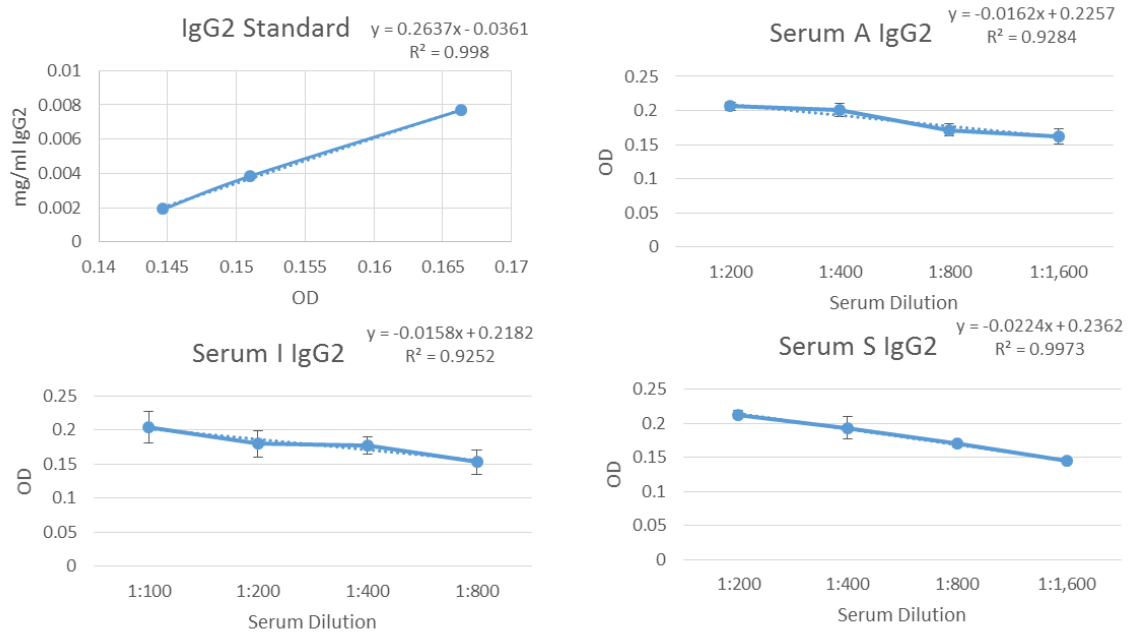


Figure 37: Quantification of IgG2

Once total antibodies for each donor was quantified, influenza specific antibodies in the optimized ELISA system were determined for two of the donors. The first donor, donor A shown in Figure 38 did not have a difference in influenza specific antibodies between pre and post flu vaccine. Also, IgG2 antibodies to H1 were highly variable and could not be measured. Interestingly, this volunteer was actively exposed to the virus in a controlled environment during the research process and thus chronic exposure to this virus could influence the appearance of influenza antibodies after vaccination.

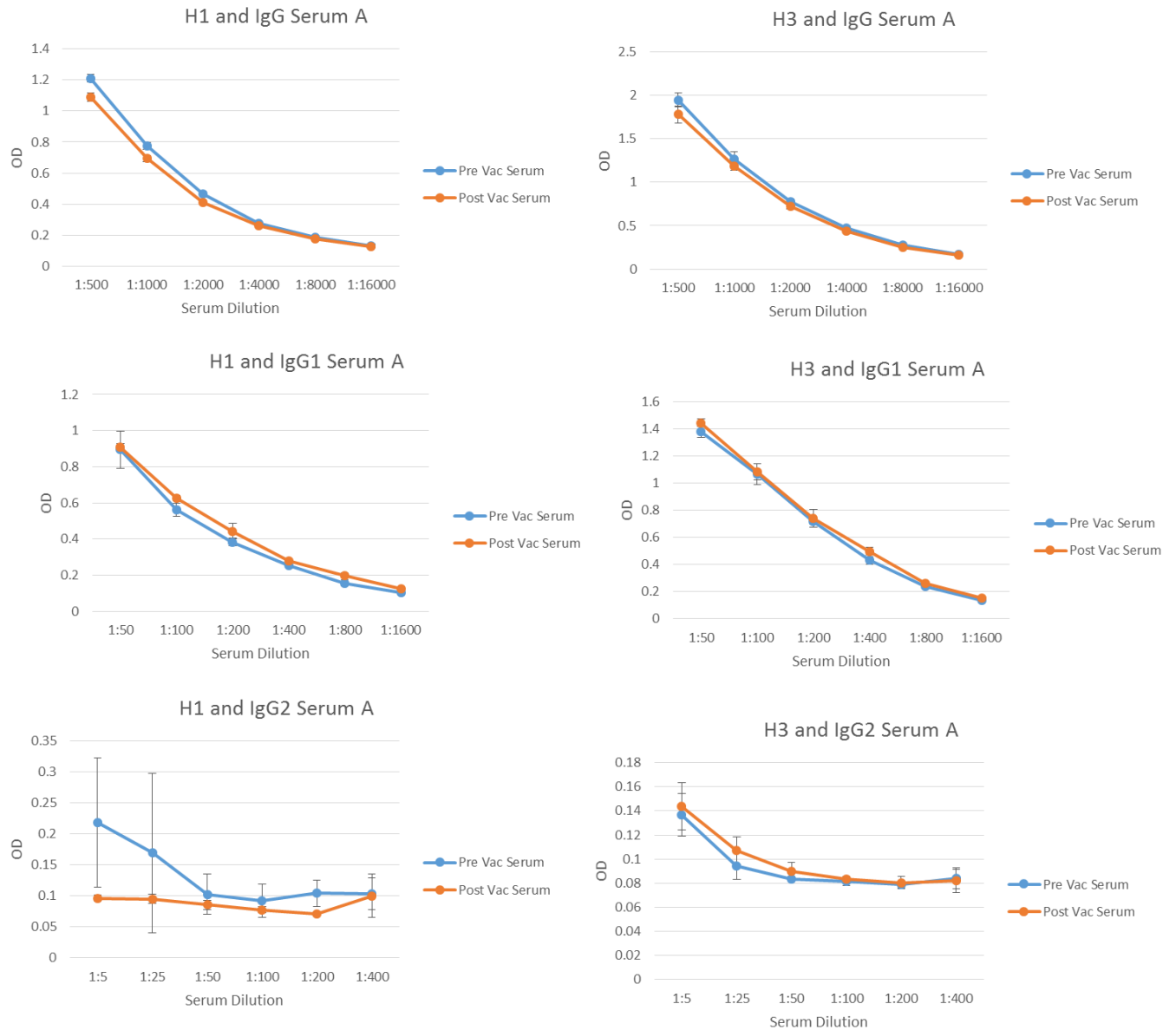


Figure 38: Influenza specific antibodies donor A

To insure that the assays were properly working, another volunteer serum pre and post flu vaccination was used in the optimized system who had not had exposure to the

Influenza A virus. Serum S showed a difference in the concentration of influenza specific antibodies after vaccination with the seasonal flu vaccine, seen in Figure 39. IgG2 for this individual was undetectable as seen with the previous donor. At 30 days post influenza vaccine, the majority of the influenza antibodies should be of the IgG1 isotype because immunologic memory has developed, as described in the introduction.

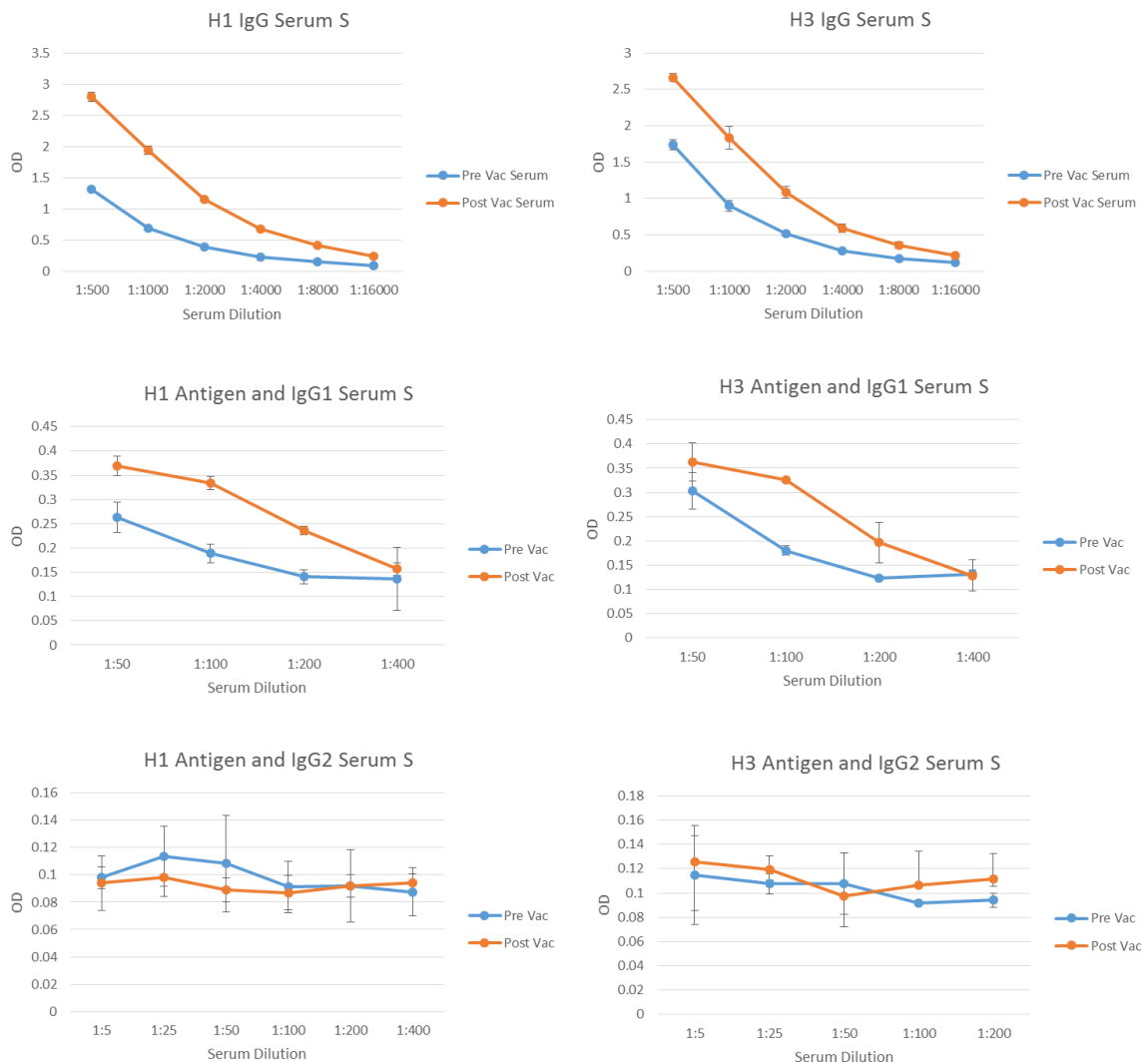


Figure 39: Influenza specific antibodies donor S

Serum from volunteer S was also used to determine presence of influenza specific (H1 or H3) antibodies of the IgG3 and IgG4 subclasses and the IgM isotype. Figure 40 shows the data for this experiment. Anti-IgG3 was detectable above background. However, Anti-IgG4 was not detectable, as expected because it is the antibody in lowest concentration.

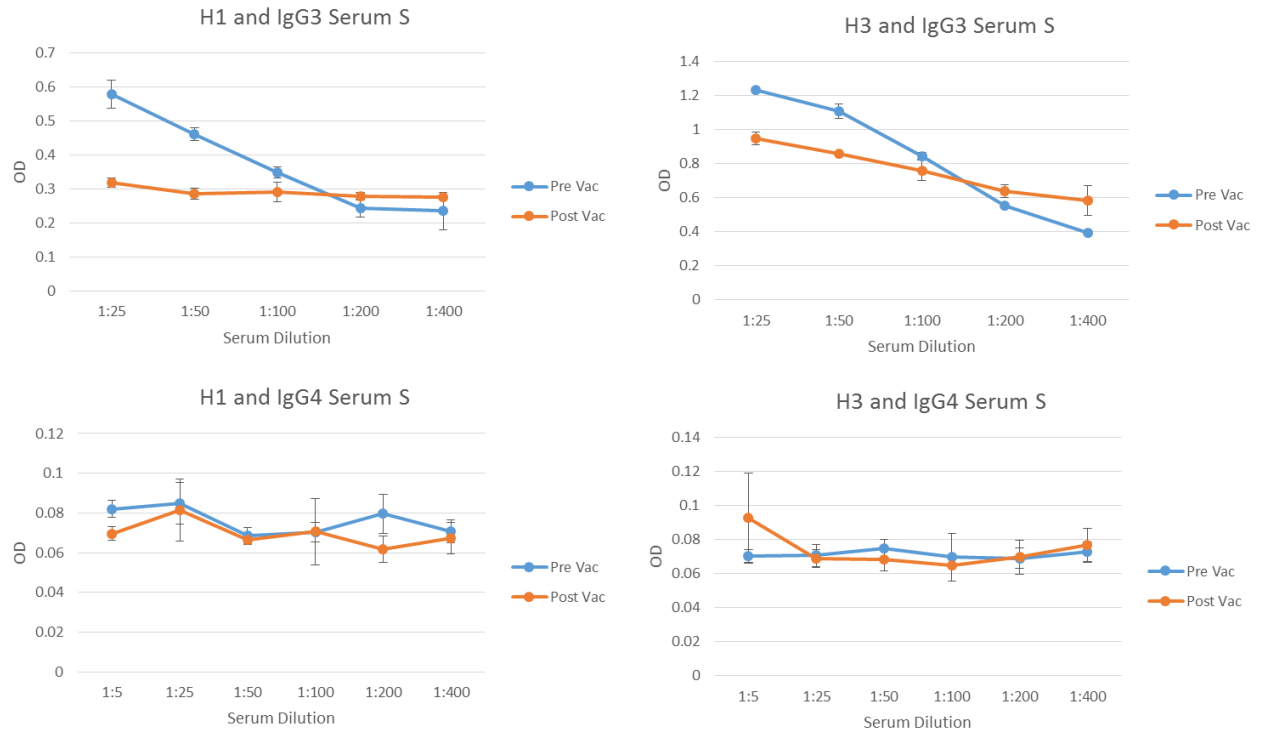


Figure 40: Influenza specific antibodies donor S

In conclusion, this ELISA was optimized to detect H1 and H3 antigen specific antibodies for total IgG, IgM, and the subclasses IgG1, IgG2, IgG3, and IgG4. There was an increase in influenza specific antibodies after vaccination seen in IgG1.

Chapter 3: Dendritic Cell Production and Infection

Section 1: Differentiation of Monocytes to Dendritic Cells

1.1 Methods

Purified CD14⁺ cells were counted and split into 12 wells of a 12-well tissue culture plate. 1 ml of 2x DC media (see appendix for recipe) and 6.25×10^4 cells per well. The plate lid was secured, and placed in an incubator at 37 degrees Celsius 5% CO₂. Attachment of monocytes to the bottom of each well was observed. Fresh 2x DC media was made and media was changed in each well on day 3. The plates were checked for attached and unattached cells before and after media change, and put back into the incubator. Day 7 after the cells were plated the culture was prepared for H₁N₁ viral infection. Each well was washed three times with 1 ml of DMEM-10%FCS. The cells were counted using a hemocytometer as described. Flow analysis was completed as previously described. The switch from CD14 to CD11c and CD80 indicated transition from monocyte to DC. DCs can also be detected by observing attached monocytes vs unattached DCs.

1.2 Results

Cytokine concentration in the DC media had to be initially optimized, to determine the concentration of GM-CSF and IL-4 to be used to get the highest yield of DCs. A 1x and 2x DC media solution was made and tested. Cells were analyzed using flow cytometry as previously described, and labeled for CD11c, a DC marker. Typical results are shown below in Figure 41. A 2x DC media solution was determined to be

optimal, because of the increase in CD11c compared to control with no cytokines and 1x media. 2x DC media was 94% CD11c+, where 1x was 91% CD11c+. The majority of the cells are positive for CD11c. Compared with the monocytes separated before culture in chapter two, all cells were negative for CD11c which demonstrates that culture conditions enhanced differentiation of the monocytes to DCs.

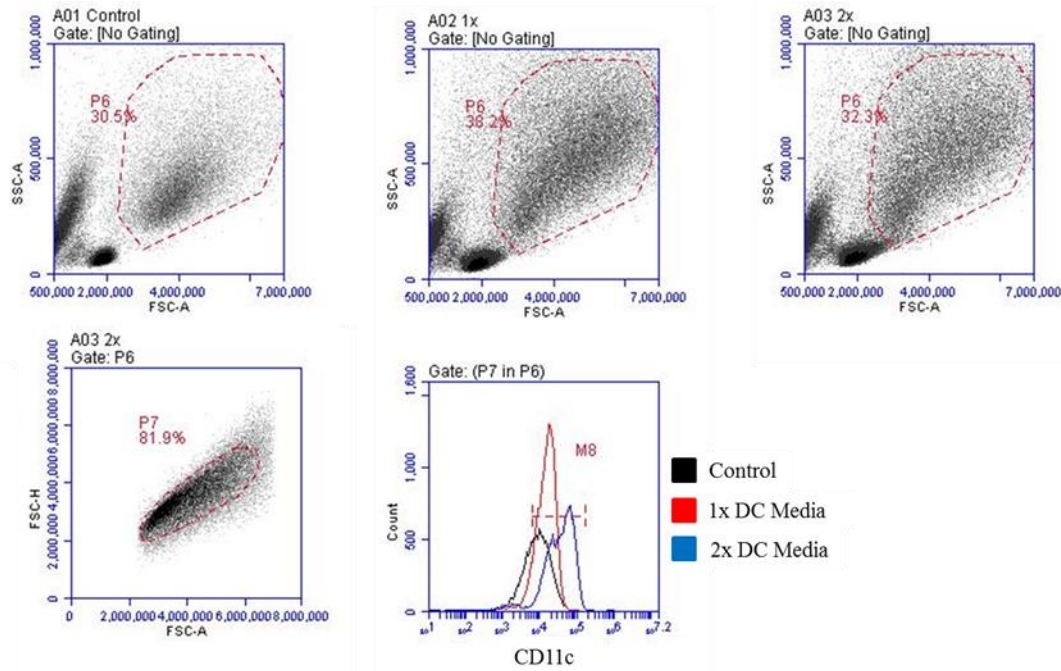


Figure 41: DC production, Donor A, 11-13-12 M8: Control: 65.84% 1x DC media: 91.05% 2x DC media: 94.15%. 2x DC media had a higher percent positive for CD11c, and was determined to be the optimal concentration of cytokines for DC culture.

Photographs of cells in the DC culture were taken at the beginning of culture, before and after media change on day 3, and on the last day of culture. Figure 42 below shows typical cells in these different stages of culture. The first photographs taken 15 hours after culture show cells that have attached to the bottom of the plate. This is expected because they cells are monocytes, which are adherent. On day 3, the media was

changed, and cells are seen still attached. This shows that cells are not washed away at this time point. This is expected because the monocytes are not DCs yet and should still be attached to the plate. The last photographs show the cells at day 7 of the culture before they are washed and pooled for infection.

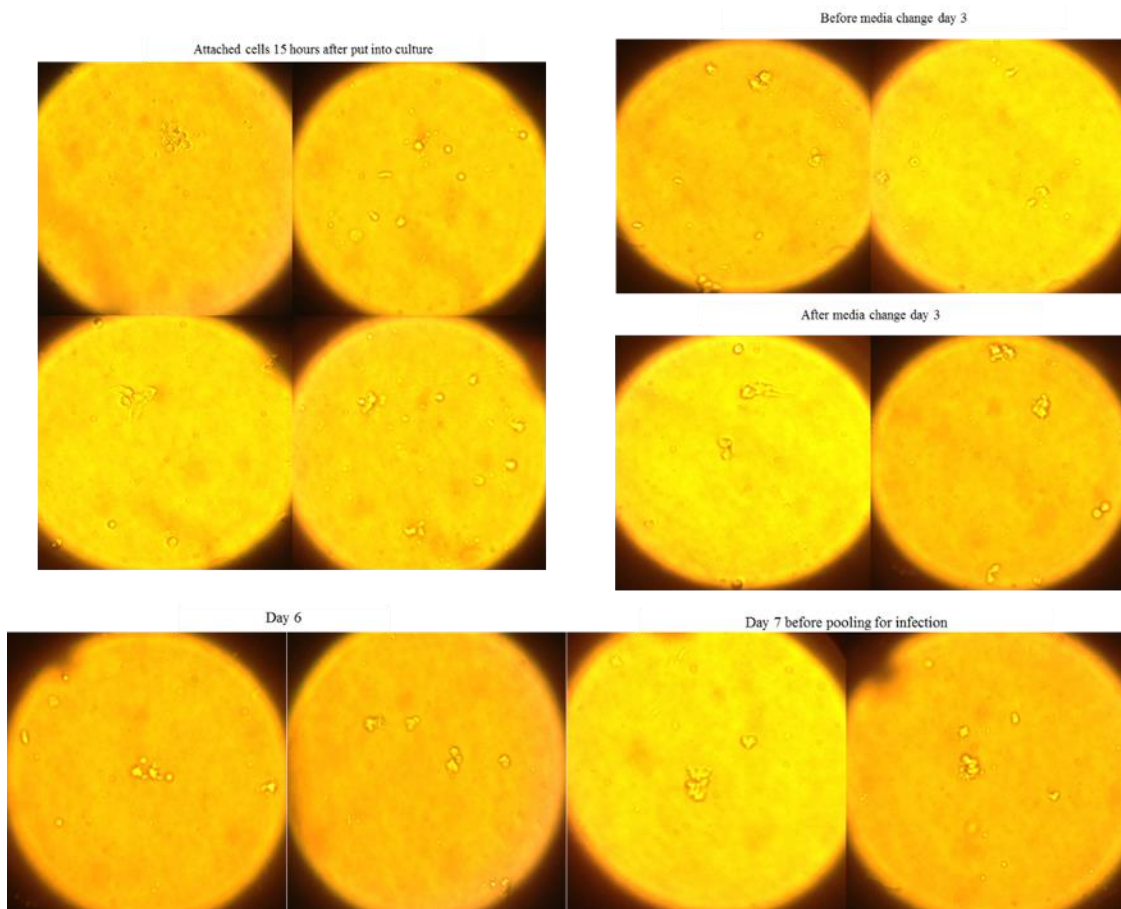


Figure 42: Cells in DC culture

In conclusion, the DC media was optimized to produce monocyte derived DCs. This was confirmed by analyzing the presence of CD11c, a marker for DCs⁴⁵, after 7 days of culture as seen in Figure 41.

Section 2: Infection of Dendritic cells with *A/California/07/2009 (H₁N₁pdm)*

2.1 Methods

Influenza virus was heat inactivated using established protocols³⁵. To confirm the virus was inactivated, 1:10 dilutions of inactivated influenza were seeded onto a prepared 96 well tissue culture plates containing MDCK cells at confluence in Influenza Virus Growth Medium. The TCID₅₀ assay was completed, and wells were checked daily for CPE. CPE was not observed in the wells containing inactivated virus, which confirmed the heat inactivation was successful.

Monocyte Derived Dendritic Cells were produced as previously described. DCs were collected from the supernatant of the culture into a 15 ml tube, and wells were washed three times with 1 ml of DMEM-5%FCS. The contents were pooled together, and DCs were counted as previously described. Based on cell number, DCs were split into separate tubes. Ten MOI of H₁N₁ virus was used (infectious and heat inactivated), as well as one tube for mock infection that did receive any virus. The cells were pelleted by spinning at 250xG for 10 minutes, and the pellet was resuspended in the assigned concentration of virus in 5 mls of 1x DMEM containing 2ug/ml of TPCK-Treated Trypsin with no FCS. Tubes were gently agitated, and placed in a 37 degree Celsius water bath for 40 minutes, mixing every 10 minutes during incubation. After the incubation, the tubes were transferred to the tissue culture incubator at 37 degrees Celsius 5% CO₂, with the lid slightly cracked for gas exchange with the tube rested at an angle. The tubes were incubated for 4 hours to allow for infection of the DCs. After incubation, 3 mls of DMEM-10%FCS was added to each tube, and the DCs in each treatment were pelleted by spinning at 250xG for 10 minutes. These cells were resuspended into 1 ml of

DMEM-10%FCS and washed again. Cells were counted using established protocols, and cells were separated for flow analysis.

2.2 Results

A TCID₅₀ Assay was completed as previously described in Chapter 1 using heat-inactivated virus. No CPE was observed in any of the wells compared with the controls, as seen in Figure 43. This confirmed that the virus had been heat-inactivated following the procedure.

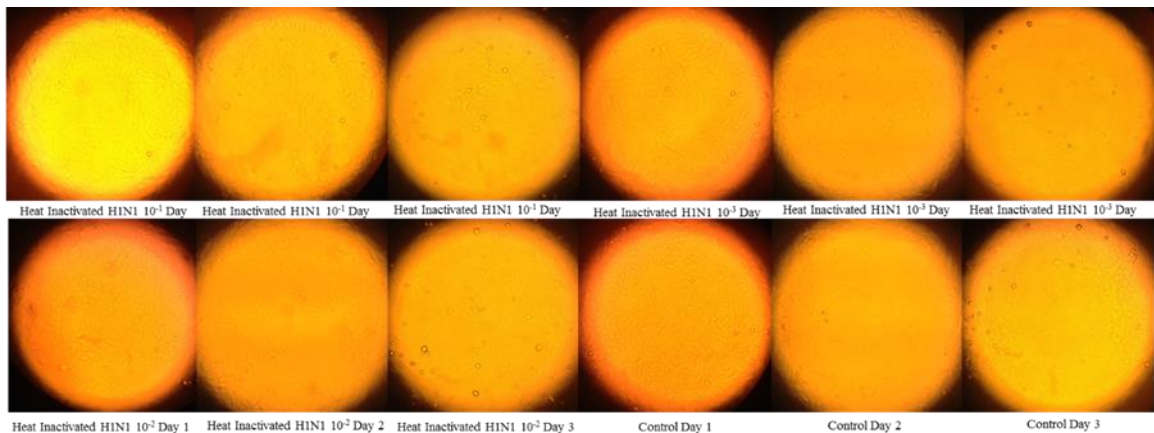


Figure 43: TCID₅₀ Results of heat inactivated H₁N₁. No CPE seen, which confirms that virus were inactivated.

Section 2: Detection of Markers

2.1 Methods

Markers used for flow analysis were determined to work by labeling of total MNCs, following previously described protocols. Activation makers were tested in the same way on MNCs activated by lipopolysaccharide (LPS) to determine that the monoclonal antibodies worked as expected. Briefly, MNCs after separation were resuspended in 0.1 µg/ml LPS, 1 µg/ml, or 10 µg/ml of LPS in 1x DMEM. Tubes were incubated for 2 hours at 37 degrees Celsius 5% CO₂ with the lids cracked to allow for gas

exchange. After incubation, the cells were washed by spinning at 250xG for 10 minutes and the pellet was resuspended for labeling and flow analysis. Monoclonal antibody flurophore conjugates to CD14, CD83, CD11c, CD40, CD80, and HLA-DR were used.

Labeling of infected and mock infected DCs for flow analysis was completed as previously described. Specifically monoclonal antibody flurophore conjugates to CD40, CD80, CD11c, and HLA-DR were used.

2.2 Results

The LPS activation was analyzed using flow cytometry. The results are seen below in Figure 44. A percentage of MNCs became larger and more granular, as seen in P6 gate on the side and forward scatter graphs. This indicated that cells were activated. Activation markers CD40 and HLA-DR increased in the LPS activated cells compared to the control, and also increased in brightness as indicated in Figure 44. An increase in brightness shows that there is more of that marker being expressed on the cell surface. If a cell becomes activated, it would be expected that more activation markers would be expressed. This experiment showed the antibodies were working as expected and could be used in the DC infection experiments.

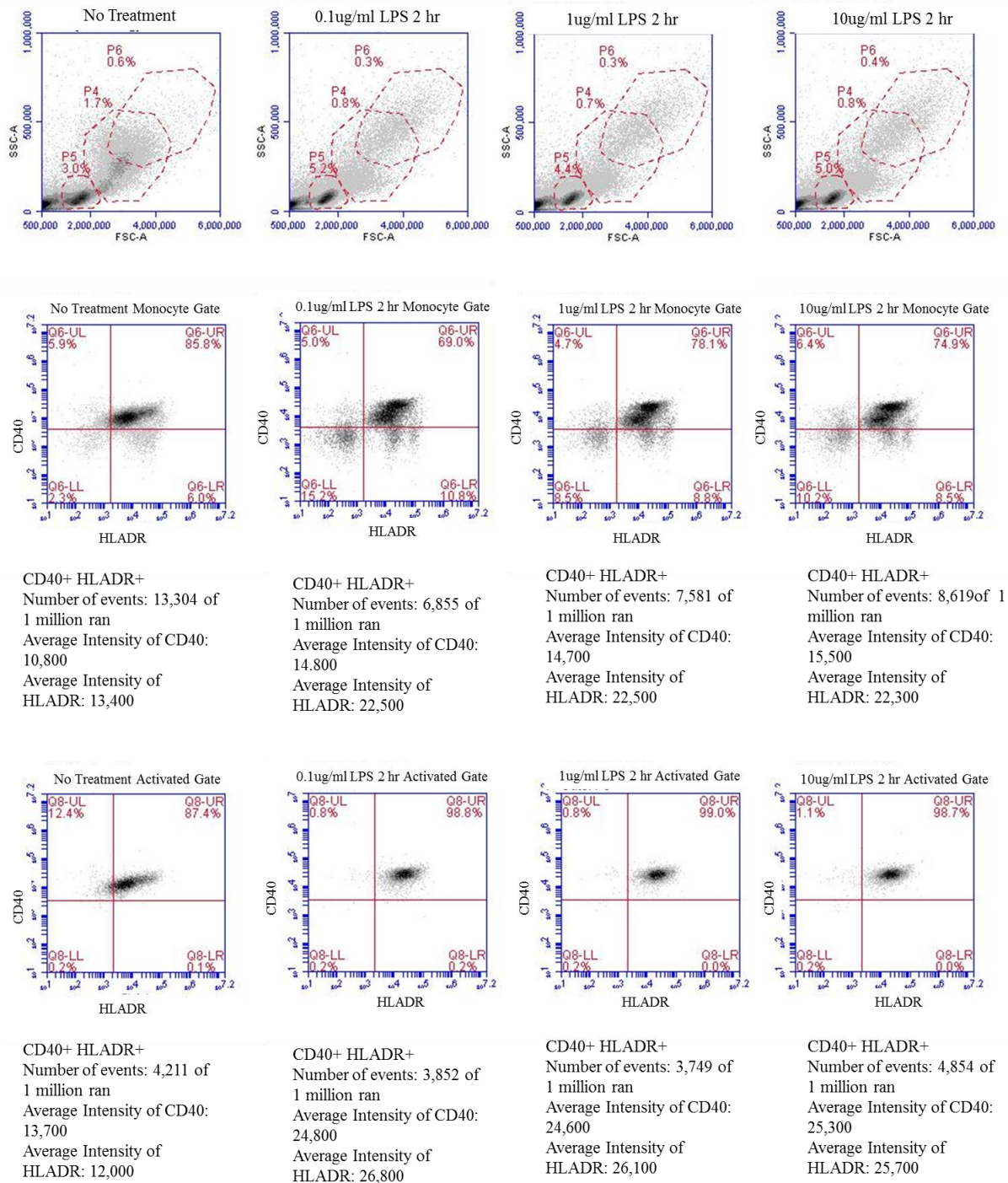


Figure 44: LPS stimulation of DCs. Cells were activated successfully by LPS, as seen by the increase of cells in gate P6 (the activated gate), that contains cells that are larger and more complex. Activation markers were higher in LPS activated cells compared to the untreated controls

Infectious and heat inactivated virus were used in conjunction with mock infected controls to infect monocyte derived DCs. This infection was completed in independent replicates, and typical results can be seen in Figure 45 below.

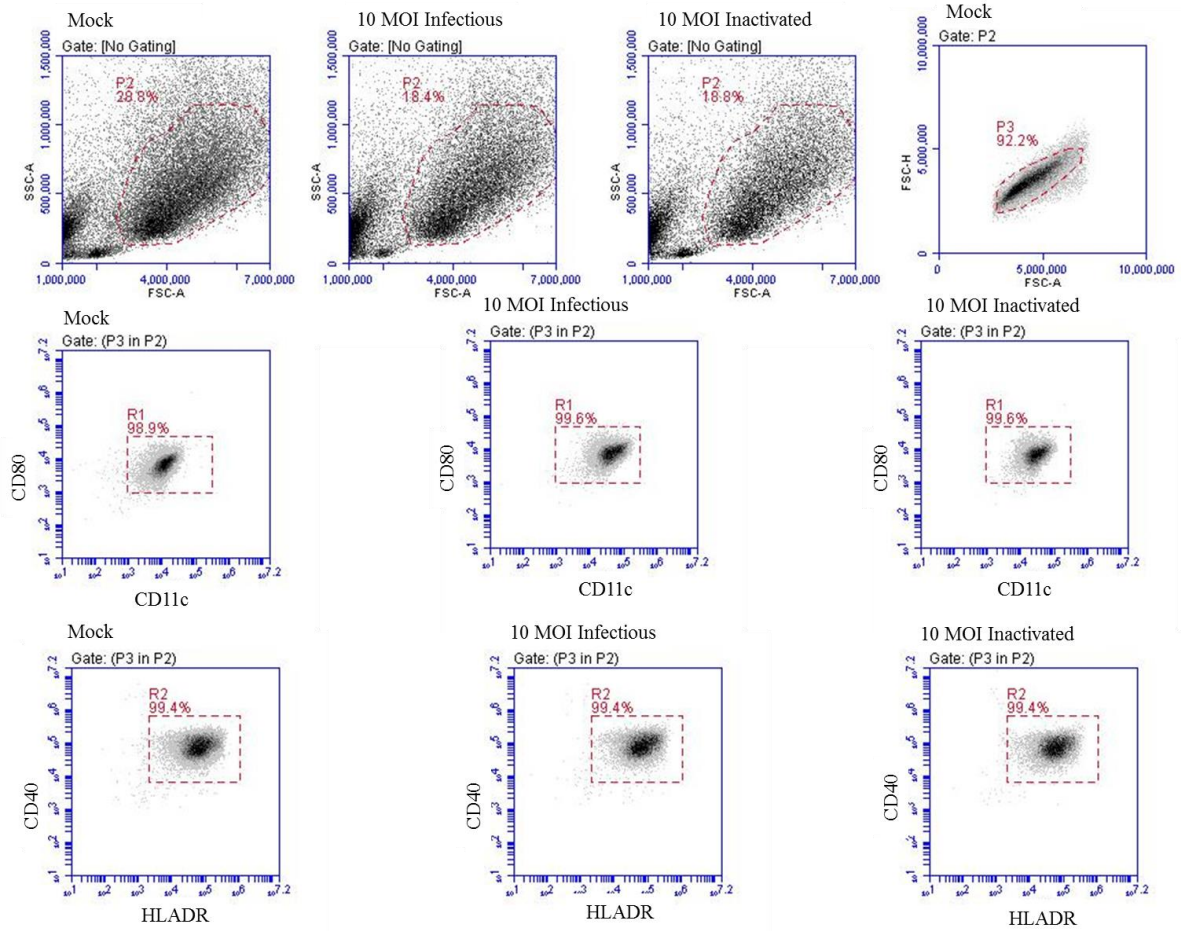


Figure 45: Infection of DC with 10 MOI of infectious and heat-inactivated virus corresponding to 10 MOI of infectious virus and mock infected controls.

Figure 45 of the DC infection shows that the majority of the cells in all of the treatments were positive for activation markers and DC markers. To determine if there was a difference between any of the treatments the brightness of the markers was

analyzed. There was no observable difference between the brightness of markers for CD80, CD40, and HLA-DR. However the brightness of CD11c appeared to increase. Using Welch's t test and the z distribution (z distribution is used because the number of samples in each treatment is larger than 1000), the differences in the brightness of different markers can be compared to the control mock infected DCs and determined if the difference is significant at different confidence intervals. Below in Table 10, the data from each of the infection experiments is shown along with the highest confidence level that was significant. Figure 46 shows the brightness of CD11c for these two experiments displayed in a histogram. Mock infected is labeled in black, red is infectious virus, and blue is inactivated virus. A clear increase in CD11c is seen in the DC with the virus versus the mock controls.

Table 10: CD11c mean brightness of DC infection, 10 MOI infectious and heat inactivated virus corresponding to 10 MOI of infectious virus and mock infected controls.

Sample	Mean	Confidence Level	p value
Optimized DC infection Donor C experiment 1			
Mock Infected	12,111	-	-
10 MOI Infectious	49,772	80%	0.2
10 MOI Inactivated	32,135	70%	0.3
Optimized DC infection Donor C experiment 2			
Mock Infected	8,183	-	-
10 MOI Infectious	51,935	95%	0.05
10 MOI Inactivated	19,542	90%	0.1

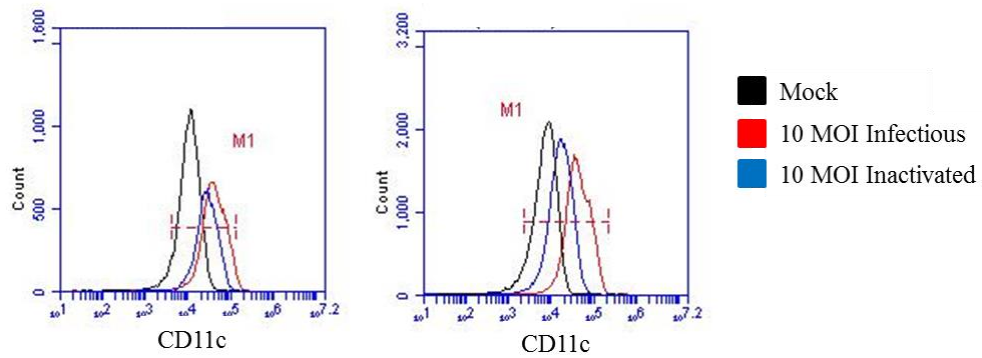


Figure 46: Brightness of CD11c for two experiments. Graph on the left from experiment 1, graph on the right from experiment 2. DC with 10 MOI infectious virus had the brightest CD11c (red) followed by the DC with inactivated virus (blue) compared to the mock controls (black)

In summary, the increase in brightness of CD11c indicates a difference in the expression of CD11c on DCs infected with H₁N₁ compared to cells that were loaded with the same quantity of inactivated virions.

Discussion

Influenza A virus infections continue to cause significant morbidity and mortality. Extensive vaccine production time, viral antigenic variability, and low vaccine efficacy contribute to the annual influenza pandemics and seasonal epidemics. A better understanding of human immune responses to Influenza A strains could result in more effective next generation vaccines.

The specific aim of this study was to determine the expression of activation markers in H₁N₁-infected DCs. To this end, influenza virus was propagated to make a stock for future experiments. This was done successfully in tissue culture using MDCK cells. MDCK-propagated virus was titrated by two different methods: hemagglutination and a Tissue Culture Infectious Dose 50% (TCID₅₀) assays. H₃N₂ could not be grown in MDCK cells as efficiently as H₁N₁. Shown in Table 3 the stock H₃N₂ from the IRR had almost four times more total viral particles than the stock H₁N₁, as determined by a HAU titer of 128 in H₃N₂ compared to 32 in H₁N₁. However, H₃N₂ had less of infectious particles with a titer of 3.9×10^4 PFU/ml versus H₁N₁ titer of 3.9×10^5 PFU/ml. These results show that the virus stocks of H₃N₂ had more noninfectious particles than H₁N₁. MDCK cells were used to propagate this stock virus. Infectious particles are required for a productive infection and propagation. A competition between non-infectious and infectious virions could result in interference as seen in the lack of development of CPE with H₃N₂ in MDCK cells. Consequently, we used H₁N₁ in the experiments involving the viral infection of dendritic cells.

A method was optimized to separate monocytes from mononuclear cells with high yield and purity (up to 95%). These monocytes were then placed into tissue culture with optimized concentration of cytokines GM-CSF and IL-4 to produce monocyte derived dendritic cells (DCs). These DCs were infected with *A/California/07/2009 (H₁N₁pdm)*, and checked for the expression of activation markers.

We hypothesized that the immune response against infectious virus induces a different pathway than inactivated virus. This will have an impact on the antibody response against virus presented in two different ways by DCs. Therefore, a difference in marker expression was expected to be observed when comparing the DCs that were infected with 10 MOI of infectious virus and a quantity corresponding to 10 MOI of inactivated virus.

Results in Table 10 demonstrate a four to six fold increase in mean brightness of the CD11c marker for the actively infected dendritic cells compared to mock-infected controls. However, DCs which were treated with a quantity corresponding to 10 MOI of inactivated virus showed approximately a 3 fold increase in mean brightness for the CD11c marker compared to mock infected controls.

CD11c, a marker for DCs, binds CD54, or Intracellular Adhesion Marker 1. These are both involved in cellular activation, particularly in activation of T cells, and enhancement of the immune response. When a DC is infected with infectious virus, the virus will use the cellular machinery to replicate itself. By increasing the expression of CD11c, the DC initiates a cascade of events that includes activation of T cells. We have demonstrated that this increase in expression of CD11c is occurring in DC infected with virus, but it is also occurring at a lower amount in DCs loaded with inactivated H₁N₁

virus. The inactivated virus will not replicate to produce infectious particles inside a target cell, and thus is generating a response similar to inactivated flu vaccines. Our observations positively correlates with the lower immune response induced by the inactivated vaccines.

We would expect to see an increase in activation markers such as CD40 and HLA-DR (MHC Class II) in infected DCs, but in these experiments enhanced expression was not observed. MHC Class II on antigen-presenting cells like DC, presents extracellular antigens to T helper cells, which is required for adaptive humoral immunity to H1N1. The experiment conducted to determine activation marker expression was designed to study these markers 4 hours post infection. It is conceivable that expression of other activation markers may require additional time post infection. Future studies may involve longer infection time to study this. MHC II and CD40 molecules are involved in the specific and second signal for activation of T cells respectively. Whereas CD11c is involved in the recruitment of T cells. Therefore, expression of adhesion molecule CD11c early (4 hours after infection) seems like the first step of a logical sequence of events in the overall mechanism of activation of T cells. The higher expression of CD11c in infected cells compared to dendritic cells loaded with inactivated virus is in agreement with a stronger response against viral infection compared to inactivated vaccines.

The future goal of this research is to understand the interaction between different populations of human B cells in DCs loaded with inactivated virus as well as infected DCs in the antibody response to Influenza A infection *in vitro*. For this purpose, a method was optimized to separate B cells from mononuclear cells. Minority B cell populations were also identified and analyzed successfully, providing for future study of

MZBCs, a B cell population of interest involved in the early immune response. Sensitive H1 and H3 specific ELISA assays were developed which enabled detection of IgM, and subclasses IgG1, IgG2, IgG3, and IgG4. Detection of these Influenza A-specific subclasses will be useful when studying formation of these antibodies in the co-culture of influenza infected DCs and different B cell populations. This *in vitro* model will provide a better understanding of the early innate immune responses to Influenza A including the cellular interactions required for successful resolution of H₁N₁ infection. Ultimately information derived from these studies may help in the development of more effective next-generation vaccines against Influenza A.

Appendices

Appendix A: Consent form for healthy volunteers

Consent form for healthy volunteers

TITLE:

Marginal Zone B Cells in the early antibody response to influenza infection in humans

AGREEMENT TO PARTICIPATE:

This signed consent is to certify my willingness to participate in this investigational (research) study.

PURPOSE OF STUDY:

The purpose of this research is to study the induction of antibodies upon infection with influenza in vitro. I am being asked to donate blood because I do not have an active influenza infection at this time.

TREATMENT(S)/PROCEDURE(S):

I will be asked to donate approximately 30 milliliters of blood (~2 tablespoons) on three different occasions (at least one month apart) over period of a year. This blood will be collected by venipuncture (using a needle to obtain blood from my arm). Blood will be collected by a trained professional at Wright State University.

BENEFITS AND RISKS:

The potential risks associated with venipuncture are excessive bleeding, fainting, feeling light-headed, development of a hematoma (bruising caused by blood accumulating under the skin), and infection (a slight risk any time the skin is broken). There may be a need for multiple punctures to locate a vein. I understand that there is no direct benefit to me other than helping to increase understanding influenza infection.

COSTS:

There will be no costs to me for my participation in this study.

REMUNERATION:

I will not be paid for my participation in this study.

CONFIDENTIALITY:

The researchers will be collecting demographic information about me (name, age, sex). All this information will be kept locked to maintain confidentiality. My identity will not be disclosed in any publication, or directly on the samples.

WHOM TO CONTACT:

If I have questions about this research study, or have a research-related injury to report, I can contact the researcher Cheryl Conley at 937-775-2306. If I have general questions about giving consent or my rights as a research participant in this research study, I can call the Wright State University Institutional Review Board at 937-775-4462.

VOLUNTARY CONSENT:

I understand that I am free to refuse to participate in this study or to withdraw at any time. My decision to participate or to not participate will not adversely affect relationship to this institution or cause a loss of benefits to which I might otherwise be entitled.

My signature below means that I have freely agreed to participate in this investigational study.

SIGNATURE/DATE LINES:

(Typed Name/Signature of Participant) (Date)

(Investigator obtaining Consent) (Date)

Appendix B: Reagent List

Bicarbonate buffer:

1.59 g Na_2CO_3 , 2.93 g NaHCO_3

Fill up to 1 L volume distilled water, pH to 8.6, store at room temperature.

10x PBS Buffer:

2.28 g NaH_2PO_4 , 11.5 g Na_2HPO_4 , 43.84 g NaCl , 400 ml of dH_2O , pH to 7.0. Fill up to 500 ml final volume with distilled water, store at room temperature.

1x PBS Buffer:

12.5 ml of 10x PBS and 112.5 ml of distilled water, store at room temperature.

1x PBS- 0.1% Tween wash buffer (sterile):

1125 μl of 1x PBS- 10% Tween, Fill up to 125 ml with 1x PBS, store at room temperature.

Blocking Buffer:

5% non-fat dry milk in 1x PBS-0.1% Tween. 2.25 g of Kroger or Meijer non-fat dried milk, 1125 μl of 1x PBS- 10% Tween. Fill up to 45 ml with 1X PBS buffer.

Store on ice or frozen overnight (wrap cap in parafilm if freezing).

Cell Buffer:

1% BSA 1mM EDTA 1xPBS

Flow Fixing Solution:

1% PFA 1mM EDTA 1xPBS

1x Homemade Red Blood Cell Lysis Buffer:

150mM NH₄Cl

10mM KHCO₃

1mM EDTA

Separation and Labeling Buffer:

0.5% Biotin free BSA 2mMEDTA 1xPBS

20x DC Production Media:

1.25 µl of BD Pharmigen Recombinant Human IL-4 (CAT#554605, 100 µg/ml,
0.4-5x10⁸ units/mg)

0.4 µl of BD Pharmigen Recombinant Human GM-CSF (CAT# 550068, 200
µg/ml, 0.1-1x10⁹ units/mg)

1% Penicillin-Streptomycin (100 units/ml Pen and 100 µg/ml Strep) (Pen-Strep)

10% Heat-inactivated fetal calf serum (FCS)

Up to a final volume of 5 mls of 1xDMEM

Dynabead Buffer:

0.1% Biotin free BSA

2mM EDTA

1xPBS

DMEM-5:

1% Pen-Strep (stock 1,000 U/ml Pen 1mg/ml Strep)

5% FCS

1x Dulbecco's Modified Eagle Medium (DMEM)

DMEM-10:

1% Pen-Strep (stock 1,000 U/ml Pen 1mg/ml Strep)

10% Heat-inactivated fetal calf serum

1x FCS

Wash Medium:

1% Pen-Strep (stock 1,000 U/ml Pen 1mg/ml Strep)

1xDMEM

TPCK-Treated Trypsin Working Stock:

2 mg/ml TPCK-Treated Trypsin

1xDMEM

Influenza Virus Growth Media

2 µg/ml TPCK-Treated Trypsin

1% Pen-Strep

1xDMEM

TCID₅₀% Viral Dilution Media

1 µg/ml TPCK-Treated Trypsin

1% Pen-Strep

1xDMEM

Appendix C: ELISA Antibodies

ELISA Method	Name	CAT#	Lot#	Dilution
Method #1	Pierce Goat Anti-Human IgG Lambda	31131	ME1418821	1:40
Method #1	Pierce Goat Anti-Human IgG Kappa	31129	MG1437581	1:40
Method #1, Method #3	BD Pharmigen Biotin Mouse Anti-Human IgG	555785	76951	1:1000
Method #1, Method #3	BD Pharmigen Biotin Mouse Anti-Human IgG1	555869	02372	1:500
Method #1, Method #3	BD Pharmigen Biotin Mouse Anti-Human IgG2	555874	07283	1:500
Method #1, Method #3	Abcam Mouse Anti-Human IgG3 HRPeroxidase	AB99829	GR33599	1:1000
Method #1, Method #3	BD Pharmigen Biotin Mouse Anti-Human IgG4	555882	02539	1:1000
Method #1	Pierce Goat Anti-Human IgG Peroxidase	31413	ML1490538	1:5000
Method #2	BD Pharmigen Purified Mouse Anti-Human IgG	555784	10689	1:50
Method #2	BD Pharmigen Purified Mouse Anti-Human IgG1	555868	19501	1:100
Method #2	BD Pharmigen Purified Mouse Anti-Human IgG2	555873	04895	1:100

Method #2	BD Pharmigen Biotin Mouse Anti-Human Ig Kappa Light Chain	555790	05989	1:1000
Method #2	BD Pharmigen Biotin Mouse Anti-Human Ig Lambda Light Chain	555794	00529	1:1000
Method #3	Influenza Reagent Resource Influenza A (H1) pdm09 Control Antigen	FR-1184	1314H1AG	1:50
Method #3	Influenza Reagent Resource Influenza A (H3) Control Antigen	FR-43	58685890	1:50
Method #3	BD Pharmigen Biotin Mouse Anti-Human IgM	555781	E03419-1634	1:500
Method #3	Influenza Reagent Resource Mouse Monoclonal Antibody Influenza Type A H3	FR-54	61807464	1:50
Method #3	Influenza Reagent Resource Mouse Monoclonal Antibody Influenza Type A H1 pdm091	FR-572	61807466	1:50
Method #3	Influenza Reagent	FR-51	59059154	1:50

	Resource Mouse Monoclonal Antibody Influenza A pool			
Method #3	Thermo Scientific Stabilized Peroxidase Conjugated Goat Anti0Mouse H+L IgG	32430	OE185747	1:500

Table 11: ELISA Antibodies

Works Cited

1. Ostrowski, M., M. Vermeulen, O. Zabal, P.I. Zamorano, A.M. Sadr, J.R. Geffner, O.J. Lopez (2007). The Early Protective Thymus-Independent Antibody Response to Foot-and-Mouth Disease Virus Is Mediated by Splenic CD9+ B Lymphocytes. *J. Virology* 81(17): 9357-67.
2. Ostrowski, M., M. Vermeulen, O. Zabal, J.R. Geffner, A.M. Sadr, O.J. Lopez (2005). Impairment of Thymus-Dependent Responses by Murine Dendritic Cells Infected with Foot-and-Mouth Disease Virus. *J. Immunology* 175: 3971-79.
3. Pillai, S., A. Cariappa, S.T. Moran (2005). Marginal Zone B Cells. *Annu. Rev. Immunol* 23: 161-96.
4. Weill, J.C., S. Weller, C.A. Reynaud (2009). Human Marginal Zone B Cells. *Annu. Rev. Immunol* 27: 267-85.
5. Lee B. O., J. Rangel-Moreno, J.E. Moyron-Quiroz, M. Makris, F. Sprague, F.E. Lund, T.D. Randall (2005) CD4 T Cell-Independent Antibody Response Promotes Resolution of Primary Influenza Infection and Helps to Prevent Reinfection. *J Immunol* 175(9): 5827-38.
6. Gonchoroff, N.J., A.P. Kendal, D.J. Phillips, C.B. Reimer (1982). Immunoglobulin M and G Antibody Response to Type- and Subtype-Specific Antigens After Primary and Secondary Exposures of Mice to Influenza A Viruses. *Infect Immun* 36(2): 510-7.

7. Lottenbach, K.R., C.M. Mink, S.J. Barenkamp, E.L. Anderson, S.M. Homan, D.C. Powers (1999). Age-Associated Differences in Immunoglobulin G1 (IgG1) and IgG2 subclass Antibodies to Pneumococcal Polysaccharides following Vaccination. *Infection and Immunity* 67(9): 4935-38.
8. Kruetzmann, S., M.M. Rosado, H. Weber, U. Germing, O. Tournilhac, H.H. Peter, R. Berner, A. Peters, T. Boehm, A. Plebani, I. Quinti, R. Carsetti (2003). Human Immunoglobulin M Memory B Cells Controlling Streptococcus Pneumoniae Infections are Generated in the Spleen. *J Exp Med* 197: 939-45.
9. Haye, K., S. Burmakina, T. Moran, A. Garcia-Sastre, A. Fernandez-Sesma (2009). The NS1 Protein of a Human Influenza Virus Inhibits Type I Interferon Production and the Induction of Antiviral Responses in Primary Human Dendritic and Respiratory Epithelial Cells. *J Virol* 83(13): 6849-62.
10. Giordani, L., M. Sanchez, I. Libri, M.G. Quaranta, B. Mattioli, M. Viora (2009). IFN-alpha Amplifies Human Naive B Cell TLR-9-Mediated Activation and Ig Production. *J Leukoc Biol* 86(2): 261-71.
11. Simmon, Jessie (2009). The Comparison of Co-Stimulatory Surface Molecule Expression on Human Monocyte-Derived Dendritic Cells Infected with Two Strains of Influenza Virus. Master of Science Thesis. Northern Michigan University.
12. Gordon, C. L., P.D.R. Johnson, M. Permezel, N.E. Holmes, G. Gutteridge, C.F. McDonald, D.P. Eisen, A.J. Stewardson, J. Edington, P.G.P. Charles, N. Crinis, M.J. Black, J.Torresi, M.L. Grayson (2010). Association Between Severe

- Pandemic 2009 Influenza A (H₁N₁) Virus Infection and Immunoglobulin G2 Subclass Deficiency. *CID* 50: 672-678.
13. Carter, John and Venetia Saunders. *Virology Principles and Applications*. West Sussex: John Wiley and Sons LTD, 2007.
 14. Hamilton, Robert G. (1987). The Human IgG Subclass Measurements in the Clinical Laboratory. *Clinical Chemistry* 33: 1707-1725.
 15. Zimmerli, W., A. Schaffner, C. Scheidegger, R. Scherz, P.J. Spath (1991). Humoral immune response to pneumococcal antigen 23-f in an asplenic patient with recurrent fulminant pneumococcaemia. *J. of Infection* 22:59-69.
 16. Wilschut, Jan, Janet McElhaney, Abraham Palache. *Influenza*. 2nd Ed. New York: Mosby Elsevier, 2006.
 17. *Influenza*. World Health Organization, April 2009. Web. 15 July 2013.
<<http://www.who.int/mediacentre/factsheets/fs211/en/index.html>>.
 18. Dawood, Fatimah et al (2012). Estimate global mortality associated with the first 12 months of 2009 pandemic influenza A H₁N₁ virus circulation: a modeling study. *The Lancet/Infection* 12:687-695.
 19. Dushoff, Jonathan et al (2005). Mortality due to Influenza in the United States- An Annualized Regression Approach Using Multiple-Cause Mortality Data. *American Journal of Epidemiology* 163:181-187.
 20. Rodak, Bernadette, George Fritsma, Kathryn Doig. *Haematology Clinical Principles and Applications*. 3rd edition. St. Louis: Saunders Elsevier, 2007.

21. Osvaldo Lopez (2013). *Immune Response Against Viruses Producing Acute Disease, Influenza Virus*. Personal Collection of Osvaldo Lopez, Wright State University, Dayton, Ohio.
22. Szretter, Kristy, Amanda Ballish, Jacqueline Katz (2006). Influenza: Propagation, Quantification, and Storage. *Current Protocols in Microbiology* 15G.1.1-15G.1.22.
23. Parham, Peter. *The Immune System*. 3rd edition. New York: Garland Science, Taylor and Francis Group, 2009.
24. Van De Sandt, Carolien et al (2012). "Evasion of Influenza A Viruses from Innate and Adaptive Immune Responses." *Viruses* 4: 1438-1476.
25. Plotkin, S.A., W.A. Orenstein, P.A. Offit. *Vaccines*. 5th edition. Philadelphia, W.B. Saunders Co, 2008.
26. *Seasonal Influenza (Flu)*. Centers for Disease Control and Prevention, 9 March 2011. Web. 22 October 2013.
<<http://www.cdc.gov/flu/professionals/vaccination/virusqa.htm>>.
27. *Seasonal Influenza (Flu), Key Facts about Seasonal Flu Vaccine*. Centers for Disease Control and Prevention, 19 September 2013. Web. 22 October 2013.
<<http://www.cdc.gov/flu/protect/keyfacts.htm>>.
28. Gerdil, Catherine (2003). "The Annual Production Cycle for Influenza Vaccine." *Vaccine* 21:1776-1779.
29. *Seasonal Influenza (Flu), Selecting Viruses for the Seasonal Influenza Vaccine*. Centers for Disease Control and Prevention, 26 September 2013. Web. 22 October 2013. < <http://www.cdc.gov/flu/about/season/vaccine-selection.htm>>.

30. *Pandemic Influenza Vaccine Manufacturing Process and Timeline*. World Health Organization, 9 August 2009. Web. 22 October 2013.
<http://www.who.int/csr/disease/swineflu/notes/h1n1_vaccine_20090806/en/>.
31. Moldoveanu, Z et al (1995). "Human Immune Responses to Influenza Virus Vaccines Administered by Systemic or Mucosal Routes." *Vaccine* 13:1006-1012.
32. CLS Limited (2013). *Afluria Influenza Vaccine: Package Insert*. Parksville, Victoria, Australia: Author.
33. *Converting TCID50 to Plaque Forming Units (PFU)*. ATCC, 25 July 2012. Web. 9 October 2013
<<http://www.atcc.org/Global/FAQs/4/8/Converting%20TCID50%20to%20plaque%20forming%20units%20PFU-124.aspx>>
34. Crowther, John R. (2009). *The Elisa Guidebook*. New York, NY: Humana Press.
35. Bender, Armin et al (1995). "Inactivated Influenza Virus, when Presented on Dendritic Cells, Elicits Human CD8+ Cytolytic T Cell Responses." *J. Exp. Med* 182: 1663-1671.
36. Morbidity and Mortality Weekly Report, 21 February 2014. Center for Disease Control and Prevention. Volume 63, Number 7. Web. 37 March 2014.
<http://www.cdc.gov/mmwr/pdf/wk/mm6307.pdf>
37. National Early Season Flu Vaccination Coverage, 12 December 2013. Center for Disease Control and Prevention. Web. 27 March 2014.
<http://www.cdc.gov/flu/fluview/nifs-estimates-nov2013.htm>
38. BD Accuri C6. BD Biosciences. Web. 21 march 2014.
<http://www.bdbiosciences.com/instruments/accuri/features/index.jsp>

39. Rogers, Clare. Multicolor Flow Cytometry: Setup and Optimization on the BD Accuri C6 Flow Cytometer. Webinar. BD Biosciences.
http://www.bdbiosciences.com/documents/webinar_092111_Accuri_Multicolor.pdf
40. Racine, Rachel et al (2011). "IgM Production by Bone Marrow Plasmablasts Contributes to Long-Term Protection against Intracellular Bacterial Infection." *J. Immunology* 186:1011-1021.
41. Banchereau, Jaques and Ralph Steinman (1998). "Dendritic cells and the control of immunity." *Nature* 392:245-252.
42. Spackman, E (2008). *Avian Influenza Virus*. Totowa, NJ: Humana Press.
43. Hystopaque 1083. Package insert. Sigma. Retrieved from web 1 May 2014.
<http://www.sigmaaldrich.com/content/dam/sigma-aldrich/docs/Sigma/Product_Information_Sheet/10831pis.pdf>
44. Types of Vaccines. National Institute of Allergy and Infectious Disease. 3 April 2012. Web. 6 May 2014.
<<http://www.niaid.nih.gov/topics/vaccines/understanding/pages/typesvaccines.aspx>>.
45. *Cellular Antigens Guide* (2nd ed.). eBioscience. Requested from ebioscience.com.